PHILIPS

APPLICATION BOOK

PHILIPS

ELECTRONIC COMPONENTS AND MATERIALS

APPLICATIONS OF INFRARED DETECTORS

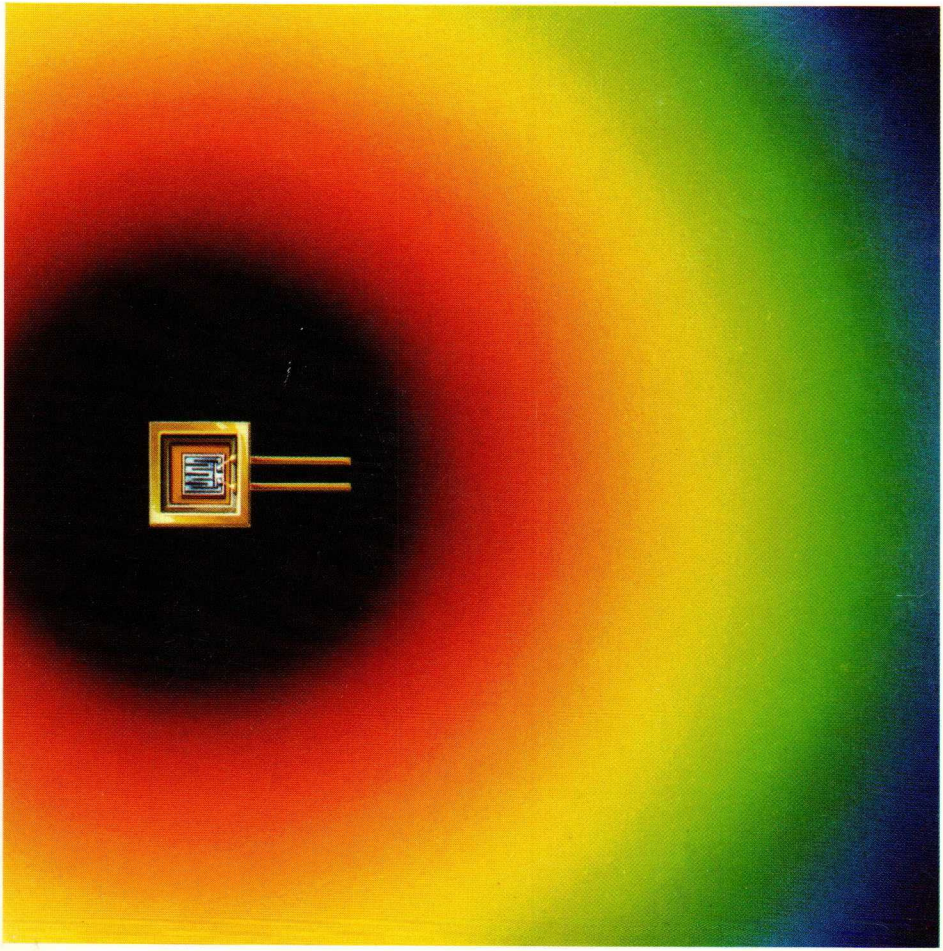

APPLICATIONS OF INFRARED DETECTORS

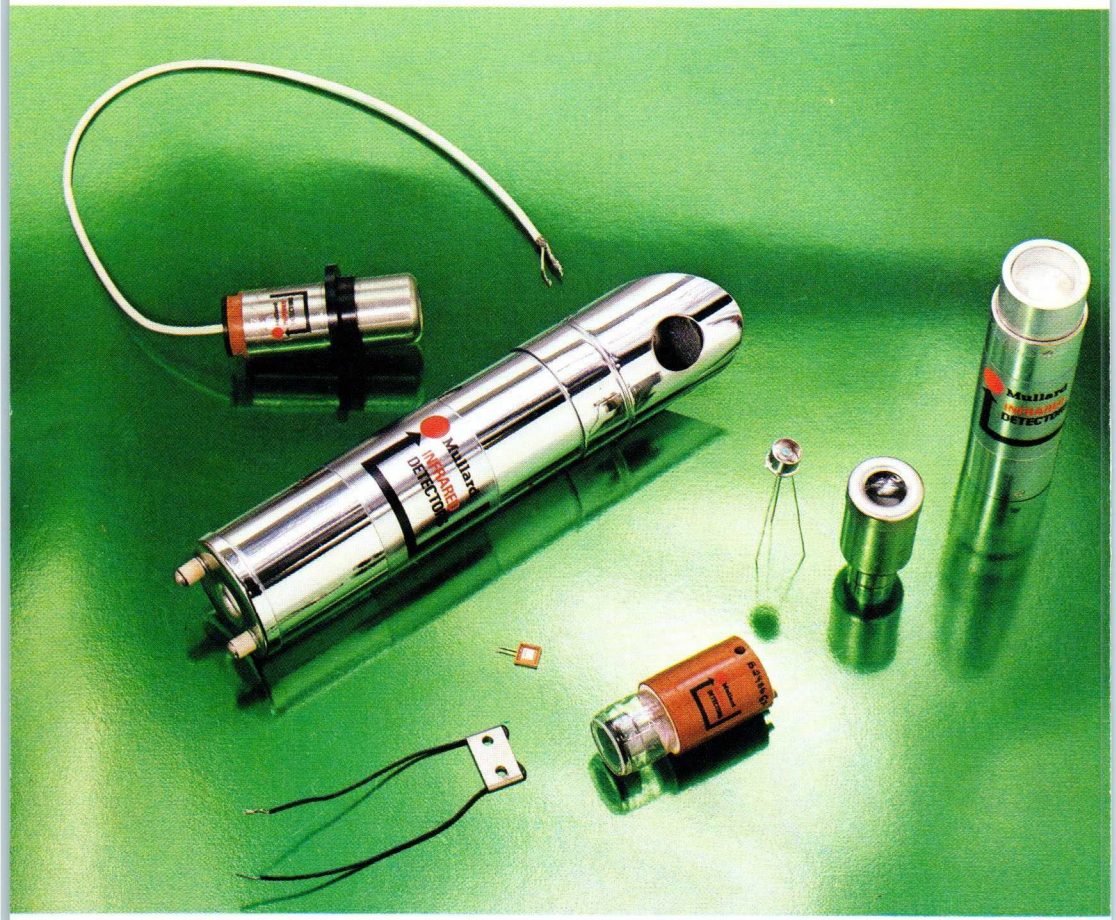
Mullard
INFRARED
DETECTOR
Mullard
INFRARED
DETECTOR

Applications of Infrared Detectors

PUBLICATIONS DEPARTMENT
ELECTRONIC COMPONENTS AND MATERIALS DIVISION

EINDHOVEN - The Netherlands

September 1971

FOREWORD

Infrared detection, infrared measurement, and infrared imaging are finding increasingly numerous and varied uses in industry and medicine. This book gives a brief account of the relevant theory of infrared detection and several typical applications. Circuits of prototypes are provided.

Temperature measurements with high resolution are now attainable with infrared detectors and their associated circuits. No contact is necessary between the detector and the area whose temperature is being measured; the response time can be as short as 100ns, and the object itself can even be in motion.

The presence or the arrival of an object whose temperature is significantly different from that of the background can be detected with other arrangements of infrared detectors and their circuits. The output can be used for control or alarm applications.

A complete thermal picture to indicate the superficial temperature over a given area of a scene can be provided by more complex infrared detection systems. This thermal image can be presented on a normal cathode ray tube (for example, in an oscilloscope).

ACKNOWLEDGEMENTS

The authors of this book are named in the Contents list. They are members of the Applications Group of the Electron-optical Department, Mullard Southampton. They wish to acknowledge the guidance and assistance provided by J. A. Ingham in the experimental work and the preparation of the text.

The book has been edited by F. A. Sowan of Central Technical Services, Mullard Limited.

CONTENTS

The Electronic Components and Materials Division of Philips supplies the infrared detectors, but not the equipments described in this book.

CHAPTER 1

INFRARED DETECTORS AND THEIR APPLICATIONS

INTRODUCTION

The nature of infrared radiation is discussed first in this chapter, and then follow descriptions of methods of detection and a number of applications of the present range of detectors.

Infrared radiation is physically of the same form as visible radiation (light), but in many of its interactions with matter it behaves rather differently. The wavelength of infrared radiation is longer than that of radiation in the visible region, causing it to lie 'beyond the red' when a spectrum is formed by a prism from an incandescent source. It was in this way that the existence of infrared radiation was deduced by Sir William Herschel in 1800. The similarity of the natures of infrared and visible radiation was shown by the fact that both could be polarised. The wavelength of infrared radiation was determined by interferometric measurements soon after 1830. Subsequent work showed that there is no upper limit to the wavelength of such radiation, and it has now been studied at wavelengths where it merges with electromagnetic radiation generated by microwave techniques.

The essential property which distinguishes infrared radiation from light is thus its wavelength. A convenient unit for measurement is the micrometre (μm) which is 10^{-6} metre. The micrometre is equal to the micron, μ, a term still used but now deprecated. Similarly deprecated is the term mμ, being 10^{-3} micron. In the shorter wavelength region, the nanometre (10^{-9} metre) may be used.

The Ångstrom unit, Å, which is 10^{-10} metre, is commonly used in optical physics. These units of wavelength are compared in Table 1, which must be read from the lefthand side.

The infrared region begins at the wavelength which is just too long for the eye to see (0·75μm); its other limit is not clearly defined, but it is often

TABLE 1

Comparison of units of length

	Å	nm	μm	mm	cm	m
Å	= 1	10^{-1}	10^{-4}	10^{-7}	10^{-8}	10^{-10}
nm	= 10	1	10^{-3}	10^{-6}	10^{-7}	10^{-9}
μm	= 10^{4}	10^{3}	1	10^{-3}	10^{-4}	10^{-6}
mm	= 10^{7}	10^{6}	10^{3}	1	10^{-1}	10^{-3}
cm	= 10^{8}	10^{7}	10^{4}	10	1	10^{-2}
m	= 10^{10}	10^{9}	10^{6}	10^{3}	10^{2}	1

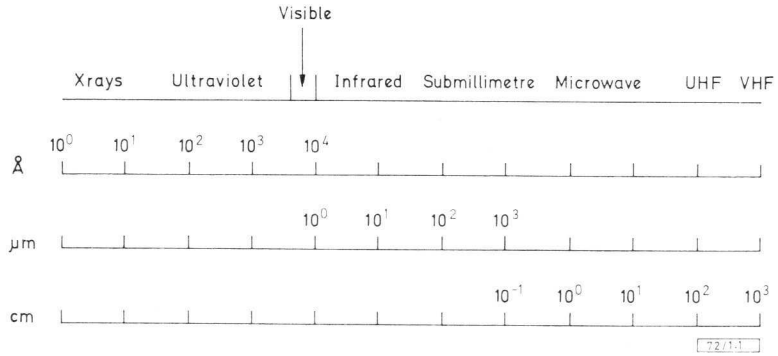

Fig. 1.1—Electromagnetic spectrum

taken to be 1000μm, where the microwave region begins. This limit depends on whether optical or microwave techniques are being considered. Fig. 1.1 illustrates the relation of the infrared region to other parts of the electromagnetic spectrum.

The infrared region is often divided into 'near' (0·75 to 1·5μm), 'intermediate' (1·5 to 10μm) and 'far' (beyond 10μm) regions, and the region beyond 300μm is often referred to as the 'submillimetre' region.

SOURCES OF INFRARED RADIATION

Electromagnetic radiation is emitted by any object at any temperature above absolute zero (−273°C), but the amount emitted and its distribution with wavelength depend on the temperature and emissivity of the body.

The emissivity denotes the ratio of the actual emission from the body to that from a hypothetical source called a 'black body' at the same temperature. The emissivity generally varies with wavelength.

The properties of a 'black body' radiator may be calculated theoretically. Three points about it are of particular importance:

1) The total energy radiated (W_{tot}) is proportional to the fourth power of the absolute temperature T (°C+273):

$$W_{tot} = \sigma T^4$$

where σ is Stefan's constant, which is approximately equal to $5{\cdot}67 \times 10^{-12}$Wcm^{-2}degK^{-4}.

2) The curve of variation of energy per interval of wavelength ($W_\lambda d\lambda$) is always of the same shape, following Planck's law:

$$W_\lambda D\lambda = \frac{C_1 \lambda^{-5} d\lambda}{\exp(C_2/\lambda T) - 1}$$

where C_1 and C_2 are constants, given by

$$C_1 = 3{\cdot}7 \times 10^{-12} \text{Wcm}^2$$
$$C_2 = 1{\cdot}44 \text{cm deg.}$$

This is plotted in Fig. 1.2 for some typical source temperatures.

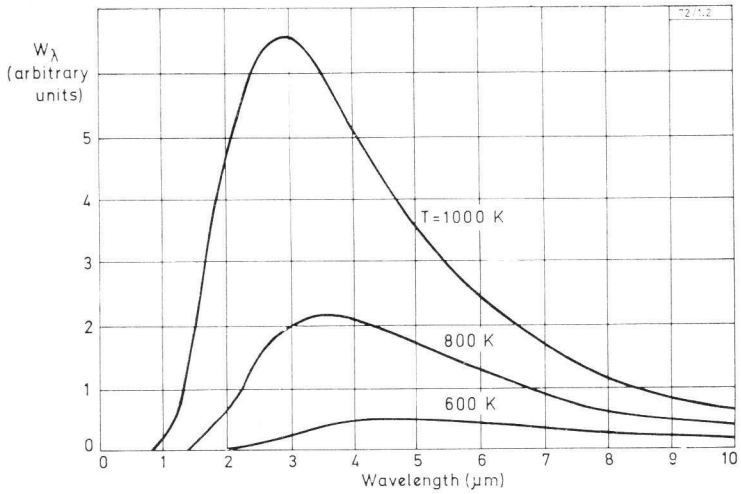

Fig 1.2—Variation of energy per interval of wavelength with wavelength (Planck's Law)

3) The wavelength of the peak emission is a simple function of the absolute temperature (Wien's displacement law). The wavelength in μm is:

$$\lambda_{pk} \simeq 2900/T.$$

Many real objects are similar to the hypothetical 'black body', and it is possible to make an experimental source approaching the theoretical very closely by taking an almost complete hollow sphere or a narrow cone at a uniform temperature.

Application of the equation for peak wavelength to the sun (at 6000K) shows peak emission at 0·5μm or 5000Å, in the visible region. An object at, say, 900K (common for a furnace) will emit most at about 3μm; one at room temperature (300K), at 10μm. Thus the range from the visible limit to 10μm is a very suitable wavelength region for measuring radiation from common objects, and hence detecting their presence or determining their temperature.

Although many interesting sources of infrared radiation are close to 'black body' sources, some sources such as flames and lasers emit over a narrow wavelength range. Normal tungsten filament lamps, although producing visible radiation, emit peak radiation in the near-infrared region. Gallium arsenide electroluminescent diodes, when forward-biased, produce monochromatic radiation at 0·9μm which may be modulated at very high frequencies.

TRANSMISSION OF INFRARED RADIATION

Although infrared radiation is similar to light, it is important to realise that, because something is transparent or opaque in the visible region, it is not necessarily so in the infrared. Thus, for example, ordinary clear glass is transparent up to only about 2·5μm in the infrared region. On the other hand, semiconductor materials such as germanium and silicon, opaque in the visible, are transparent in the infrared region beyond 1·8 and 1μm respectively.

An important factor in transmission over long distances is the atmosphere, and Fig. 1.3 shows typical transmission percentages over a path of one mile. The 'transparent' regions in this figure (in, for example, 8 to 13μm) are referred to as 'windows'.

Interference filters which enable narrow bands of radiation to be selected, or 'cut-on' and 'cut-off' characteristics of any form to be achieved, are important components often used in infrared systems.

DETECTION OF INFRARED RADIATION

As infrared radiation is a form of electromagnetic energy, it is, of course, possible to detect it by absorbing it and hence converting the

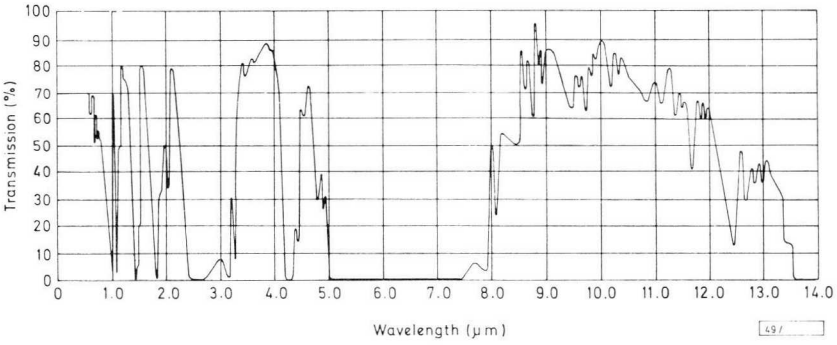

Fig. 1.3—Atmospheric transmission of infrared radiation over one mile

energy to heat. This is the basis of early experiments using a blackened thermometer bulb. However, this method is slow, insensitive and inconvenient; a device that gives an electrical output is more desirable.

Thermal detectors

Detectors which measure radiation by means of the change of temperature of an absorbing material are called thermal detectors. The output from the element may be in the form of a thermal e.m.f. (thermocouple detector), a change in resistance (thermistor bolometer), the movement of a diaphragm caused by the expansion of a gas (pneumatic detector) which may lead to the change of illumination of a subsidiary photocell (Golay cell), or changes in the electrical polarisation of certain crystals with temperature (pyroelectric detector).

Thermal detectors respond to any wavelength radiation that is absorbed, and can thus, by 'blackening' the surface, be made to respond over a wide range of wavelengths. However, because the temperature of the sensing element must change, they are in general slow, taking one hundredth to one tenth of a second to respond.

Quantum detectors

The alternative method of detecting infrared radiation depends on the interaction of the radiation with electrons in a solid, causing the electrons to be excited to a higher energy state. These effects depend on the quantum nature of radiation, and detectors using them are called quantum detectors.

The quantum theory states that radiation of a given wavelength λ is composed of 'particles' each of individual energy proportional to $1/\lambda$. Hence, if a transition of electrons from one state to another, requiring an

energy W, is considered, it will occur only if the wavelength is such that λ is less than some critical value. The idealised response of a quantum detector is as shown in Fig. 1.4.

The rising form of the curve is due to the fact that, as the wavelength increases, the number of quanta for a given amount of energy increases, and since the output is controlled by the number of electrons excited, it

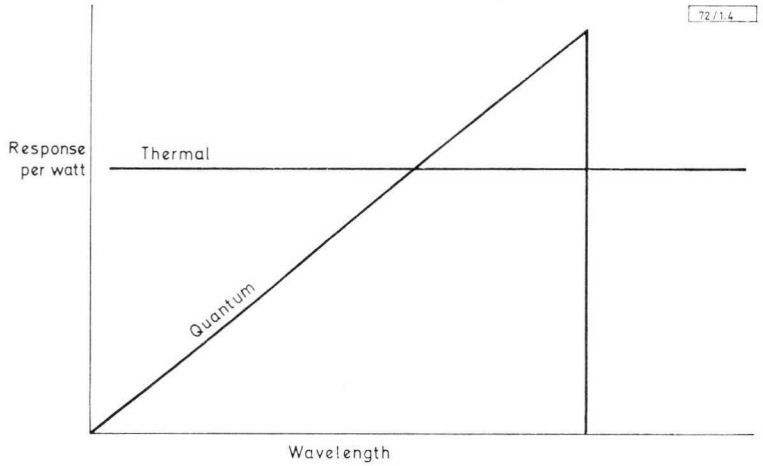

Fig. 1.4—Idealised response characteristic for quantum and thermal detectors

also rises. Fig 1.4 also shows the idealised response of a thermal detector; as this type of detector measures the energy directly, the response per watt is constant.

To use this quantum effect, it is necessary to be able to excite electrons from one state to another in which their electrical properties are different. One way is by photoemission, when electrons are given enough energy to escape from a solid and flow through a vacuum to give a current. However, surfaces require rather high energies for the release of electrons, and this effect can be used only in the visible and near infrared (to about 1μm). However, inside a semiconducting material the properties of an electron in the valence band are very different from when it is in the conduction band: in an n-type semiconducting material, the electrons in the valence band are unable to contribute to the conduction. If excited to the conduction band, however, they can do so, as also can the 'hole' left behind in the valence band. Thus the conductivity is increased, and the material may be used as a photoconductor to detect radiation. If the absorption occurs near a p-n junction, the excited carriers are swept away

by the junction electric field and give a current in the external circuit. Devices using such effects are known as photodiodes and phototransistors.

If it is desired to detect radiation at long wavelengths in the infrared region, a small amount of excitation energy is required. Some detectors make use of the release of an electron from an added impurity atom, which needs less energy than for an excitation across the band gap. Such devices are impurity photoconductors. The transitions required for several types of quantum detector are compared in Fig. 1.5.

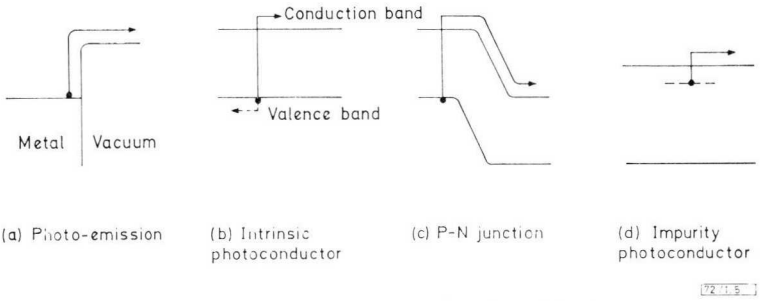

Fig. 1.5—Energy transitions in quantum detectors

The fact that smaller energies are required at the longer wavelengths for quantum detectors has one important consequence. The smaller energy requirement allows the excitation of electrons by thermal agitation of the solid, and this is a random effect that gives rise to electrical noise in the output. Thus, for good sensitivity it is necessary to cool the semiconducting element. This may necessitate only a thermoelectric cooler to maintain a temperature just below room temperature, or it may demand the use of liquid helium, boiling at 4·2K, depending on the application.

SOME IMPORTANT DETECTOR PROPERTIES

Full discussion of the properties of infrared detectors will be found in standard text books. Those outlined below are the most relevant to the purposes of this book.

Responsivity

The purpose of a detector is to convert infrared radiation into an electrical signal; thus the basic property defining the performance is the ratio of electrical output (volts or amperes) to the incident energy (watts) on the sensitive area of the detector. This quantity is called the responsivity. It is important to note the type of radiation specified in connection with the responsivity. It may be radiation at one specific wavelength (monochromatic radiation), which is often chosen to be the wavelength of peak

sensitivity (to give peak responsivity), or it may be black-body radiation from a source at a specified temperature, often 500K (to give black-body responsivity). In this case, some of the incident radiation is in wavelength regions where the detector is not sensitive, but the whole of the radiation is counted in calculating this responsivity. Of course, the black-body responsivity is always less than the peak responsivity. The responsivity will also vary with the modulation frequency of the radiation because of the finite time-constant of the photo-effect.

Noise equivalent power (N.E.P.)

The importance of cooling to reduce noise has been mentioned. Such electrical noise sets a limit to the smallest radiation level that can be detected. The noise of a detector is usually quoted as the root mean square value of the electrical output measured in a bandwidth of 1Hz at some specified centre frequency, under typical operating conditions for the detector. This quantity may be independent of frequency over some range, when it is said to show white noise in that range, or it may vary with frequency. For white noise, the magnitude measured is proportional to the square root of the bandwidth, so the performance is often quoted as volts per unit bandwidth ($VHz^{-\frac{1}{2}}$).

Although a low noise enables smaller energies to be detected, it may make the design of suitable amplifiers difficult. To get the best performance, the amplifier noise must be low. It is thus often of importance to know the ratio of the detector noise to the value of Johnson noise in a resistor, at room temperature, of magnitude equal to that of the detector. This ratio may be quoted as a noise factor.

In testing a detector intended for measuring small quantities of radiation, the signal-to-noise ratio may be measured. This depends on a number of test conditions, such as the radiation energy used, the frequency of modulation of the energy and of the noise measured, and the bandwidth. A more useful quantity is the noise equivalent power, or N.E.P. This is the amount of energy that will give a signal equal to the noise in a bandwidth of 1Hz. It is, in general, a function of the wavelength and of the frequency of measurement. It is equal to the noise (per unit bandwidth) divided by the responsivity.

Area normalised detectivity (D*)

As one might expect, all the above quantities vary with the size and shape of the sensitive area of detectors, even if made of the same material prepared by the same process. However, it is found (and supported by theory) that for similarly made detectors, the N.E.P. is often proportional to the square root of the area of the detector. Thus a quantity called the

area normalised detectivity, with symbol D* ('D star') and equal to (Area)$^{\frac{1}{2}}$/N.E.P., is commonly used to compare and specify detectors. From what has been stated, it will be seen that this quantity depends on the wavelength or black-body temperature of radiation used, and the frequency of measurement of signal and noise. It is therefore written as, for example, D* (5μm, 800, 1), implying a value at a wavelength of 5μm and a frequency of 800Hz, the '1' indicating the normalisation to unit bandwidth. Alternatively, if a black-body radiation source is concerned, the definition may be, for example, D* (500K, 90, 1). The dimensions of this commonly used quantity are cmHz$^{\frac{1}{2}}$W^{-1}, and, as opposed to the N.E.P., it has the merit of taking a higher value for better-performance cells.

OPTIMUM PERFORMANCE CONDITIONS

Photoconductive cells must have a bias current passed through them to make the changes of resistance appear as a voltage; photodiodes may also require bias. All the properties discussed above will vary with the bias, and an optimum bias exists for detectivity and, often, for responsivity. This bias will certainly vary with the semiconductor material used, the shape of the sensitive area, and to some small extent from detector to detector of identical construction. A typical form of variation is shown in Fig. 1.6. It

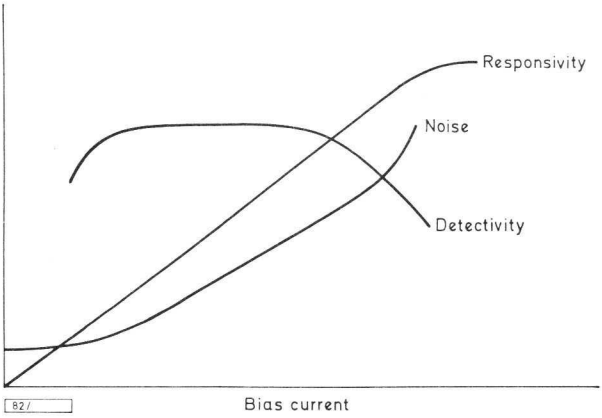

Fig. 1.6—Typical variation of detector properties with bias

will be seen that, with low bias, the noise is independent of bias, being equal to Johnson noise, while the responsivity rises linearly, hence the detectivity rises. There is a region where both vary proportionally to current, while at higher operating currents, the noise tends to rise more rapidly than linearly, and the signal less rapidly than linearly. The most suitable operating range for optimum signal-to-noise can be seen in Fig. 1.6.

PRACTICAL INFRARED DETECTORS

The detector most suitable for any given wavelength is usually one with its peak sensitivity at or only just greater than the wavelength in question. There are two reasons for this. Firstly, detectors that are sensitive to wavelengths that are much longer than are necessary require more cooling to reduce internal thermal noise. Secondly, there is a theoretical limit to the detectivity set by the amount of radiation the detector receives in its sensitive band from the thermal background radiation, usually at 300K. This radiation is noisy in nature, gives rise to a limiting noise in the detector, and limits the attainable detectivity to what is called the background limited, or BLIP, value. For wavelengths up to 10μm, this limiting value falls with wavelength, so that any sensitivity beyond the required wavelength is likely to be detrimental.

Fig. 1.7 shows this limitation, with the performance of some typical detectors that are discussed below. The materials used are stated, with the operating temperature and the field of view (F.O.V.). It will be seen that some detectors show performance above the theoretical limit. This is because they have a cooled aperture restricting their field of view and hence the amount of background radiation received.

Silicon and germanium photodetectors

Silicon and germanium, sensitive up to 1μm and 1·8μm respectively, are well-known in applications which usually require a tungsten light source. As this emits in the visible region, they are often not thought of as infrared detectors; but 90% of the radiation from a typical tungsten lamp is in the infrared region, much of it lying within the spectral bands covered by silicon and germanium.

The properties and applications of silicon and germanium photodetectors are not considered further here, except to point out that they are available as diodes or transistors, and that many specialised forms of silicon diode are available, such as cells having high operating speeds, and solar cells.

Lead sulphide detectors

Next in increasing wavelength of peak sensitivity is lead sulphide (PbS). This material must be prepared in a way very different from silicon and germanium to give good photosensitivity. It may be deposited by evaporation, in which case a small vacuum capsule is used. The layer is treated during and after deposition to give a high sensitivity. The typical detectivity D* (2·2μm, 800, 1) at the peak wavelength is 6×10^{10}cmHz$^{\frac{1}{2}}$W^{-1}.

The evaporation technique is limited in the size and shape of the elements that can conveniently be made. An alternative process is to deposit the lead

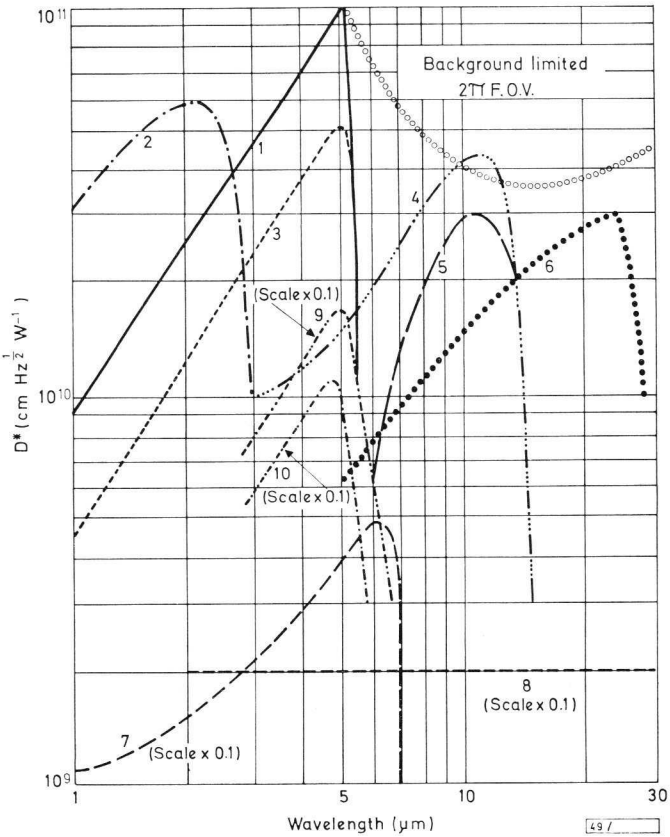

Fig. 1.7—Spectral response of infrared devices

1)	InSb 77K, 60 ° FOV	6)	Ge: Cu 4·2K, 60 ° FOV
2)	Pbs 300K, 2π FOV	7)*	InSb 300K, 2π FOV
3)	InSb 77K, 2π FOV	8)*	TGS bolometer
4)	Cd Hg Te 77K, 60 ° FOV	9)*	Cd Hg Te −80 °C
5)	Ge: Hg 35K, 60 ° FOV	10)*	Cd Hg Te 295K

* scale ×0.1

sulphide layer by chemical reaction on to a suitable insulating substrate. This allows the formation of a layer that can be cut into a wide range of shapes and sizes, including arrays of elements.

All lead sulphide cells have a high impedance (of the order of a megohm per square) and rather long time-constants (typically 100 to 400μs) compared with the other detectors considered here. In normal circumstances, PbS detectors provide adequate sensitivity at room temperature.

However, their performance may be enhanced by cooling to an optimum temperature of about −30°C (243K).

Indium antimonide detectors

The best performance from indium antimonide (InSb) is achieved by cooling to liquid nitrogen temperature (77K), when detectivities near the background-limited value can be obtained. However, indium antimonide also has many uses at higher temperatures. It is the only currently available semiconductor material that will respond to 7μm at room temperature.

Photoconductive detectors are made from doped single crystals, prepared in a way similar to that used for germanium and silicon. These crystals are then cut into elements of the required size and made as thin as possible. At room temperature, the resistivity is low, giving detectors with resistances of about 5Ω/square. The most useful forms are thus either long thin strips, or areas made up of a number of such strips laid in parallel but connected electrically in series. The effect of temperature on performance is rather large at these temperatures, and a good heatsink is required for the element. Cooling to, say, 0°C gives improved performance, and these detectors are ideally suited to thermoelectric refrigeration. The response time is very short (about 50ns) and the detectivity D* (6μm, 800, 1) is up to 8×10^8cm $Hz^{\frac{1}{2}}W^{-1}$.

Cooled detector elements are made in a similar way, the main difference being in the doping of the single crystal material. The sensitive element must be mounted in an enclosure suitable for cooling. This is usually a small glass dewar vessel with infrared transmitting window, and the cooling may be achieved either by using liquid nitrogen at 77K (either simply pouring liquid nitrogen into a vessel, or using a liquid nitrogen transfer system for continuous operation) or by means of a miniature Joule-Thomson expansion liquefier.

Cooling increases the resistance to a more convenient value (about 2kΩ/square) and elements covering a wide range of shapes and sizes may be made. This includes arrays of elements as small as 100μm square with as many as 100 in one assembly. Detectors are 'background limited', hence the use of a cooled aperture as part of the assembly improves the detectivity. Without such apertures, a value of D* (5·3μm, 800, 1) of 5×10^{10}cm $Hz^{\frac{1}{2}}W^{-1}$ is achieved. With a restricted field of view, values of over 1×10^{11}cm $Hz^{\frac{1}{2}}W^{-1}$ are possible.

Mercury cadmium telluride detectors (MCT)

For wavelengths beyond 5 to 7μm it has been necessary to rely on doped germanium detectors which require cooling to below liquid nitrogen temperatures. Recent developments, however, have led to the use of a

mixed crystal of cadmium telluride and mercury telluride which can be made to have a peak response over a range of wavelengths depending on the ratio of cadmium to mercury. The particular interest in this material is for detectors matching the 8 to 13μm atmospheric window. This wavelength range includes the peak of radiation from 300K sources at 10μm, and also the CO_2 laser radiation at 10·6μm. This material has the advantage that operation approaching the background limit is obtainable at 77K (liquid nitrogen temperature), hence the cooling techniques available for InSb detectors can be applied.

Elements are made by techniques similar to those used for InSb, and the elements are mounted in similar dewars, with the difference that a window transparent in the 8 to 13μm range is required. For this purpose, silicon with an antireflection coating is very suitable.

The resistance of elements is typically lower than that of InSb, for example 20 to 100Ω for a square element; but this does not create serious problems as the noise level is substantially above Johnson noise. As stated above, detectors can be background limited, and detectivities of up to 8×10^{10}cm $Hz^{\frac{1}{2}}W^{-1}$ at 10μm with a 60° cooled aperture are possible.

Current developments are concerned with the use of mercury cadmium telluride at other wavelengths. If the cadmium to mercury ratio is adjusted to give a response peaking at 5μm at 300K operating temperature, peak detectivities greater than that of InSb (at the same temperature) by a factor of 5 have been achieved. It is possible that this mixed crystal may thus replace InSb in applications requiring high detectivity but not allowing of cooling.

Doped germanium detectors

In doped germanium detectors the radiation is absorbed by electrons in the impurities, and this leads to a lower absorption coefficient, hence the need for thicker specimens. It is also essential to cool the element so that the electrons are initially in the impurity centres ready to be excited.

The germanium must be extremely pure apart from the intentionally added impurities. Mercury and copper are the two most widely used additives. Mercury responds to 14μm and requires cooling below 40K. This can be done with liquid hydrogen produced by a Joule-Thomson liquefier, or by using liquid helium or neon. Another method of cooling is to use a closed-cycle expansion engine working with, for example, helium. Copper responds to 25μm, and requires a temperature below 10K, achieved with liquid helium. In both cases, a wide range of element sizes and shapes is possible. A cooled aperture is usually essential, and with a field of view of 60°, peak wavelength detectivities of over 10^{10}cm $Hz^{\frac{1}{2}}W^{-1}$ are obtained.

Indium antimonide extrinsic detectors

For specialised applications of infrared radiation beyond 50μm, detectors have been developed which are faster than thermal detectors. One such device uses impurity levels in indium antimonide, giving a very low activation energy. It is necessary to operate such devices at a temperature below that of helium boiling at atmospheric pressure, so the helium must be in a low-pressure container. The response of such devices extends through to the submillimetre and microwave regions.

Pyroelectric bolometers

Of the many effects used to make bolometers, the pyroelectric effect is the most recent, and one that allows improvements in bolometer performance. The pyroelectric effect occurs in certain crystals with a complex structure in which there is an inbuilt electrical polarisation which is a function of temperature. Changes of temperature therefore result in changes in the charge at the surface of the crystal which can be detected by a high-impedance amplifier. Many crystals show this effect, but the most useful known at present is triglycine sulphate $(NH_2\ CH_2\ COOH)_3\ H_2\ SO_4$—known as TGS.

In most other thermal detectors, operation is usually at frequencies below that set by the thermal time-constant, but in the pyroelectric detector, frequencies above that value are used. This is because, though the signal output will fall with frequency, so will the noise, and a constant signal-to-noise ratio is obtained. The performance is largely limited by amplifier noise which will limit the frequency range of constant signal-to-noise when the noise voltage generator of the amplifier becomes significant. This frequency will depend on the sensitive area, and can be in the range 1 to 10kHz.

Because of the high impedance of the detector element (essentially a capacitor) and the importance of amplifier noise, detectors are made with integral amplifiers.

The pyroelectric bolometer can have essentially constant detectivity over the wavelength range from 2μm to some hundreds of micrometres, depending on the window material used; and detectivities of over 10^8 cm $Hz^{\frac{1}{2}}W^{-1}$ are achieved with sensitive areas between 0·4mm^2 and 15mm^2.

This type of detector, with good detectivity and frequency response and the ability to operate without cooling, has many applications in thermal detection (where the sensitivity to 10μm is used) and in spectrometry and gas analysis, using the large wavelength coverage.

APPLICATIONS OF INFRARED DETECTORS

The range of infrared detectors now available gives coverage of the whole infrared spectrum. Although the applications of these detectors are numerous, they fall into two general classes. One depends on the properties of black-body radiation for purposes of measurement and control; the other depends on the optical properties of materials (solid, liquid, and gaseous) in the infrared region as aids to analysis and control. These two classes are discussed below.

BLACK-BODY OBJECTS

In the first class, the applications use the black-body emission which is emitted from all objects at temperatures above absolute zero. Fig. 1.8 shows the distribution of energy from black bodies at three temperatures, the rapid increase in total radiation, and the shift of the peak of the energy distribution to shorter wavelengths. The useful spectral ranges of the types

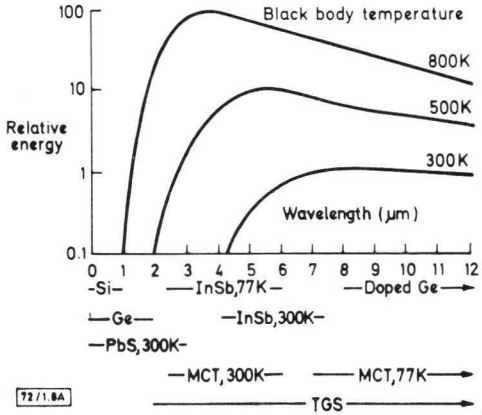

Fig. 1.8—Energy distribution from a black body at three temperatures

of detector most commonly available are also shown in Fig. 1.8. The graph indicates the desirability of choosing a detector to match the spectral output of the source of interest. For example, for a source at 300K a detector responding to at least 10μm is desirable although, for practical reasons, a detector of, say, indium antimonide may be preferred. A lead sulphide detector is unlikely to be of any use.

A detector responding in the correct wavelength region can be used in three types of application. It can be used for detection of an object, measurement of its temperature, or formation of a thermal picture. These will be considered in turn.

Detection

It is obvious that the emission from the object of interest must be different from that of the background by a significant amount. This clearly occurs with what are known as 'hot 'bodies (for example, a flame), but difficulties may be encountered with objects near room temperature.

Some objects, assumed here to approximate to a black body, are listed in Table 2 with their radiation outputs indicated. Whether or not one of these objects can be detected against the room temperature background

TABLE 2

Radiation from various objects

Object	Temperature	Total radiation	Radiation between 0 and 5μm
	(°C)	(W/m^2)	(W/m^2)
Ice	0	320	2·2
Room temperature	22	430	5·2
Human face	34	505	7·7
A cup of tea	60	700	24·5

depends on whether or not enough of the radiation can be focused onto the detector to give a change of signal greater than the noise of the detector and amplifier, and greater than any extraneous noise. It might be necessary, therefore, to use a large aperture in the collecting optical system for the greatest sensitivity. A narrow bandwidth, giving a long response time, will decrease the noise and lead to a greater sensitivity. It will also be necessary to detect a change in the output to indicate the presence of the object. Such a system can be made either to detect the passing of objects whose temperatures are within a few degrees of the background temperature or, by scanning the optical system over the scene, to detect a stationary object. The principles of the system are shown in Fig. 1.9

Some of the phenomena detected by such systems are: unauthorised presence of human beings, the occurrence of an overheated part of a mechanical system (overheated axle-boxes on trains, for example), the difference between fertile and infertile eggs coming out of an incubator, or the presence of hot spots on overhead cables.

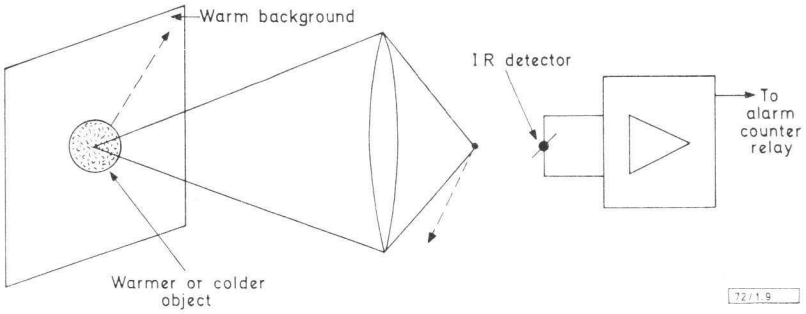

Fig. 1.9—Detection of moving object with temperature different from that of the background

With objects at significantly higher temperatures than the background it is not necessary to detect the difference between the radiation from the object and its background, but just to set the system to respond to a given radiation input.

Another approach to detection is possible if the emission is fluctuating, as in the case of many flames. Then an a.c. coupled amplifier can be used to respond to the fluctuation frequency of the emission.

There are many extensions to the techniques mentioned. For example, the output may be used for counting, to control a servo-system in a tracking mode or, with two channels, to measure time intervals and hence speed.

Temperature measurements

To attain the accuracy essential for temperature measurement by means of the emitted infrared radiation, it is usually necessary to measure the difference in detector output when viewing the object and a reference source alternately. This is because the voltage across the detector is usually a function of the temperature of the detector itself, as well as that of the object being viewed, and drifts in the detector temperature could mask the output produced by the object. The measurement of the difference between the test source and the reference can be effected by using a radiation chopper, often a rotating segmented disc. In this case, the output a.c. signal is related to the difference between the emission of the object and that of the chopper blade. For objects above 100°C, the radiation from a room-temperature chopper can usually be ignored, although this depends to some extent on the wavelength response of the detector used. For lower temperatures, the output is related to the difference between

object temperature and chopper blade temperature unless the image of a reference source is reflected by the chopper blade back onto the detector when the object is obscured. Fig. 1.10 illustrates a simple system.

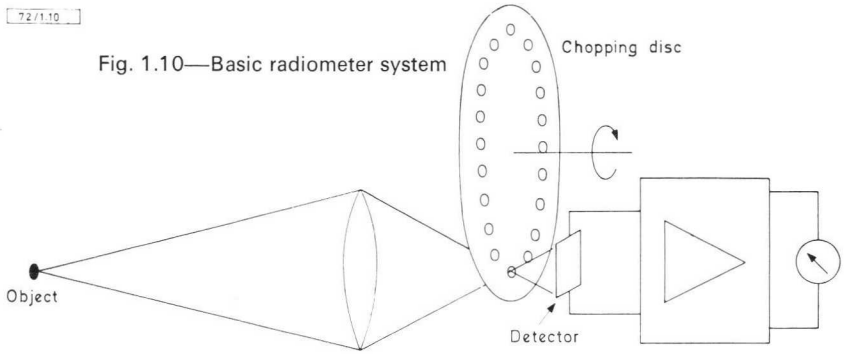

Fig. 1.10—Basic radiometer system

Chopping the radiation has the further advantage that a.c. amplifiers can be used, and the bandwidth can be limited to reduce the noise. The frequency of chopping can be chosen so that the noise figure of detector and amplifier is lowest.

It may be necessary, for absolute measurements, to take account of the fact that the emissivity of the object is not unity. However, because of the rapid change of emission with temperature, the absence of such a correction does not always have a very marked effect on the temperature indicated.

The advantages of radiation measurements of temperature lie primarily in the fact that no contact need be made with the object under investigation. Thus the temperature of the object is not seriously disturbed, and moving objects present no difficulty. Furthermore, in many cases, no special surface preparation is necessary, unless the surface has a very low emissivity.

The applications for these techniques are too numerous to list here. Two extreme examples may be mentioned; these are the determination of temperatures of parts of integrated circuits in operation, and the measurement of the temperatures of blast furnace walls.

Thermal imaging

The need for thermal imaging frequently arises when the location of those parts of an object where the temperature is of interest are not known or specified. Measurements could be made point by point with a radiometer, but it is often more convenient or essential to have a picture of the emission differences, and hence of temperature differences, presented directly. Thus there is considerable interest in devices that give such thermal pictures.

The requirement may be for an indication of the hot areas, or for actual

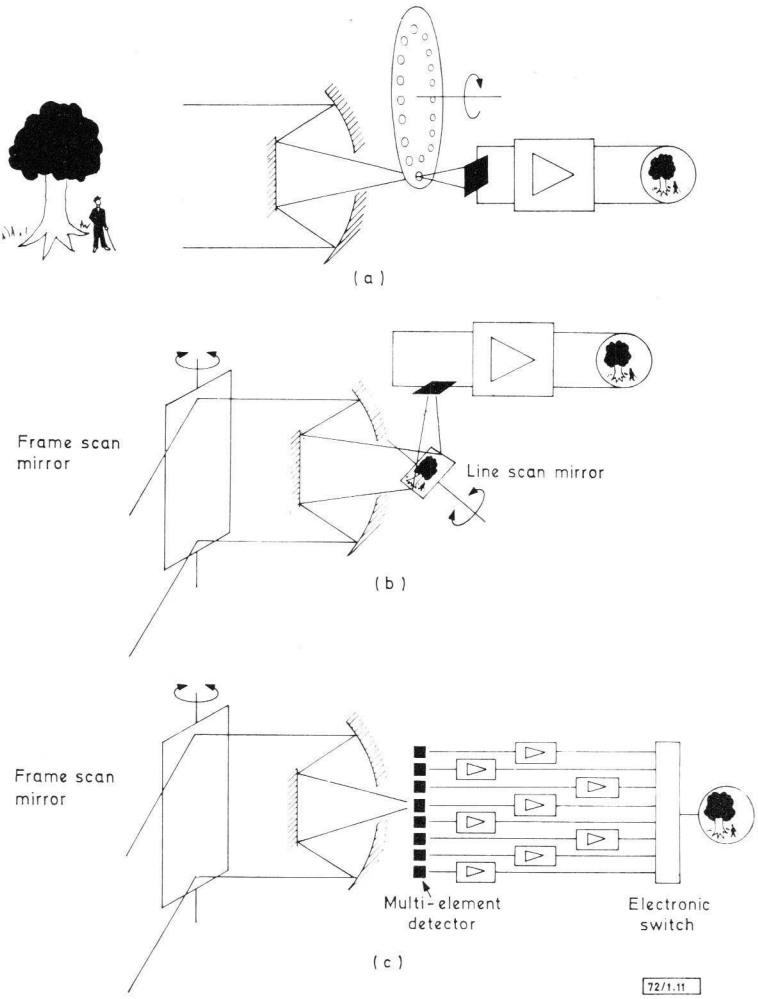

Fig. 1.11—Methods of obtaining information for television display
a) Nipkow disc scanner
b) Double mirror scanner
c) Multi-element detector scanner

temperature measurements of selected points in the picture. A television type of display tube is the most convenient method of displaying the picture. The information to make up this picture can be obtained in a number of ways, as illustrated in Fig. 1.11. One technique scans an image

(produced by lens or mirror system) by means of a disc containing a spiral of holes known as a Nipkow disc. A detector behind the disc generates an electrical waveform which can be used as the video signal for the display. In a second system, the image of the scene is made to move in a television-raster type of movement over a small detector by the synchronised movements of two mirrors giving line and frame scans. In a third method, greater sensitivity may be achieved by using an array of detectors, one to give each line of the picture, with electronic switching to give the required waveform.

The most well-known application for these techniques is in the medical field, but many industrial applications have also been proposed and tried.

INFRARED ABSORPTION ANALYSIS AND CONTROL

The applications considered above all depend on differences in the emission from objects. Another large class of applications depends on the change of absorption produced by materials, in either the solid, liquid, or gaseous form. The field of chemical analysis by infrared absorption spectroscopy is now well known. It depends on the fact that the absorption, particularly of organic materials, is characteristic of a particular compound or type of chemical structure. Application of such techniques outside the laboratory is expected to grow rapidly with the availability of rugged and sensitive semiconductor detectors. Improvements of sensitivity, speed of response, and wavelength coverage are expected to widen still further the scope of this type of measurement. Much work is being done to improve gas analysis, which must often be performed in situ and must give a rapid read-out. Such measurements are of growing importance in control systems as widely varied as those for power station exhaust gases, and anaesthetics. Other applications, not requiring on-line control, include detecting leaks in piped gas systems or hermetically sealed electronic equipment.

COMPARISON OF CELL PARAMETERS

The Table on pp 24 and 25 compares the major electrical parameters of nine commonly-used types of photoconductive detector.

The two lines showing different types of signal/noise ratio enable a comparison to be made of different detectors in various types of optical system.

The line relating to constant total radiation of 1μW implies that in this case the smaller detectors are subject to a greater radiant excitance (W/m^2). This is the case when the optical system is focusing the total radiation (watts) on to the cell area. In such a system a smaller area cell will produce a higher signal. It must be remembered, however, that

higher quality optics are required in order to utilise this effect.

In the line relating to constant intensity of $1\mu W/cm^2$ the total radiant power (watts) on each cell under consideration is varying directly as its area. Thus where the optics remain unchanged, and different types of detector are inserted in the field, this will be the relevant column for signal/noise comparison.

'Black-body temp. at λ_{pk}' is the black-body source temperature which has peak emission coincident with the peak response of the detector. It is a rough indication of the type of source for which the detector is appropriate.

Figs. 1.12 to 1.17 give additional information relating to infrared technology.

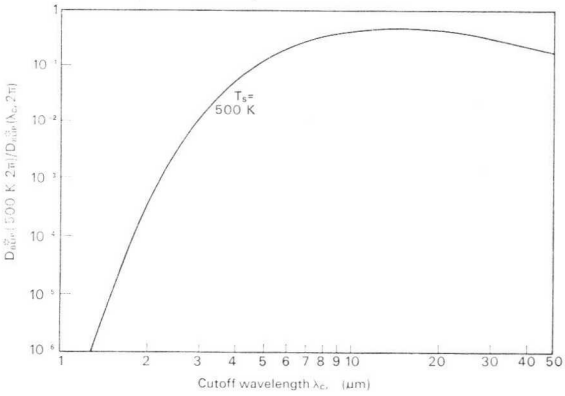

Fig. 1.12—Variation of black-body detectivity to monochromatic detectivity versus cut-off wavelength for photon detectors

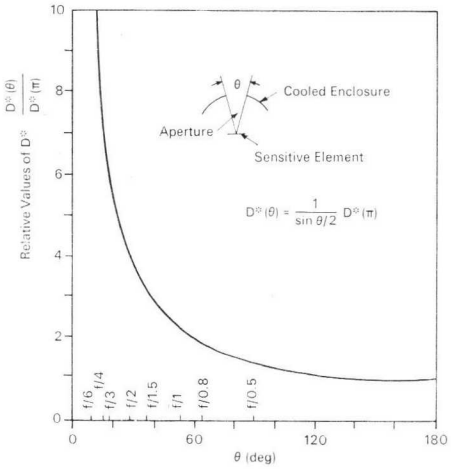

Fig. 1.13—Theoretical dependence of D* on angular field of view for background limited detectors

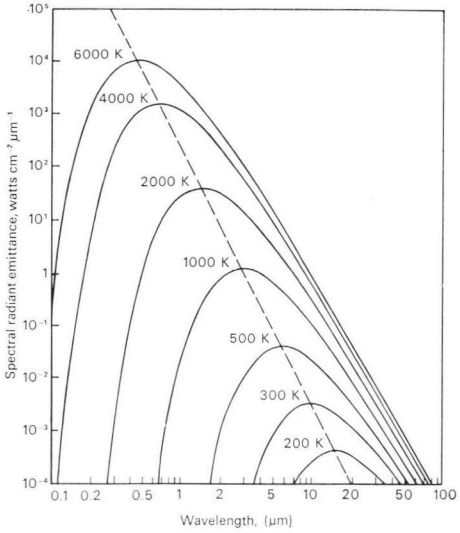

Fig. 1.14—Spectral radiant emittance of a black body as a function of wavelength at various temperatures. The maximum spectral radiant emittance at a given temperature falls on the broken line.

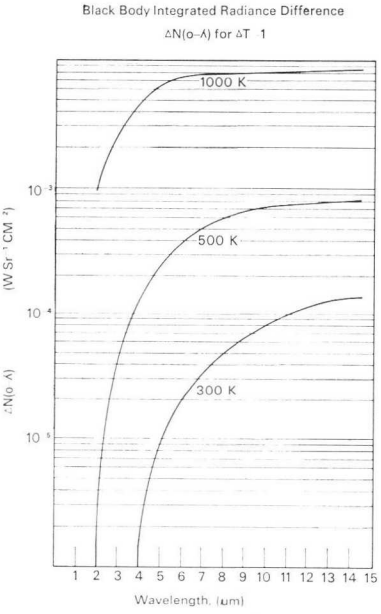

Fig. 1.15—Black-body integrated radiance difference

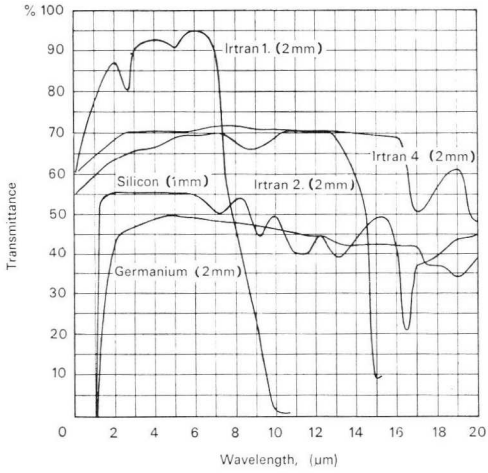

Figs. 1.16(a) and (b)—Spectral transmission of commonly used materials

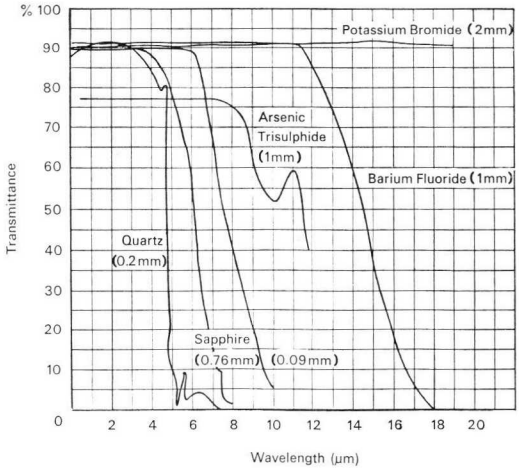

Fig. 1.17—Spectroscopic energy conversions

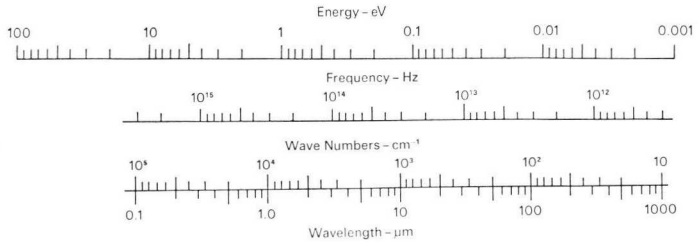

INFRARED DETECTOR PARAMETERS

Cooled types: 77K

	InSb RPY51	InSb RPY56	InSb ORP13	MCT	
$R_{cell(min)}$	1·2k	130	20k	20	Ω
$R_{cell(max)}$	3·5k	350	60k	1k	Ω
I_{bias}	0·7	10	1·0	10	mA
P_{bias}	10	20	40	10	mW
V_s	9×10^{-3}	125×10^{-6}	7×10^{-3}	$0{\cdot}5\times10^{-3}$	V
V_s'	$22{\cdot}5\times10^{-6}$	38×10^{-6}	210×10^{-6}	$0{\cdot}26\times10^{-6}$	V
I_s	4×10^{-6}	$0{\cdot}5\times10^{-6}$	$0{\cdot}175\times10^{-6}$	6×10^{-6}	A
V_n	26×10^{-9}	17×10^{-9}	112×10^{-9}	$2{\cdot}4\times10^{-9}$	$VHz^{-\frac{1}{2}}$
V_s/V_n	350×10^3	7×10^3	65×10^3	210×10^3	—
V_s'/V_n	866	$2{\cdot}2\times10^3$	$1{\cdot}9\times10^3$	110	—
Rise-time	2·5	4·8	5·0	1·0	μs
λ_{pk}	5·3	5·3	5·3	9·5 to 15	μm
Black-body temp. at λ_{pk}	275	275	275	+30 to −80	°C
Element dimensions	0·5×0·5	8×5	6×0·5	0·23×0·23	mm

R_{cell} = cell resistance

I_{bias} = optimum bias current

P_{bias} = bias power at I_{bias}

V_s = open-circuit signal voltage for 1μW of incident black-body radiation

INFRARED DETECTOR PARAMETERS
Uncooled types: room temperature

	InSb ORP10	InSb RPY77	InSb RPY79	PbS 61SV	PbS RPY75/76	
$R_{cell(min)}$	30	500	100	1M	0·2M	Ω
$R_{cell(max)}$	120	1·5k	300	4M	1M	Ω
I_{bias}	55	10	10	0·02	0·06	mA
P_{bias}	225	80	20	1·6	2·5	mW
V_s	$0{\cdot}3\times10^{-6}$	$1{\cdot}7\times10^{-6}$	$1{\cdot}7\times10^{-6}$	$1{\cdot}3\times10^{-3}$	$1{\cdot}2\times10^{-3}$	V
V_s'	9×10^{-9}	68×10^{-9}	17×10^{-9}	470×10^{-6}	12×10^{-6}	V
I_s	4×10^{-9}	$2{\cdot}6\times10^{-9}$	$8{\cdot}5\times10^{-9}$	$0{\cdot}9\times10^{-9}$	2×10^{-9}	A
V_n	$1{\cdot}0\times10^{-9}$	7×10^{-9}	7×10^{-9}	$1{\cdot}2\times10^{-6}$	$1{\cdot}2\times10^{-6}$	$VHz^{-\frac{1}{2}}$
V_s/V_n	300	243	243	1×10^3	1×10^3	—
V_s'/V_n	9	10	2·4	400	10	—
Rise-time	0·1	0·1	0·1	100	250	μs
λ_{pk}	6·2	5 to 7	5 to 7	2·2	2·2	μm
Black-body temp. at λ_{pk}	190	300 to 140	300 to 140	1050	1050	°C
Element dimensions	$6\times0{\cdot}5$	2×2	1×1	6×6	1×1	mm

V_s' = open-circuit signal voltage for 1μW/cm² incident black-body radiation

I_s = short-circuit signal current for 1μW of incident black-body radiation

V_n = noise voltage

All figures are typical

CHAPTER 2

BIASING AND AMPLIFYING TECHNIQUES FOR PHOTOCONDUCTIVE DETECTORS

The biasing and amplifying methods that are adopted for use with photoconductive detectors can have a considerable effect on the environmental stability of the system. The stability of equipment performance will also be affected by variations of detector parameters due to production tolerances.

There are three different methods of biasing photoconductive detectors:

1) Constant current.
2) Constant voltage.
3) Constant power.

Each of these methods maintains the appropriate electrical quantity approximately constant over a wide range of cell resistance. Each method will have a particular effect on system performance.

The input impedance of the following amplifier will also have a significant effect on system performance. This impedance can be either much higher than cell resistance (voltage amplification) or much lower than cell resistance (current amplification).

Each combination of biasing method and amplifier impedance will have a specific effect on system stability.

To understand the effects of different methods of biasing and amplifying, three facts concerning photoconductive detectors must be noted:

1) Responsivity is approximately proportional to the square of cell resistance.
2) Responsivity is approximately linear with bias current.
3) The peak of the cell signal-to-noise curve occurs at approximately the same bias power for every cell of a given type.

If we first consider the combination of constant current bias and a voltage amplifier, it can be seen from fact (1) that the output of the system will vary directly with responsivity variation. In other words, changes in detector resistance will have no effect on bias current or amplifier gain. If a current amplifier were used, then the gain of the amplifier would increase as the reciprocal of cell resistance. This would reduce the effects of changes of cell responsivity. If, also, constant voltage bias were used then changes in cell resistance would produce changes in cell bias current. This again would tend to reduce the effects of varying cell responsivity (see fact 2). Each of these two methods will alter the output from the system by a factor $1/R_{cell}$. The two used together will increase this to a factor $1/R_{cell}^2$. Hence the combination tends to minimise the cell characteristic described in fact (1).

Fact (3) can be utilised in systems where constant signal-to-noise ratio is of greatest importance. This is achieved by employing a constant power biasing system.

Some practical methods of obtaining the different forms of bias are discussed and analysed in the following section.

EVALUATION OF BIASING METHODS

Constant current

The simplest approximation to a constant current bias system is when the bias voltage source is applied to the detector cell through a resistor of high value compared with cell resistance variation. By choosing a value of resistor that is higher than the cell resistance, noise contribution from the resistor is minimised.

The bias current can be selected to give optimum signal-to-noise performance for the particular cell to be used. This is a most likely situation for cooled cells where the temperature is constant, and usually a test certificate is supplied with each cell quoting optimum bias current.

When a spread of cell resistance has to be considered, then variations of signal and signal-to-noise ratio must be tolerated. If the bias is chosen for a typical cell, then cells with a higher resistance value will produce a higher signal and noise level, but the signal-to-noise ratio is degraded. Lower resistance cells will again produce degraded signal-to-noise ratio, and both signal and noise will be at a reduced level.

By using a low-impedance input amplifier the variation of signal and noise level will be reduced, but the signal-to-noise ratio will still suffer the same deterioration.

The gain of this type of system will vary as $1/R_{cell}$.

The noise voltage V_n produced by this biasing system is given by

$$V_n = \frac{R_{cell}\sqrt{(4kTBR_B)}}{R_B + R_{cell}}. \qquad \text{(see Fig. 2.1a)} \qquad ..(1)$$

Evaluating this for an RPY51 detector fed through an R_B of 20kΩ gives a value of $V_n = 0{\cdot}6 \times 10^{-9}$ VHz$^{-\frac{1}{2}}$. This is negligible compared with cell noise which is of the order of 15×10^{-9} VHz$^{-\frac{1}{2}}$.

With high-resistance detectors requiring quite high currents for optimum bias this may not be a convenient method, and a transistor can be used as shown in Fig. 2.1b. The noise voltage V_n generated by this circuit is

$$V_n = R_{cell}\sqrt{\left(e_n^2/R_e^2 + i_n^2 + \frac{4kTB}{R_e}\right)} \qquad \text{(see Fig. 2.1b)} \qquad ..(2)$$

where e_n and i_n are the equivalent noise generators of the transistor, and

$$e_n^2 = 2kTBr_e + 4kTBr_b \qquad i_n^2 \simeq 2kTB/h_{fe}r_e.$$

B = bandwidth k = Boltzmann's constant.

An RPY51 biased at 0·7mA and with a BC109 transistor in the circuit of Fig. 2.1b gives a noise voltage of 6×10^{-9} VHz$^{-\frac{1}{2}}$. The above equations are calculated on the assumption that the cell is noiseless. Therefore to calculate the effective noise figure with a typical detector in circuit the following expression can be used.

$$\text{N.F.} = \frac{V_n^2 + V_{n(cell)}^2}{V_{n(cell)}^2}. \qquad ..(3)$$

Constant voltage

If minimum variation of signal level with variation of detector resistance is of prime importance, then constant voltage bias followed by a current amplifier would be recommended. The simplest method of achieving this is with the circuit of Fig. 2.1c. This will give as good a signal-to-noise performance as a constant current bias system followed by a voltage amplifier if both the transistor and the cell are working at optimum current. Since the transistor emitter current is also the cell bias current, this optimum may be difficult to achieve.

This method of biasing and amplifying produces a responsivity correction factor of $1/R_{cell}^2$. This should maintain a reasonably constant voltage signal at the amplifier output despite changes in the value of R_{cell}. Signal-to-noise ratio will, however, be degraded in the case of cell resistance values above and below the chosen datum. If the system is designed on a resistance datum level which is the harmonic mean of the total expected variation, then bias power will vary symmetrically about the datum.

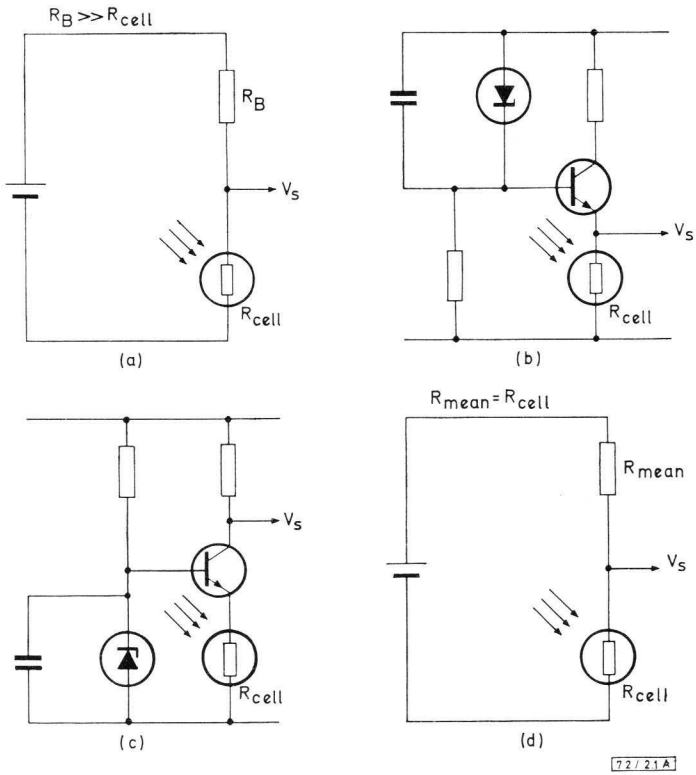

Fig. 2.1—(a) Constant current bias system
(b) Constant current bias with transistor
(c) Constant voltage bias system
(d) Constant power bias system

The noise contributed by the transistor in this circuit is given by

$$V_n = \sqrt{(i_n^2 R_{cell}^2 + e_n^2)}.$$

With an RPY51 detector and a BC109 transistor, typical values put in this equation give a noise voltage of 7×10^{-9} $VHz^{-\frac{1}{2}}$.

This is a much higher value of noise than with passive biasing, but the circuit can generally have a voltage gain of about ten so that subsequent amplification will cause very little degradation of noise figure.

Constant power

Where constancy of signal-to-noise ratio is the prime consideration, constant power biasing is recommended. The effect is achieved by feeding

Type of bias	Amplifier Z_{in}	Compensation for R_{cell} variation	Major virtue	Signal-to-noise ratio	Source of noise (denominator)	Circuit Fig. No.	Stability of bias power for R_{cell} variation*	Bias power % change for 3:1 R_{cell} change
Constant current	Low	$\propto R$	Low noise	$\frac{V_s(R_C+R_B)}{R_C\sqrt{(4kTBR_B)}}$	Bias resistor	2·1a	$\frac{R_{C1}}{R_{CC}}$	± 50
Constant current	High	None	Low noise	$\frac{V_s}{\sqrt{[(i_nR_C)^2+e_n^2]}}$	Voltage amplifier	2·3	$\frac{R_{C1}}{R_{CC}}$	
Constant voltage	Low	$\propto R^2$	Signal stability	$\frac{V_s}{\sqrt{[(i_nR_C)^2+e_n^2]}}$	Transistor	2·1c	$\frac{R_{CC}}{R_{C1}}$	± 50
Constant voltage	Low	$\propto R^2$	Signal stability	$\frac{V_s}{R_C\sqrt{\left(i_n^2+\frac{e_n^2}{R_b}+\frac{4kTB}{R_B}\right)}}$	Transistor and bias resistor	2·4	$\frac{R_{CC}}{R_{C1}}$	
Constant power	Low	$\propto R^{1.5}$	Signal-to-noise stability	$\frac{V_s}{\sqrt{(4kTBR_B)}}$	Bias resistor	2·1d	$\frac{4R_{CE}R_{C1}}{(R_{C1}+R_{CC})^2}$	-6
Constant power	High	None	Signal-to-noise stability	$\frac{V_s}{\sqrt{(4kTBR_B)}}$	Bias resistor	2·1d	$\frac{4R_{CE}R_{C1}}{(R_{C1}+R_{CC})^2}$	

$R_C = R_{cell}$ = cell resistance
R_b = total external base resistance
R_{C1} = one extreme of production spread of R_C

R_{CC} = mean of R_C variation (arithmetic mean for constant current cases, harmonic for constant voltage, geometric for constant power)

V_s = open-circuit cell voltage signal

*factor for calculation of bias power when $R_C = R_{C1}$

the cell bias current through a resistor of value equal to the geometric mean of the expected cell resistance variation (Fig. 2.1d).

Biasing by this method will mean a larger noise contribution from the bias resistor. The equation for bias noise is the same as Eq. 1, but of course R_B is a lower value and V_n is higher. With an RPY51 detector the bias noise voltage is $2{\cdot}5 \times 10^{-9}$ $VHz^{-\frac{1}{2}}$. This noise could be reduced in many applications by the introduction of a choke or LC filter in series with the bias resistor.

A constant power bias system should be followed by a current amplifier. This prevents attenuation of voltage signals by the bias resistor and helps to stabilise the signal level. With this system the responsivity correction factor will be about $1/R_{cell}^{1{\cdot}5}$. Thus correction is not quite as good as with the constant voltage bias circuit followed by a current amplifier.

The Table on page 30 summarises the effect of various combinations of biasing method and high and low amplifier input impedances. It also summarises the noise contribution of each biasing method, and in the last two columns indicates how a centre value of cell resistance should be chosen for minimum parameter variation.

BIASING AND AMPLIFIER CIRCUITS

The next twelve pages give practical biasing systems and amplifier circuits for the commonly-used cooled and uncooled detectors whose parameters are given on pages 24 and 25.

Cell type		Description Page No.	Fig. No.
Cooled	Uncooled		
RPY51 constant power biasing		32	2·2
RPY51 constant current biasing		32	2·3
RPY56		34	2·4
ORP13		34	2·5
MCT		36	2·6
	ORP10	38	2·7
	RPY77	38	2·8
	RPY79	40	2·9
	61SV	40	2·10
	RPY75/76	42	2·11
	RPY75/76	42	2·12

COOLED DETECTORS

Circuits are given for several types of cooled detector.

Amplifiers for RPY51

Fig. 2.2 shows a constant power biasing system followed by a current amplifier (low input impedance). This system is designed to give an acceptable noise performance and a high voltage gain, and to be optimised for signal-to-noise ratio with all detectors of the RPY51 specification.

Noise generated by the amplifier and biasing resistor R_B referred to the amplifier input is given by:

$$V_n = \frac{R_{cell}}{R_{fb}} \sqrt{\left(KR_{fb} + i_n^2 R_{fb}^2 + e_n^2 \frac{(R_{fb}+R_b)^2}{R_b^2} + \frac{KR_{fb}^2}{R_B} \right)} \quad \ldots(4)$$

where

$K = 4kTB$

R_b = total external resistance at the transistor base.

Amplifier performance is as follows:

Voltage gain	250 typ. (designed to vary with cell resistance)
Current gain	21
Input impedance	80Ω
Output impedance	27kΩ
Bandwidth	1MHz
Noise voltage V_n	15×10^{-9} $VHz^{-\frac{1}{2}}$ (From Eq.4)
Noise figure with typical cell	3dB

The circuit of Fig. 2.3 shows a constant current biasing arrangement followed by a voltage feedback amplifier. In this system noise contribution from the biasing resistor and amplifier is less than in the circuit of Fig. 2.2. There is, however, no compensation for different values of cell resistance.

Amplifier and bias resistor noise referred to the input of the amplifier is given approximately by:

$$V_n \simeq \sqrt{\left(e_n^2 + i_n^2 R_{cell}^2 + KR_B \left(\frac{R_{cell}}{R_B + R_{cell}} \right)^2 + KR_e \right)} \quad \ldots(5)$$

when $R_{cell} \ll$ amplifier input impedance.

The performance of this system is as follows:

Voltage gain	250
Input impedance	40kΩ
Output impedance	1kΩ
Bandwidth	>1MHz
Noise voltage V_n	6×10^{-9} $VHz^{-\frac{1}{2}}$
Noise figure with typical cell	0·8dB

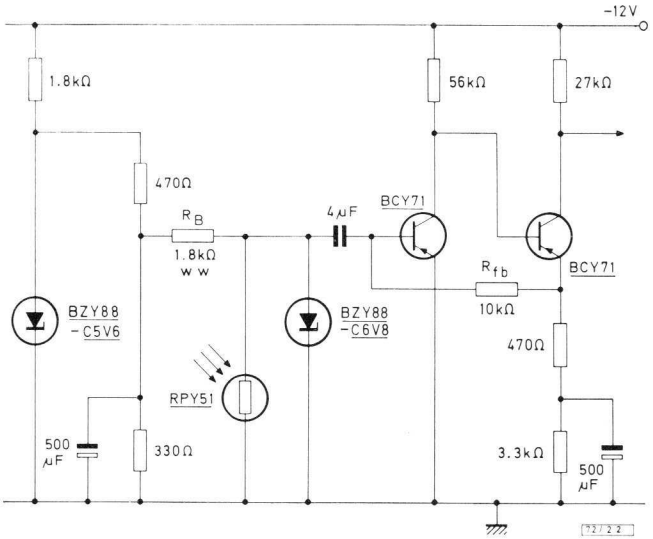

Fig. 2.2—Constant power bias system followed by current amplifier for RPY51

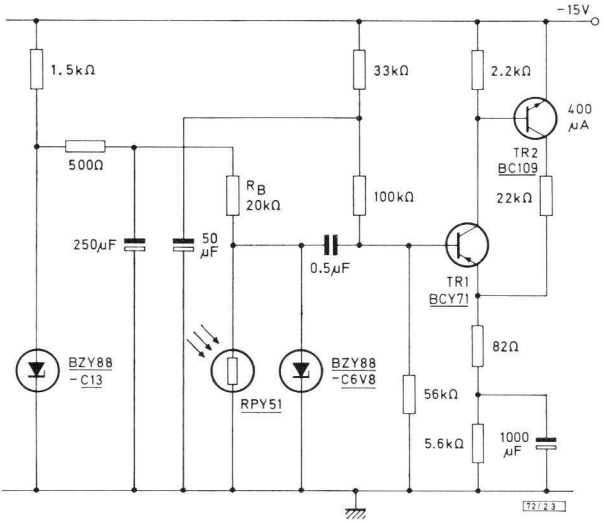

Fig. 2.3— Constant current bias system followed by voltage feedback amplifier for RPY51

Constant voltage bias circuit for RPY56

A constant voltage bias circuit for use with the RPY56 is shown in Fig. 2.4. The cell is placed in the emitter of TR_2, the base of which is taken to a regulated voltage. However, because of the high value of bias current required by the RPY56 (10mA approx), transistor TR_2 does not supply all the biasing current to the cell. As TR_2 is biased to a collector current of about 1 mA, it is working at a reasonably low noise level; the input impedance at TR_2 emitter is also sufficiently low for good current transfer from the cell. This value of collector current also enables a suitably high value of collector load to be used, giving the stage a typical voltage gain of 50. The main bias current is provided by TR_1. The noise generated by this stage is shunted off by C_1. Thus the only significant noise contributed by the stage is that generated by R_B.

The total noise generated by the transistors and resistor R_B is given by:

$$V_n = \sqrt{\left(\frac{KR_{cell}^2}{R_B} + i_n^2 R_{cell}^2 + \frac{e_n^2(R_B + R_{cell})^2}{R_B^2}\right)} \qquad \ldots(6)$$

System performance is as follows:

Voltage gain	50 typ. (designed to vary with cell resistance)
Current gain	unity
Input impedance	25Ω
Output impedance	10kΩ
Bandwidth	>1MHz
Noise voltage	8×10^{-9} VHz$^{-\frac{1}{2}}$
Noise figure with typical detector	3dB

Circuit of constant power bias type suitable for ORP13

A circuit of the constant power bias type for use with the ORP13 is shown in Fig. 2.5. Since the ORP13 is a high-resistance type, the emitter current of the first transistor of the amplifier must be very low. Transistors of the BC109 series are most suitable for operation at low emitter currents.

In the circuit of Fig. 2.5, TR_1 is biased to a collector current of 30μA, which is near optimum for noise figure when a source impedance of 20kΩ is considered. The ORP13 detector is biased directly through a resistor of value equal to the mean value of expected cell production spreads. Thus near-optimum bias conditions will be obtained with any production ORP13.

This circuit is of the same type as that shown in Fig. 2.2, and the noise voltage of the amplifier and biasing resistor referred to the input can be calculated from Eq. 4.

Owing to the very low transistor operating current and the high value of feedback resistor (compared with the similar circuit of Fig. 2.2), the emitter

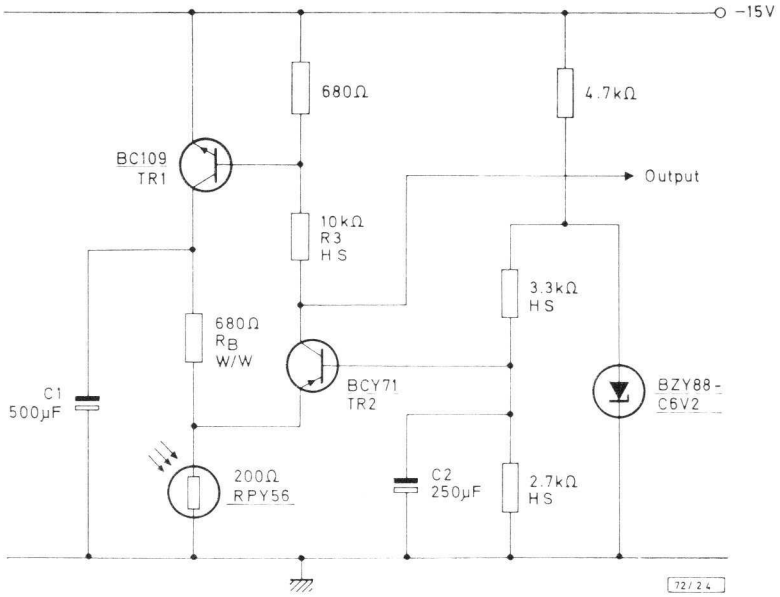

Fig. 2.4—Constant voltage bias system for RPY56

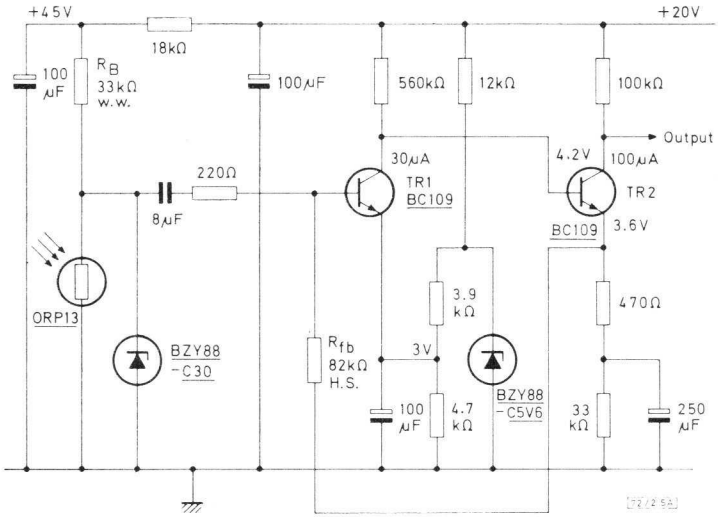

Fig. 2.5—Constant power bias system for ORP13

voltage of TR_1 has been raised. This enables a greater degree of d.c. feedback to be employed, thus improving stability of the working point.

System performance is as follows:

Voltage gain	400 typ. (designed to vary with cell resistance)
Current gain	175
Input impedance	3kΩ
Output impedance	100kΩ
Bandwidth	>0·5MHz
Noise voltage	40×10^{-9} $VHz^{-\frac{1}{2}}$
Noise figure with typical ORP13	0·8dB

Low noise amplifier for MCT detector

A low-noise amplifier circuit for use with an MCT detector is shown in Fig. 2.6. The amplifier is designed to give a good noise performance with MCT detectors biased with a constant current.

So that the collector currents of TR_2 and TR_4 are largely unaffected by variations in supply voltage, two reference voltage sources have been used. One reference is provided by the voltage regulator diode D_2 which, through transistor TR_3, sets the potential across R_4. This potential defines the operating current of transistor TR_2. Any noise generated by D_2 is decoupled by R_{10} and C_5. Transistor TR_3 provides some gain and, with the reference voltage of D_2 to its base, enables TR_4 to be connected directly to the supply rail. Thus nearly all the supply voltage is available for the output voltage swing.

The second reference voltage is provided by the base-emitter voltage of TR_1. This sets the d.c. voltage across R_5 and R_6 which defines the total current taken by TR_2 and TR_4. Thus the collector currents of both TR_2 and TR_4 are now defined. Transistor TR_1 controls the d.c. base bias voltage of TR_2 to give the desired collector current. This enables very large values of base bias resistors to be used without causing any change in operating conditions due to production spreads of h_{fe} at TR_2.

Resistor R_9 protects transistor TR_4 against damage from short-circuit of the amplifier output terminal to earth.

Transistor TR_2 (BFXLNR29) is a device specially selected for use with cells of very low resistance. With this transistor a noise figure of 3dB is obtainable with a driving source impedance of 100Ω. The MCT cell will have a noise equivalent resistance greater than 300Ω, so that good noise figures can be expected.

The effective noise voltage generated by the amplifier at its input is given approximately by:

$$V_n = \sqrt{(e_n^2 + i_n^2 + KR_e)}.$$

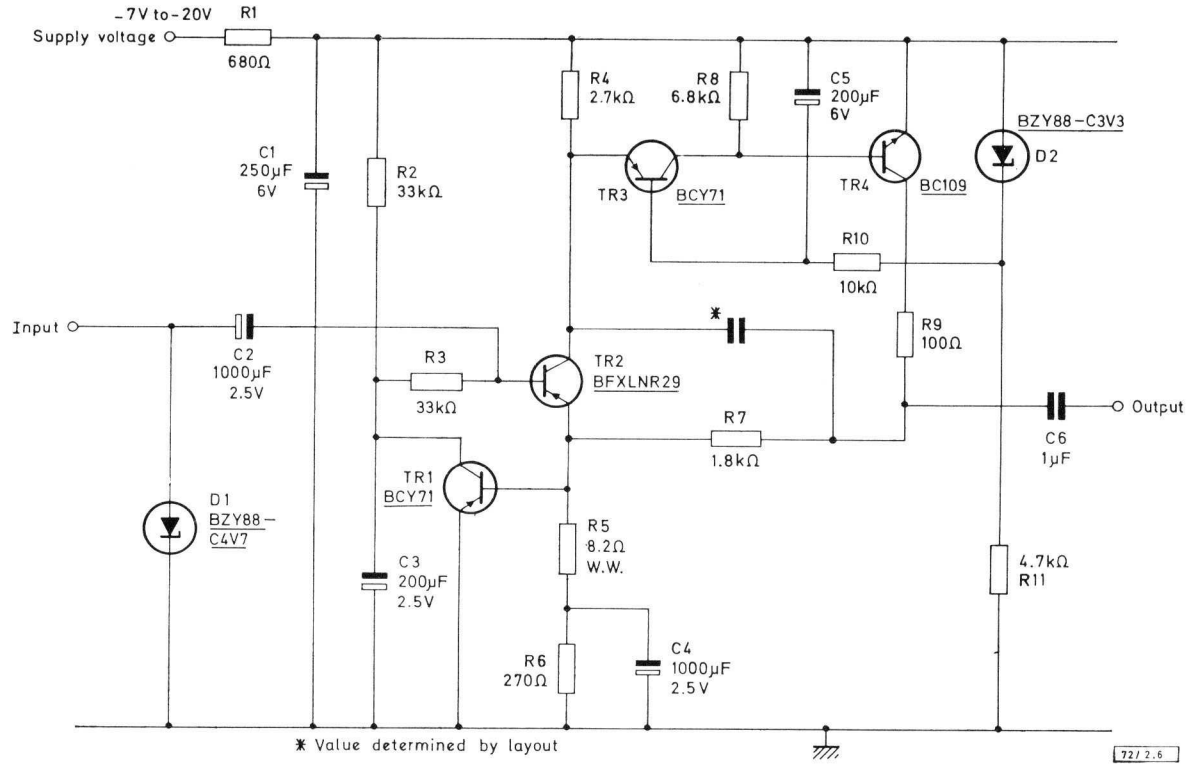

Fig. 2.6—Low-noise amplifier for MCT detector

The amplifier performance is as follows:

Voltage gain	200
Input impedance	$>15k\Omega$
Output impedance	$<100\Omega$
Bandwidth	$>1MHz$
Noise voltage at input	$1{\cdot}4\times10^{-9}VHz^{-\frac{1}{2}}$
Noise figure with typical detector	1·5dB

UNCOOLED DETECTORS

Circuits for uncooled detectors are now given.

Low-noise amplifier for ORP10

The low-noise amplifier shown in Fig. 2.7 uses four BFXLNR29 low-noise transistors in parallel as its first stage. This technique is necessary because of the extremely low d.c. resistance and noise level of ORP10 detectors. A typical ORP10 will have a d.c. resistance of 50Ω and a noise equivalent resistance of 60Ω. ($1\times10^{-9}VHz^{-\frac{1}{2}}$ expressed in r.m.s. noise volts).

When the amplifier of Fig. 2.7 is driven from a source resistance of 60 Ω, amplifier noise will be about the same level as cell noise. Thus an effective noise figure of 3dB is attainable.

Amplifier performance is as follows:

Voltage gain	220
Input impedance	$>15k\Omega$
Output impedance	$<100\Omega$
Bandwidth	$>1MHz$
Noise voltage	$0{\cdot}8\times10^{-9}VHz^{-\frac{1}{2}}$
Noise figure with typical ORP10	3dB

Biasing and amplifying circuit for RPY77 2×2mm labyrinth cell

The circuit for RPY77 detectors shown in Fig. 2.8 is similar to that of Fig. 2.4 for the RPY56 detector. The circuit is noise optimised for the RPY77 detector, however. This is a constant voltage biasing system followed by a current amplifier.

The value of R_B is critical in its effect on the noise performance of this type of circuit. If R_B is reduced in value, noise current contributed by the resistor itself is increased, and at the same time the effect of the transistor equivalent noise voltage generator is increased. Thus R_B must be made as

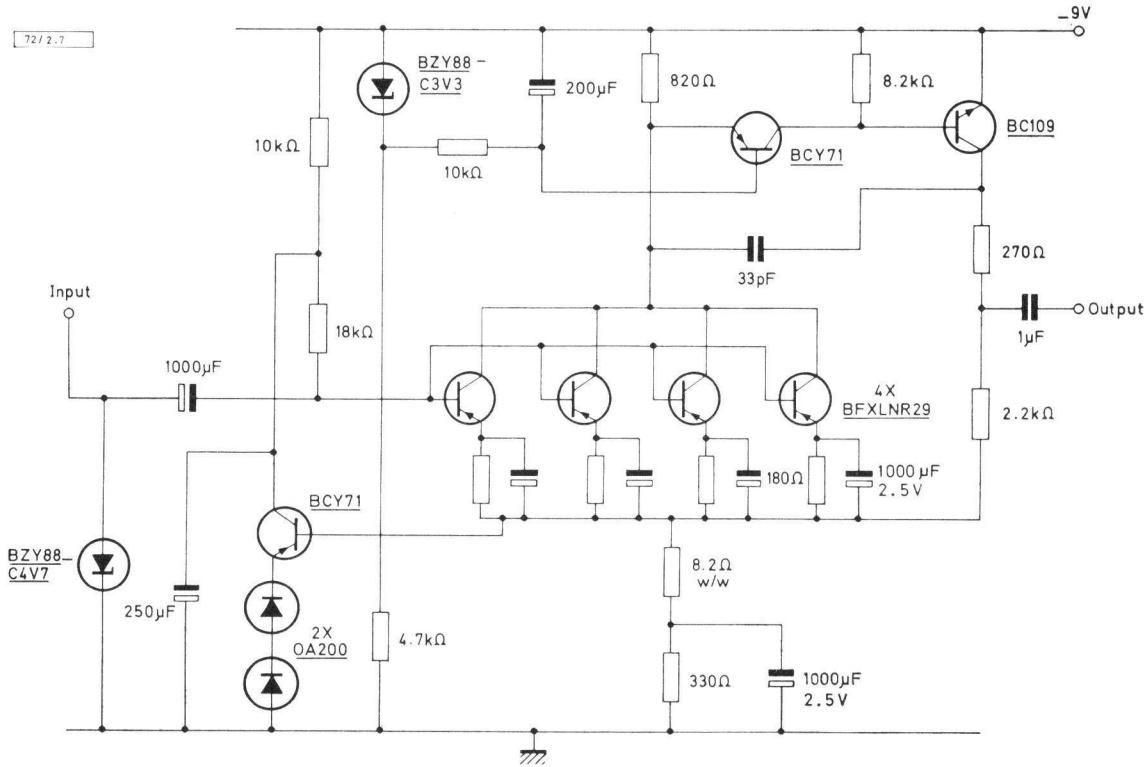

Fig. 2.7—Low-noise amplifier for ORP10

large as d.c. conditions will allow. The noise voltage generated by this circuit can be calculated from Eq. 6.

The performance of this system is as follows:

Voltage gain	40 typ. (designed to vary with cell resistance)
Current gain	unity
Input impedance	90Ω
Output impedance	33kΩ
Bandwidth	>1MHz
Noise voltage	5×10^{-9}VHz$^{-\frac{1}{2}}$
Noise figure with typical RPY77	2dB

Biasing and amplifying circuit for RPY79 1 × 1mm labyrinth cell

A circuit for the RPY79 detector is shown in Fig. 2.9 and is principally the same as that for the RPY77. The RPY79 has a lower d.c. resistance, therefore transistor TR_2 must operate at a higher collector current.

The circuit performance is:

Voltage gain	60
Current gain	unity
Input impedance	35Ω
Output impedance	22kΩ
Noise voltage	$2{\cdot}25\times10^{-9}$VHz$^{-\frac{1}{2}}$
Noise figure with typical RPY79	0·6dB

General purpose amplifier for 61SV

A general purpose amplifier for the 61SV is shown in Fig. 2.10 (p. 42). A FET is a convenient device to use in the first stage. It contributes very little noise and provides a high input impedance that will not attenuate the voltage signal developed across the detector. For the same reason the bias resistor must be of a high value. With a bias voltage supply of 200V a suitable bias resistor value is 4·7MΩ. This produces near optimum bias for all detectors and does not attenuate the signal excessively. A diode must be connected across the FET input terminals to protect it from a high-voltage transient which would occur at the moment of switching on cell bias.

Circuits for chemically deposited lead sulphide detectors RPY75/RPY76

When using chemically deposited lead sulphide detectors where signal and noise levels are high, it is recommended as a general principle that constant voltage biasing followed by a low impedance input amplifier is used. This

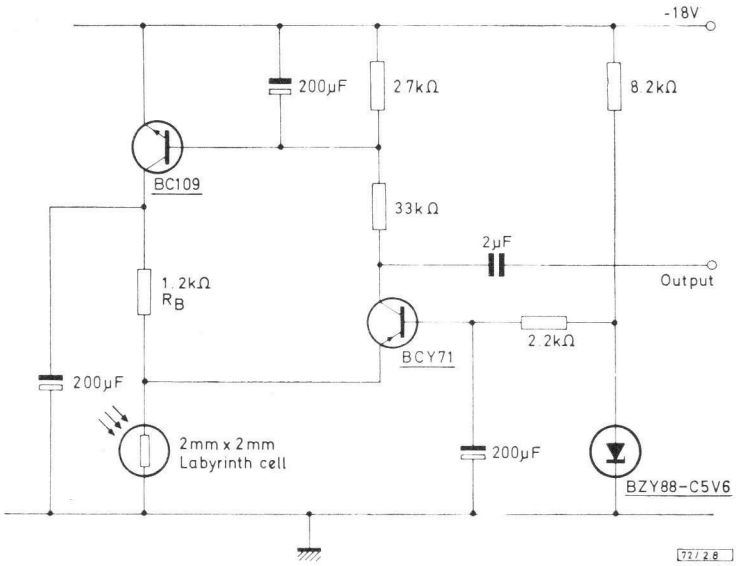

Fig. 2.8—Biasing and amplifying circuit for RPY77

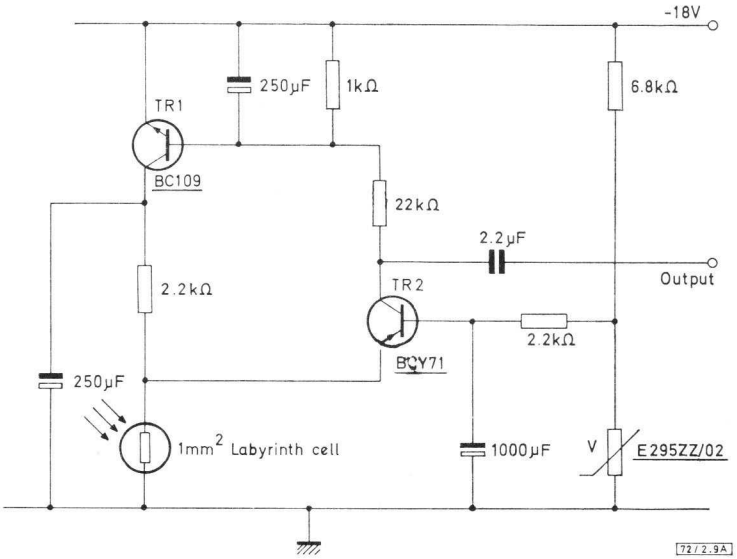

Fig. 2.9—Biasing and amplifying circuit for RPY79

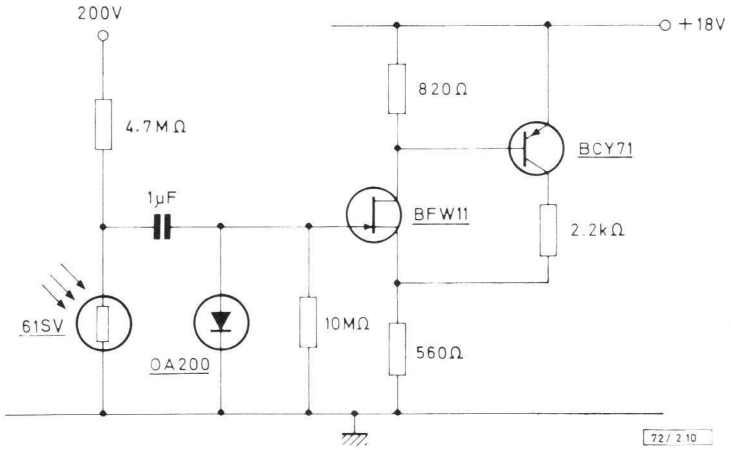

Fig. 2.10—General purpose amplifier for 61SV

will ensure minimum signal variation if cell parameters change because of temperature variation and ageing.

Circuit 1

Fig. 2.11 shows a simple transistor constant voltage biasing stage. The cell is directly connected to the low impedance of the transistor emitter which also holds a constant d.c. voltage across the cell. All of the cell signal current appears in the transistor collector. By means of a suitable collector load the signal can be converted into a voltage suitable for amplification.

In this circuit the standing collector current is the same as the bias current, and this will vary with cell resistance. Hence there is an upper limit of collector load beyond which the transistor will tend to bottom at extremes of cell resistance variation. This limits the voltage gain available from the circuit.

Circuit 2

In this circuit (Fig. 2.12) constant voltage bias is achieved by connecting the cell through a relatively low value resistor to the supply rail. The load resistor does not attenuate the signal in this case, owing to the amplifier input impedance being low compared with the cell load.

With a.c. coupling to the amplifier, changes of cell d.c. resistance do not affect amplifier performance, and high gain is possible. The values shown in Fig. 2.12 give a signal current gain of 100.

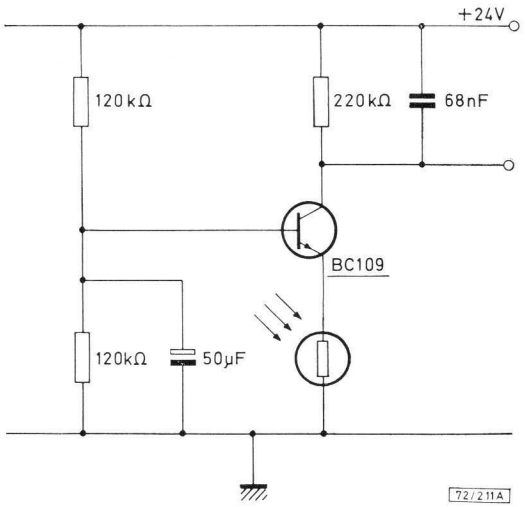

Fig. 2.11—Simple transistor constant voltage bias system for chemically deposited lead sulphide detector RPY75 or 76

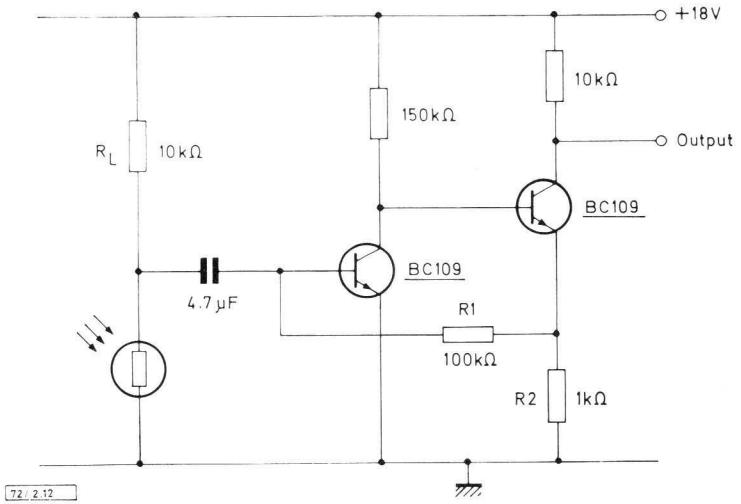

Fig. 2.12—Constant voltage bias system for chemically deposited lead sulphide detector RPY75 or 76

PROTECTION AGAINST PLUG-IN SURGE

In a number of the circuits described in this chapter a voltage regulator diode has been placed across the amplifier input terminals. This diode protects the detector from current surges which can occur at the instant of connecting a cell into a live circuit. This surge is caused by the coupling capacitor charging up when the detector is removed from the circuit. When reconnected to the circuit the cell is presented with an excessive voltage V_p with very little series resistance to limit the current. Cell resistance itself can be very low, this being particularly important with cooled cells at room temperature.

The voltage V_p can be evaluated from the expression:

$$V_p = V - V_{ZT} - V_{be}$$

where

V is the cell bias supply voltage

V_{ZT} is the transistor reverse base-emitter voltage

V_{be} is the base-emitter forward voltage of the transistor.

The base bias voltage does not affect V_p.

The effective series resistance R_p is given by:

$$R_p = R_{ZT} + r_b + R_{cell}$$

where

R_{ZT} is the reverse-breakdown impedance of the transistor emitter-base

r_b is the transistor internal base resistance.

To prevent interference with the cell output signal, the breakdown voltage of the voltage regulator diode must be chosen to be a volt or two higher than the maximum d.c. voltage across the cell. This is a straightforward choice in the case of most detectors where the voltage will not exceed 4V. If a diode of suitable voltage is chosen, then the peak of the plug-in surge cannot exceed 30mA.

However, with the ORP13 amplifier in Fig. 2.5 a diode with a voltage breakdown of 30V would be required. If the ORP13 at room temperature is plugged into this circuit, and a BZY88–C30 diode is used, a current surge of peak 300mA may flow. In this circuit it is necessary to include some extra series resistance which will cause only negligible degradation of circuit performance. If a 220Ω resistor is placed in series with the input as shown, then the peak surge current will not exceed 85mA, which is an acceptable peak for this detector at room temperature.

CHAPTER 3

FLAME-DETECTOR FIRE ALARM

Commercially available fire alarms are usually one of two basic types, namely heat detectors and smoke detectors.

With heat detectors, a dual-action thermostat operates the alarm either at a predetermined temperature (about 65°C) or when the rate of rise of temperature exceeds a given level. The main limitation of this system is that the fire must generally be well-established before the alarm is given.

The optical smoke detector relies on the presence of smoke particles in the atmosphere to operate the alarm. Since most fires produce an appreciable volume of smoke in their early stages this system has the major advantage of producing an early warning. Its limitations are set by the environment and the nature of the fire.

The system to be described here is a flame detector in which the infrared radiation from a flame results in an alarm signal from an infrared detector. The major advantage of this type of system is that an alarm signal will be produced as soon as a flame occurs in the field of view of the detector.

BASIC FIRE ALARM SYSTEM

A practical form of flame-detector fire alarm system using an infrared detector has been designed round the RPY75, RPY75A, RPY76, or RPY76A, which are small lead sulphide cells with a sensitive area of 1×1mm and a peak spectral response at 2·2μm. The fire alarm is a simple infrared detecting system requiring no mechanical chopping or elaborate optical system. Fig. 3.1 shows the overall scheme.

An amplifying stage is incorporated with a cell to form a composite detector head. This has the advantage that a large signal is generated at source so that the system is less prone to electrical interference between the source and the central alarm position. The detectors are sited, either singly or in groups, to provide a protected zone as covered by their field of view, which in this case is about 150° cone angle per detector. The operating range obviously depends on the size of flame that can be tolerated before the alarm operates.

Alarm signals from each zone are fed to separate channels in the central

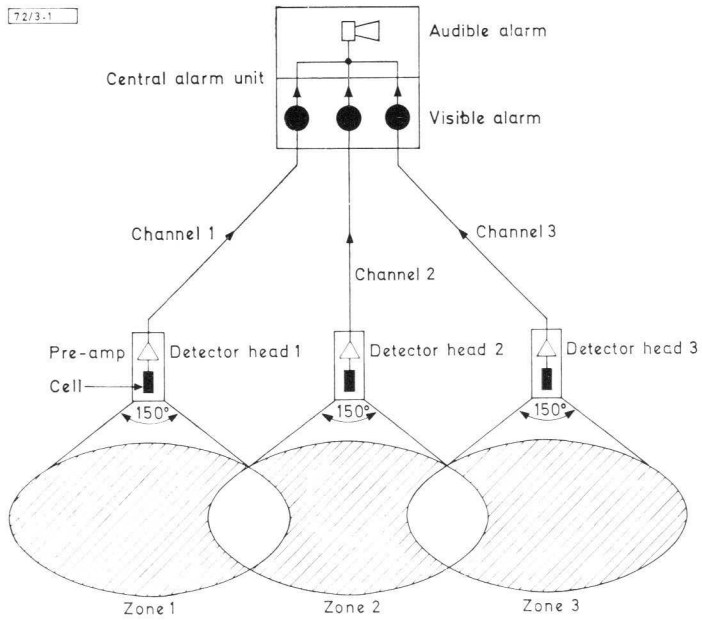

Fig. 3.1—Fire alarm system, showing protected areas

alarm position so that the location of the fire may rapidly be determined. A common form of audible alarm indicates the outbreak of a fire, while zone location is provided by indicator lamps. The prototype, the three-channel system illustrated in Fig. 3.1, is powered from a 24V supply, which could be derived from mains or batteries.

INTERFERENCE

The flame detector is based on the principle that a flickering flame acts as an intermittent source of high-energy infrared radiation to which a lead sulphide cell is extremely responsive. However, the infrared detector cannot discriminate between sources of infrared radiation, so that, when used as a flame detector in a fire alarm, it is necessary to devise methods of discriminating between true and spurious signals. For design purposes, spurious signals are classified as either continuous, such as those generated by the 100Hz radiation from a mains-powered tungsten filament lamp, or isolated transients, such as those generated by a sudden change in the background radiation level. The methods used to discriminate between the two main classes of interference are as follows.

Continuous interference

The major source of continuous interference signals is the radiation from mains-powered lighting systems, and it is particularly significant with tungsten filament lamps. As emitted radiation is not polar, lighting systems powered by 50Hz mains supply emit radiation fluctuating at 100Hz. Since this frequency is considerably higher than the typical flame flicker frequency (10 to 20Hz), the necessary discrimination is provided by making the system frequency-selective.

Transient interference

Major changes in the background level occurring, for instance, when lighting is switched on, will generate single transient signals much greater in amplitude than those from a small flickering flame. Unless the detector is carefully sited or the sensitivity of the system considerably reduced (or both), the 10 to 20Hz component of such a transient signal will provide a spurious alarm. Such limitations are not desirable in a general purpose system; therefore transient discrimination is provided by means of an integrating circuit. The output signals from the amplifier preceding this stage are limited to such an amplitude that any single pulse will not trigger the alarm, whereas a short train of pulses such as that produced by a flickering flame will quickly build up to the trigger level.

DESIGN OF DETECTOR HEAD

One must allow for the fact that the alarm system may be required to operate over a wide range of ambient temperature. Although it is primarily an indicating rather than measuring system, a reasonably consistent cell responsivity is required. This is best satisfied by operating the cell with constant voltage bias. In this condition the signal current responsivity is substantially independent of changes in cell resistance with operating temperature.

A form of constant voltage bias incorporating an active element is used (Fig. 3.2). This form of bias allows for a comparatively large value of collector load (R_L) so that a large output voltage ($i_s.R_L$) is possible. With equal base bias resistors as shown ($R_1 = R_2 = 120k\Omega$) a collector load nominally equal to the cell resistance could be used to provide an output voltage comparable to the "equivalent signal voltage" ($i_s.R_{cell}$).

However, in most circumstances allowance must be made for a rise in temperature above the nominal ambient. This rise would result in a decrease in cell resistance and hence an increase in cell current. The effect would be to drive the transistor into a bottomed state where the signal would be grossly attenuated. A load considerably smaller than the nominal cell

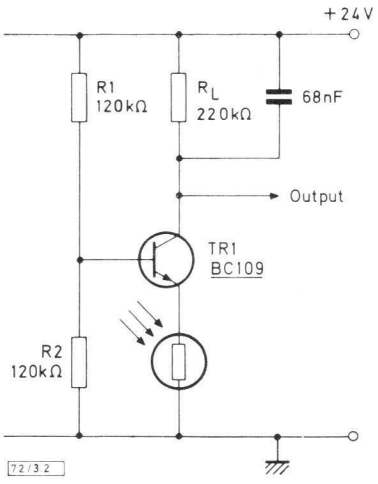

Fig. 3.2—Constant voltage bias with active element, for RPY75 or 76

resistance must therefore be used if the transistor is not to malfunction. Obviously, as R_L is decreased there is a proportional fall in the available output voltage ($i_s.R_L$). Consequently for optimum signal conditions, the load should be related to the specific cell and temperature range. Typical temperature coefficients of cell resistance are 1·6 to 2% per degC.

Tailoring the circuit to a specific cell may not always be desirable, and some loss of signal may be tolerated for the sake of standardisation. The standard load indicated (220kΩ) will allow for a 25degC rise above ambient (20°C to 45°C) for all cells above a minimum value of 400kΩ.

The continuous 100Hz radiation from any ambient lighting could result in a spurious triggering signal. With the possibility of high incident radiation levels, early attenuation is desirable to prevent the head amplifier overloading. In this circuit the necessary high-frequency attenuation may be realised by decoupling the collector load. The capacitor value 68nF is a compromise. At f = 10Hz the reactance is comparable to the load (240kΩ) whereas at f = 100Hz the reactance is considerably lower (24kΩ). This provides for a nominal 3dB attenuation at 10Hz and 20dB at 100Hz.

At a flicker frequency of 10Hz the collector impedance is about 150kΩ, which is considerably less than even the minimum limit of cell resistance (200kΩ). If high limit (1MΩ) cells are in circuit there will be considerable attenuation with the output voltage approximately 15dB down (÷6) on the equivalent signal voltage ($i_s.R_{cell}$). This need not prove a major disadvantage since the signal may be a.c. coupled to a high-gain low-noise amplifier.

A simple two-transistor amplifier incorporating negative feedback is shown

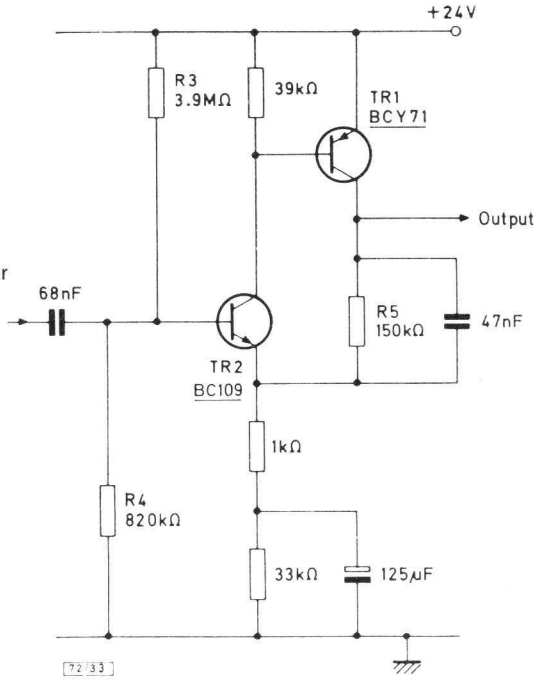

Fig. 3.3—Two-transistor amplifier with negative feedback

in Fig. 3.3. The 39kΩ load in conjunction with the V_{BE} of TR_1 (= 600mV) sets the current level in the input transistor to about 15μA. This level ensures suitable low noise performance.

With negative feedback the input resistance of TR_2 is very high (MΩ) so that the impedance is predominantly determined by the bias resistors. With R_3 = 3·9MΩ and R_4 = 820kΩ, the input impedance will be significantly greater than the source (220kΩ). These resistance values set the nominal potentials: V_B = 4·1V, V_E = 3·5V. At this level the 33kΩ emitter load defines a total current of 105μA so that, with 15μA flowing in TR_2, a nominal 90μA flows in TR_1.

Allowing for capacitor leakage (100μA in TR_1) the collector load (R_5) of 150kΩ ensures high gain without driving TR_1 into bottoming. Adequate 100Hz attenuation in the amplifier is provided by decoupling R_5 with a 47nF capacitor.

The frequency gain response of a breadboard circuit, as determined by injecting a 20mV signal in series with an upper limit (1MΩ) cell, was:

Freq.:	2·5	5·0	7·5	10	15	20	25	30	100	Hz
Overall head gain:	19	20	19	16	12·5	9·5	7·0	5·5	0·75	

CENTRAL ALARM UNIT

The central alarm unit provides both visual and audible alarm signals. Provision is made to connect each detector to a separate channel so that the location of the fire may be readily determined. Each channel contains a bistable element which switches to the ON state on receipt of an alarm pulse. In this state, both an indicator lamp and an audible alarm are activated. A suitable type of bistable circuit, which may be driven directly from a detector, is shown in Fig. 3.4. It merely consists of two transistors connected as a p-n-p-n device.

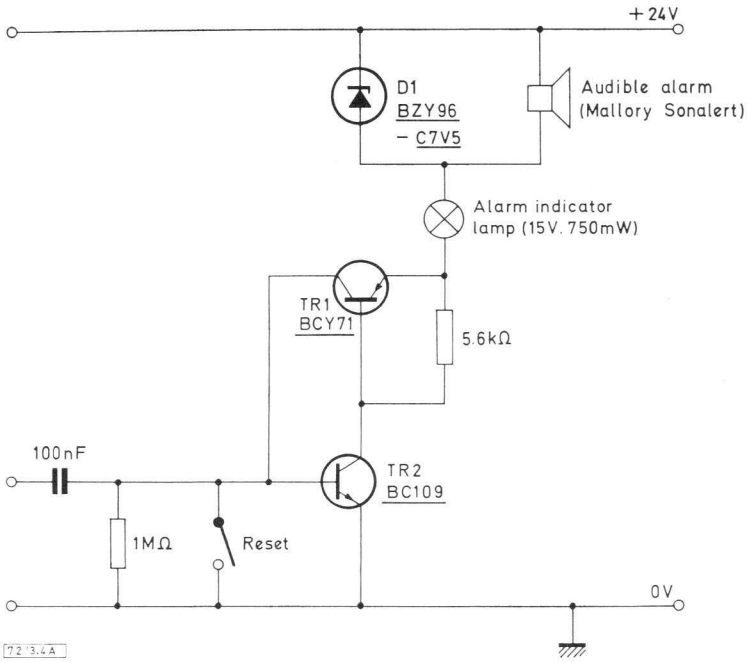

Fig. 3.4—Central alarm bistable circuit

On receiving an alarm pulse greater than the threshold voltage of the n-p-n transistor (that is, 500mV), the p-n-p-n element switches to a stable ON state. In this state, both the channel indicating lamp (15V, 750mW) and the audible alarm (Mallory 'Sonalert') are activated.

With the 24V supply allowing for 1·5V across the p-n-p-n switch and 15V across the lamp, there is 7·5V available for the 'Sonalert'. This is a suitable operating voltage for this alarm but, since it is a high-impedance

element (2kΩ), its corresponding current requirement is low (3·5mA). Most of the 50mA lamp current must therefore be diverted via a shunt path. By using a 7·5V reference diode, more than one lamp circuit can operate at the same time, yet the correct operating voltages for the lamps are maintained. The channel is reset by short-circuiting the input to the n-p-n transistor to the 0V line, cutting off the bistable circuit.

With the high gain transistors used, the base current required to switch on is negligible ($<1\mu A$) so that the switch does not load the detector. However, at high ambient temperatures, transistor leakage may be sufficient to give a spurious switch-on. This effect is eliminated by shunting the emitter base diode of the p-n-p transistor so that it does not switch on below a predetermined current level. With 5·6kΩ shunt a level of 100μA is required for switch-on.

In this simple form, use of the system is restricted since the circuit cannot discriminate between a flame and any other spurious pulse. The circuits described below overcome this difficulty.

CENTRAL-ALARM DISCRIMINATING CIRCUITS

Under normal operating conditions the system must be able to discriminate between flame flicker and the two major classes of interference signal. These are dealt with separately below.

100Hz discrimination

Under some operating conditions, there may be a very high level of continuous radiation from the lighting system. For example, if the detector faces a 60W tungsten lamp at a range of 2m, a 1·6V output signal will be generated. For the detector to operate in such an environment, further 100Hz attenuation must be introduced into the system at an early stage.

A simple method of producing the necessary voltage attenuation is by means of an RC filter. The values used (150kΩ, 100nF) provide a nominal 20dB attenuation at 100Hz and 3dB at 10Hz. With three filters (Fig. 3.5) 60dB of 100Hz attenuation is introduced. If required, this may be increased by further filters. Since there has been prior amplification in the detector head (40dB), the loss of signal caused by this filter can be tolerated. There is no loss in overall sensitivity because compensation may be provided for the fall in effective signal level by a corresponding increase in the gain of the next amplifier.

Transient signal discrimination

The second form of interference, the large transient signal, occurs, for instance, when there is a sudden change in the sunshine level or when the lighting is switched on. The interruption frequency is low and the ampli-

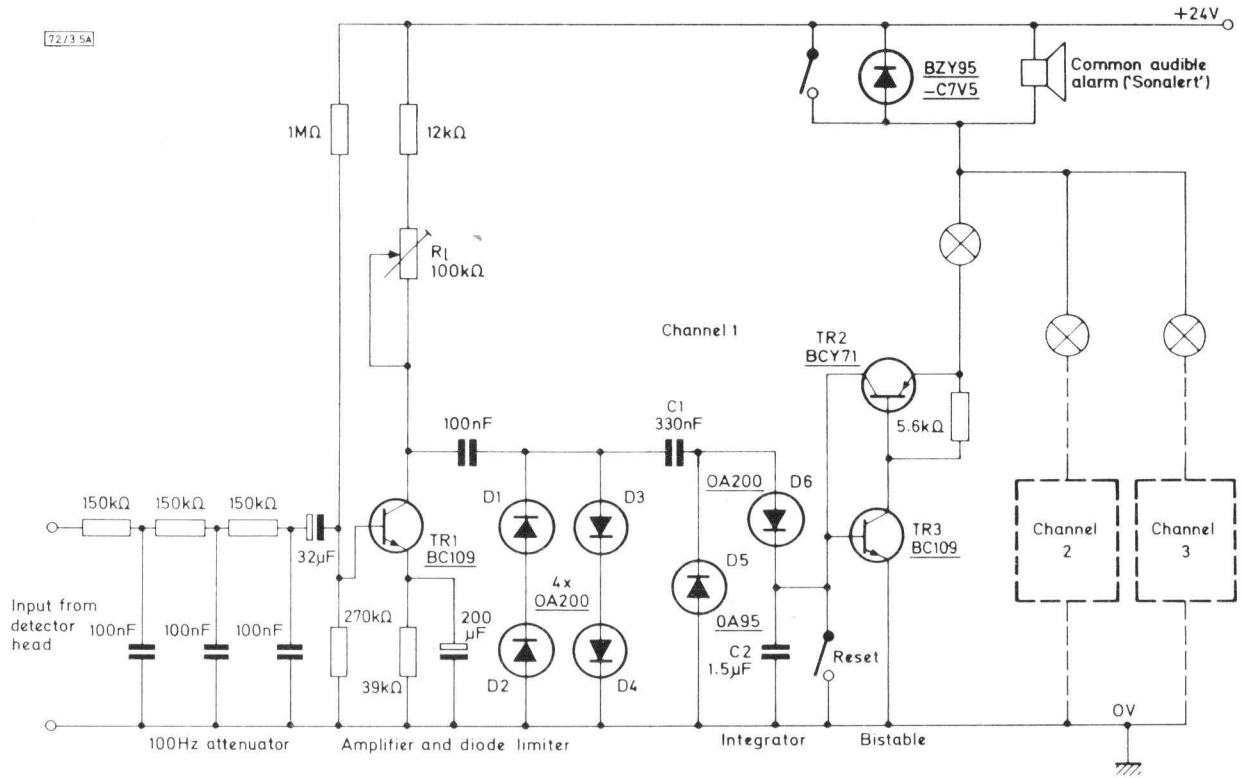

Fig. 3.5—Central alarm unit, with channel 1 shown in detail

tude indeterminate, so that a more elaborate approach than that of simple attenuation is necessary. Since this is a multichannel system, the circuitry has been kept to a minimum, but it still entails two stages: an output-limited voltage amplifier and a diode integrating circuit.

At a signal frequency of 10Hz, the attenuator is equivalent to a nominal source impedance of 100kΩ. For maximum signal transfer, the following voltage amplifier should have an input resistance greater than this value. However, as high gain is available, some loss of signal can be tolerated, and this allows some simplification of the circuit.

A low operating current is used as a simple means of providing high input resistance. At a current of 100μA, r_e is 250Ω, so that with a suitable high gain transistor ($h_{FE} > 300$), an input resistance ($h_{FE}r_e$) of 75kΩ may be obtained. In conjunction with the high-impedance bias chain, this gives an overall input resistance of 60kΩ, which does not lead to an excessive loss of signal.

With the bias chain setting the base potential at 5V, and the 39kΩ emitter resistor defining a current of 100μA, a collector load of 180kΩ can be tolerated before the transistor bottoms. In practice, the load may be preset between the limits 12 and 112kΩ by means of the variable resistor R_1 (100kΩ). With the emitter load effectively decoupled, the gain of the amplifier may be set between the corresponding limits 12 000/250 or 48, and 112 000/250 or 450. With the gain set so that a small flame flicker signal has the required detection level, large transients will be large enough to overload the amplifier. All large transient signals must have a standard amplitude before being fed to the integrating circuit, therefore some form of amplitude limiting is necessary.

The method used is to connect the output from the amplifier via a 100nF coupling capacitor to the two silicon diode chains D_1, D_2 and D_3, D_4. The forward voltage drop of the two series diodes defines the limit level to about 1V, while the reverse connection ensures that conduction occurs on both positive and negative half cycles. With this circuit, the input to the integrator is a waveform with a maximum amplitude of ±1V with respect to 24V.

On the arrival of a positive-going pulse, the capacitors C_1 and C_2 will rapidly charge via the silicon diode D_6 to the peak level. The values of C_1 and C_2 are such that they form a capacitive attenuator of 6 to 1 so that, even for the maximum input pulse of 2·0V±1·0V, the corresponding potential rise across C_2 (allowing for a forward voltage drop of 0·5V) is only 250mV. This level of input to the bistable stage is insufficient to switch it on.

At the end of the pulse, C_1 discharges rapidly through the now forward-biased diode D_5, while C_2 discharges slowly through the reverse-biased

diode D_6. Within about one second both capacitors will discharge, and the circuit will revert to its initial state. However, if within this period further pulses arrive, C_2 will progressively charge toward the peak value of the input. Once the input to TR_3 reaches about 700mV the bistable stage will switch to its stable ON state.

Sensitivity

A sensitivity control has been incorporated to enable optimum sensitivity to be realised for the prevailing conditions of ambient lighting. To form a reliable fire alarm system, the sensitivity must not be set so high as to exceed an acceptable false alarm rate.

With the minimum gain setting of the system, it is possible to detect about 8cm of flame flicker at a range of 6m within each detector head cone angle of 150°. In favourable environments where maximum sensitivity can be used, the range is doubled to 12m for an 8cm flame flicker.

Current consumption

In the normal quiescent condition, the total current drawn per channel is less than 1mA. However, with the indicator lamps used in the laboratory model, 50mA will be demanded from the supply when the channel is activated. For this reason it may be preferable to arrange mains, rather than battery, operation. A single-channel alarm system with a 'Sonalert' as the indicator would require a maximum of only 10mA when activated, therefore a portable battery-operated alarm would be practicable.

Optical filter

Discrimination against interference signals in the visible spectrum can be provided by means of an optical filter. Under conditions where this results in an improvement in the false alarm rate, the system gain can be increased. However, the overall improvement in the system sensitivity will depend on the amount of attenuation that the filter produces on the required infrared signal. For low signal attenuation, a germanium (λ_c = 1·8μm) or silicon (λ_c = 1·2μm) filter should be used.

CHAPTER 4

FLAME FAILURE PROTECTION AND FLAME PROVING

Photocell protection of oil and gas fired boilers is required to replace the slower bimetal or thermocouple systems commonly used at present.

An important factor in the choice of photocell is the spectral distribution of radiation emitted by the flame. This is dependent not only on the type of fuel used but on the efficiency of the boiler, as this controls the temperature of the flame and the constituents produced by the burning process. The gaseous or ionic constituents will produce, in general, a line spectrum of emission; while any solids present, mainly particles of carbon, will generate a continuous black-body type spectrum which will then be modified by the line absorption effects of the gaseous components (Ref. 1).

In general, gas burners using either town or natural gas (methane) will produce flames almost completely free from carbon, emitting strongly in the ultraviolet and infrared regions only. Oil burners, on the other hand, because oil is a heavy hydrocarbon, produce large amounts of carbon particles in the flame. These are subsequently burnt, if the burner is operated efficiently to avoid sooting, and the resulting flame emits strongly in the visible region.

Whereas silicon and cadmium sulphide photodetectors are limited to systems in which the flame emits visible radiation, lead sulphide cells can be used for detecting the infrared present in all flames. Furthermore, whilst visible radiation detectors may be suitable for basic protection there is a strong requirement for "solar blindness"; that is, discrimination against spurious background radiation in the visible region. Thus, systems detecting radiation in the infrared and ultraviolet are in demand. Since low-cost solid-state ultraviolet detectors do not exist, the filtered lead sulphide detector, with a response in the infrared from 1·5μm to 3·0μm, would seem to be the most suitable device for flame protection at the present time. Further discrimination against background radiation may be provided by designing the flame detection system to respond only to the flicker content of the flame. Such a system, using the RPY76A filtered lead sulphide detector, is described below.

FLAME PROVING UNIT FOR DOMESTIC GAS CENTRAL-HEATING BOILERS

This 'flame proving' unit (Fig. 4.1) is designed to provide a 'hold' current to the main gas jet relay only if a flame is present. The presence of a flame is detected by utilising the intermittent radiation produced by flame flicker. This energy irradiates a chemical lead sulphide cell so as to generate a low-frequency signal which, after suitable amplification, is made to switch and hold on a transistor. The output current may be subsequently amplified to the specific hold current necessary for a particular relay.

The system is a modified version of the 'flame detection' fire alarm system described in chapter 3.

Flame flicker provides a source of intermittent radiation that will generate an alternating signal in the chemical lead sulphide cell. The signal is initially amplified and then amplitude limited. The resultant pulses are then used to provide a charge to a capacitor which is sufficient to switch and hold on a transistor. With no flicker, and hence no pulses, the capacitor charge decays and the transistor switches off.

For this particular application the cell could be required to operate over a wide range of ambient temperature (20°C to 50°C). For a reasonably consistent value of responsivity during operation the cell should have constant voltage bias and subsequent signal current amplification.

With these high-impedance cells, constant voltage bias may be simulated by using a load resistor of a few kilohms. However, under optically saturated conditions ($R_{cell} = 30k\Omega$) the cell dissipation with a 24V supply could exceed the maximum permissible rating. The 39kΩ load used:

a) provides a nominally constant voltage bias;
b) limits the maximum possible device dissipation to about 2mW;
c) does not place stringent requirements on the following current amplifier.

The signal current is capacitively coupled to the following current amplifier. For efficient signal transfer the overall input impedance should be low. With a 39kΩ load a comparatively low value capacitor (1μF) may be tolerated. At any flame flicker >5Hz the reactance is <39kΩ. Low-frequency flame flicker (<5Hz) is attenuated, but so are the low-frequency spurious transients.

The system must become immediately operative on switch-on. The time-constant (1μF × 39kΩ) of 39ms should satisfy this requirement.

Two identical stages are used to provide an overall current gain of × 100; although in practice it may be found that the second stage and the four OA200 diodes are not needed.

Negative feedback is used to provide the required low input impedance and gain stability. The circuit does not employ decoupling capacitors, so

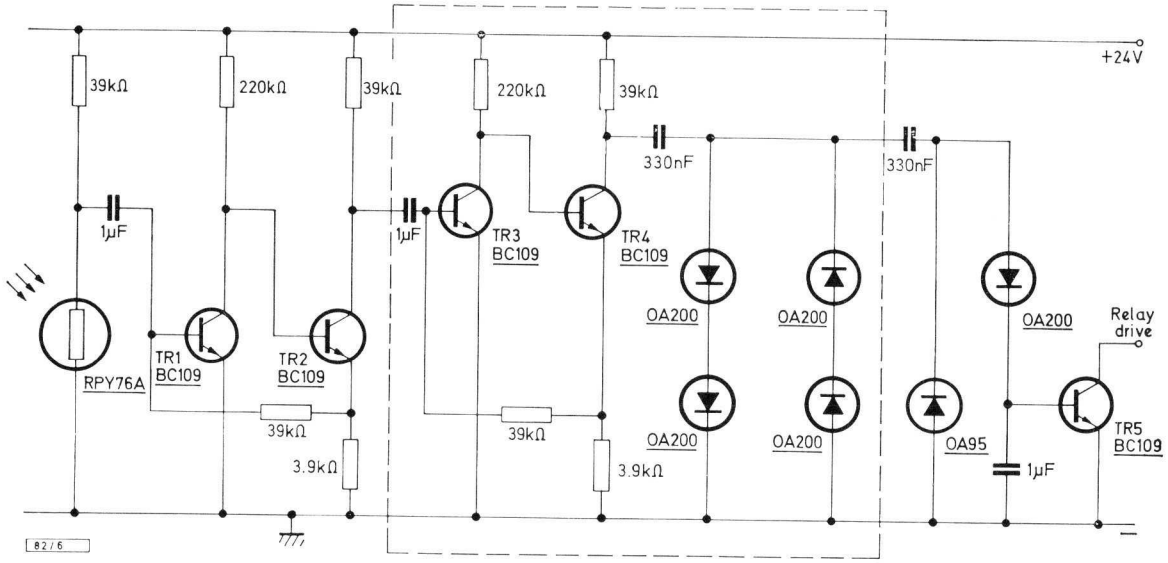

Fig. 4.1—Flame proving unit for domestic gas boiler. The boxed section may not be needed (see text).

it becomes immediately operative. The feedback to emitter resistor ratio (39kΩ/3·9kΩ) determines the nominal gain per stage (× 10). The nominal operating levels, as defined by the collector load (220kΩ) and emitter load (3·9kΩ), are 100μA and 150μA respectively.

The same technique is used for limiting and integrating as in the fire alarm system. The two diode chains limit the output from the amplifier to provide a series of pulses which have a maximum amplitude of +1V with respect to earth. After d.c. restoration these pulses progressively charge the 1μF capacitor until the 'hold' transistor switches on. They then provide sufficient base charge to keep this transistor on.

The output transistor provides the basic 'hold-on' level. In the prototype a match at a range of a few inches produces a collector current of about 1 mA. The hold transistor may be compounded with a p-n-p device (or devices) to provide the necessary hold level for any particular relay.

CHAPTER 5

PASSIVE INTRUDER ALARM

A fundamental difference between pyroelectric detectors (triglycine sulphate) and photoconductors (indium antimonide, lead sulphide) is that the former rely upon a change of temperature of the element, rather than upon the excitation of electrons by the incident radiation. Thus the spectral response of the triglycine sulphate detector depends only upon the absorption properties of the element and its associated electrical contacts; the response is substantially flat from 2μm up to the millimetre region. By the use of suitable window materials only radiation in a given wavelength range may be allowed to reach the detector.

The passive intruder alarm (Fig. 5.1) was built to demonstrate the sensitivity of the TGS detector to radiation from objects slightly above and below room temperature. The peak of the black-body emission curve for 300K lies at about 10μm: indium antimonide, with a wavelength cut-off at 7μm, will 'see' only 4% of the available energy, and lead sulphide at 3μm a negligible amount. Thus, of the uncooled detectors, the thermal detector is the most attractive for this application.

The detector used in the alarm is a standard 802CPY type, with an element size 3mm$\times$1mm; it incorporates a low-noise preamplifier with a low output impedance, so that electrical noise from external sources can be neglected.

OPTICAL CONSIDERATIONS

As stated above, the peak of the black-body curve for room temperature sources is approximately 10μm. Thus any optical elements such as lenses and windows should allow this wavelength through. A convenient lens material which transmits up to 14μm is arsenic trisulphide. The lens used in the alarm has a diameter of 25mm and a focal length of 10cm, and it is supported at the end of a plastic pipe. The detector is housed in the pipe with the element at the focus of the lens. With this arrangement the detector surveys a field of view of 30$\times$10 milliradians. Thus at 60 metres (200ft)

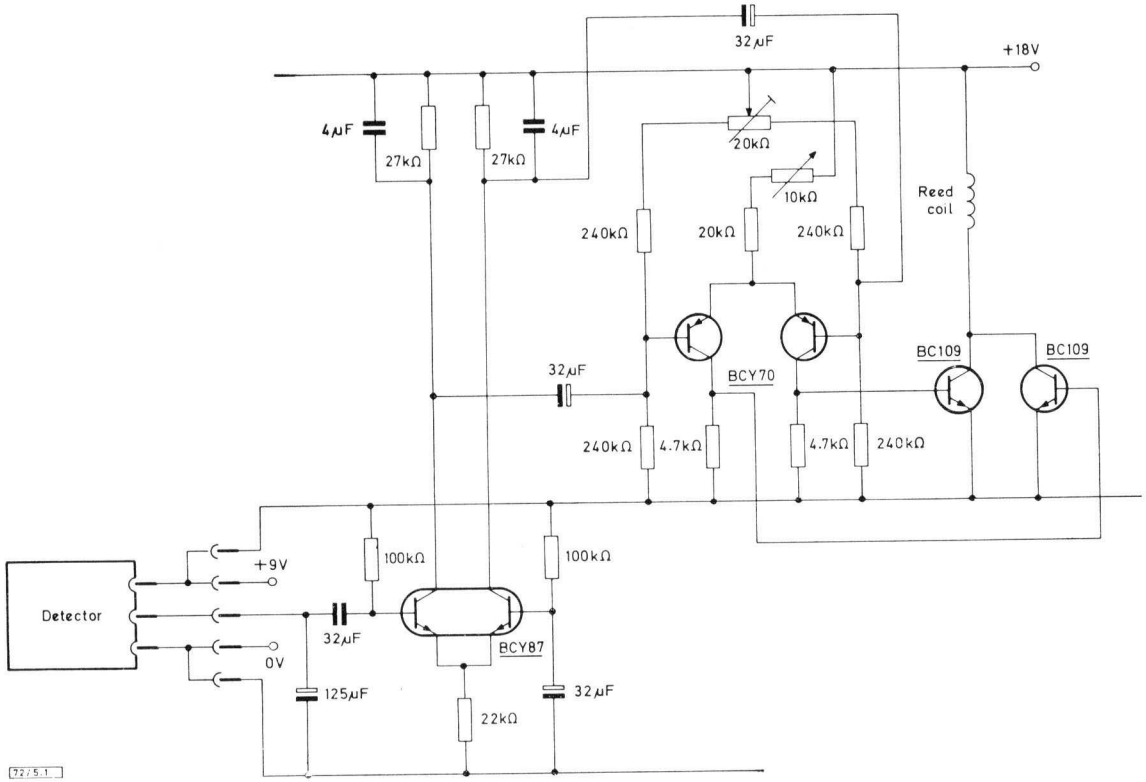

Fig. 5.1—Passive intruder alarm

the field of view is 1·8×0·6m (6×2ft). If the element is mounted with its long axis vertical, then the field of view is almost filled by an intruder at 60 metres.

The indium antimonide window fitted in front of the detector transmits radiation with wavelengths in excess of 8μm. Thus the combination of lens and window material used forms a bandpass filter of 8 to 14μm transmission which greatly reduces the effect of spectrally reflected sunlight from the background. The signal from an intruder is reduced by a factor of three by the filter.

The interior of the plastic pipe between the lens and detector has been blackened to eliminate reflections. Otherwise the edge of the field of view is blurred, leading to an apparent slowing down of the intruder.

THERMAL CONSIDERATIONS

The plastic pipe fulfils a second function—that of shielding the detector from changes in the temperature of the ambient. The part of the detector that is most sensitive to ambient changes is the field effect transistor, which will produce an output of 30mV for a 1 deg C change. The element itself will probably give rise to a change an order of magnitude less than this.

The existing thermal screening includes a plastic end cap which completes the surrounding of the detector. The detector is held in the tube by a nylon screw. The thermal arrangement appears to be adequate for normal ambient variations.

The first amplifier in the control box utilises a dual transistor to minimise any untoward thermal changes therein.

ELECTRONICS

The output impedance of the preamplifier incorporated in the detector is low (200Ω), requiring no additional circuitry to guard against pick-up in the lead to the control box. The first amplifier is a simple differential unit employing a BCY87 dual transistor. Since the current demanded by this amplifier is independent of signal, it can be supplied from the same voltage rail as the preamplifier without special decoupling. The differential gain in the first amplifier is approximately 200 with a bandwidth of 0·1 to 1·6Hz.

The first amplifier is capacitively coupled to a second differential pair. The biasing points of the two transistors may be adjusted by the 20kΩ preset potentiometer so that the two collector voltages are equal. The tail current is set by adjusting the 10kΩ potentiometer, which is set so that the two collector voltages are not quite enough to bias the final BC109 relay drivers on. Any disturbance, positive or negative, will then activate one or other of the driver transistors, and the relay will make. Thus the 10kΩ potentiometer can be used as a sensitivity control. The reed coil is a

Radiospares No. 3, with the two parts connected in parallel.

The short-circuit produced by the reed when the system is disturbed can be used to operate peripheral equipment such as a warning lamp, bell, or transmitter.

The control box is run from two PP9 9V batteries, having a life in excess of 500 hours. The five-pin socket and plug which connect the detector to the control box are wired so that the system is switched on when the detector is plugged in.

CHAPTER 6

RADIATION THERMOMETER FOR TEMPERATURES OVER 100°C

A radiation thermometer provides a means of measuring the surface temperature of an object without having to make physical contact with the surface. It has obvious applications where normal temperature detecting methods, which rely on physical contact, are either impracticable or uneconomical. A radiation thermometer determines temperature by measuring the energy emitted from the surface of the object. Its ability to do so is based on the fact that every object above absolute zero temperature emits radiation energy, and that the intensity of the radiation is a function of temperature.

One class of radiation thermometer is that based on thermal detectors in which the absorbed radiation heats the detector and causes a change in some observable property, for example its resistance. Such detectors respond to all wavelengths but, as they rely on a heating effect, their response is slow (one millisecond to ten seconds).

The other class of radiation thermometer is that based on quantum detectors in which all incident photons with the necessary minimum energy free a bound electron. Such detectors respond to a limited range of wavelengths, but their response is fast (one picosecond to one millisecond). The portable radiation thermometer described here is of this type.

The elements of the radiation thermometer are shown in Fig. 6.1. They are the collecting optical system, the radiation detector, an amplifier, and the indicator. With the instrument described here, the simplest infrared detecting techniques have been used. The collecting optical system consists of either a simple light-pipe or a lens, followed by an optical chopper which alternately passes and blocks the infrared radiation. The chopped radiation results in an alternating output signal from the detector. The signal is amplified in the preamplifier and then fed to the main amplifier. The output from the main amplifier, which has an amplitude proportional to the source temperature, is demodulated and registered on a meter.

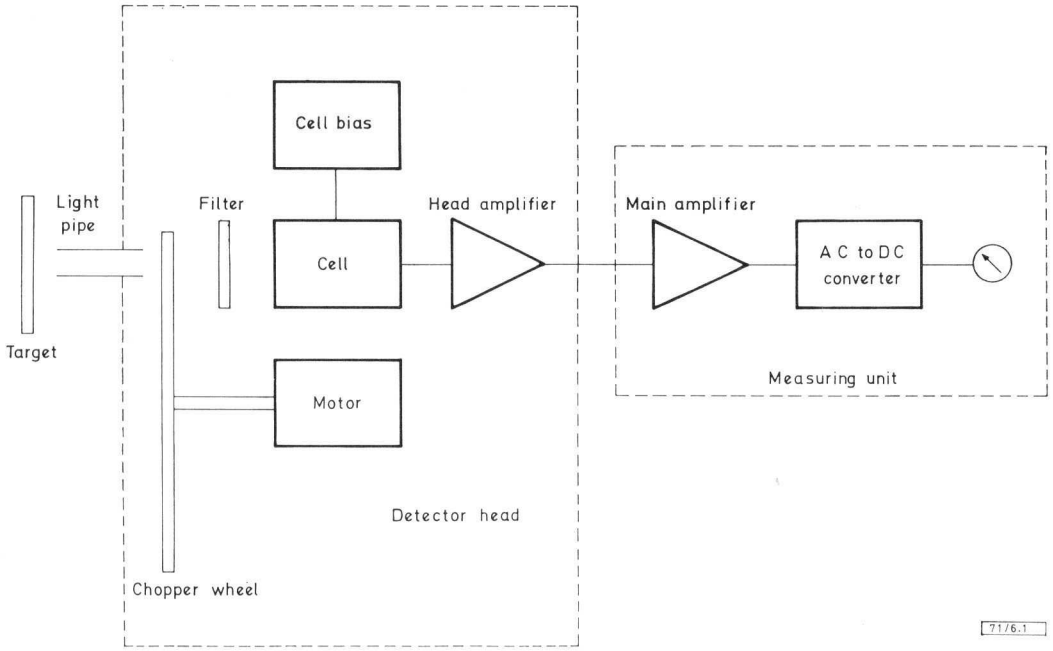

Fig. 6.1—Layout of PbS radiation thermometer

The instrument is calibrated on a perfect radiator (that is a black body) which has an emissivity of 1. Provision is made for practical target emissivities ranging from 0·1 to 1.

RADIATION DETECTOR

The choice of radiation detector has considerable influence on the design and performance of the complete instrument. For this particular portable equipment, the detector should have a high infrared sensitivity when operated at normal room temperatures. This entails the use of a detector designed to measure energy at short wavelengths where the higher photon energy $E = hc/\lambda$ obviates the need to reduce thermal noise by means of cell cooling. The cell used is the 61SV, a lead sulphide photoconductive cell with a 3dB spectral response from 1·8 to 2·8μm and a high infrared sensitivity at room temperature.

Collecting optical system

The spectral transmission band of glass, extending typically to 2·7μm, embraces the spectral response of the cell. An optical glass lens may therefore be used as the collecting system for applications where the target is remote from the measuring instrument. An alternative optical system may be used for applications where the target is at a short range: this is the light-pipe, consisting of a short length of fused silica rod within a metal casing, with a transmission band from 0·19 to 3·5μm.

Optical filter

Interference by short wavelength radiation, such as sunlight, may be attenuated by an optical filter. Semiconductor filters which have a high absorption below a critical wavelength (λ_c) are extremely suitable in this respect. If a germanium filter ($\lambda_c = 1{\cdot}8\mu m$) or silicon filter ($\lambda_c = 1{\cdot}2\mu m$) is used in conjunction with this cell, a narrow spectral response is obtained, free from solar and other visible background interference.

Lower limit of target temperature

The peak spectral emission from a perfect radiator, or black body, is a function of its absolute temperature. From the Wien displacement formula ($\lambda_m T = 2893$) it may be seen that the lower the temperature, the longer the wavelength. The general rule is therefore that the spectral emission shifts to longer wavelengths as the temperature of the body to be detected decreases. This imposes a fundamental limitation on the minimum temperature that can be detected with the short-wavelength detector used. In practice, with simple techniques, a lower limit of 100°C may be realised.

Radiation from ambient bodies

The power per unit area radiated into a hemisphere by a perfect radiator or black body is given by

$$W_{bb} = \sigma T^4,$$

where σ is the Stefan-Boltzmann constant ($5{\cdot}6697 \times 10^{-12} Wcm^{-2}degK^{-4}$).

The fall in power and the shift in peak spectral emission to longer wavelengths both have the effect of drastically reducing the sensitivity of the lead sulphide cell for objects at room temperature. For this particular application (where the minimum target temperature is 100°C) the radiation from the chopper disc itself may be regarded, for all practical purposes, as an effective zero reference, since the disc blocks the incoming radiation.

Change in cell sensitivity with ambient temperature

One limitation of the photon detector employed (61SV) is that the sensitivity is a function of the ambient temperature. For a portable radiation thermometer it is impracticable either to cool or to heat the cell to provide a constant operating temperature. Therefore a constant cell sensitivity cannot be realised. However, with the 61SV the change in signal sensitivity is consistent and may be expressed, over the range −10 to +50°C, as:

$$S_T/S_{20} = 1{\cdot}4 - (T/50)$$

where S_T and S_{20} are the sensitivities at T°C and 20°C. Thus the sensitivity changes 2% of its value at 20°C for every degC change in temperature. Therefore a constant sensitivity may be simulated if a suitable compensating circuit is used to increase the gain of the amplifier by a corresponding amount; that is, by 2% for every degC rise in temperature.

The gain compensation is made by means of a negative temperature coefficient thermistor, which of necessity must track with the cell. Since the cell and thermistor do not have the same thermal time-constant, both elements are encased in a metal block. This provides a large, common thermal mass, so that the temperature tracking is greatly improved.

Cell bias

The 61SV exhibits ohmic behaviour in that the signal for a given irradiation is linearly proportional to the applied voltage. A separate h.t. supply has been used to attain sufficient sensitivity to keep the signal clear of interference and noise at low irradiation levels. Since the 61SV is a high-impedance element (1 to 4MΩ) the current drain on this supply is low.

For a specified supply voltage the optimum signal voltage is generated across the cell when the load resistor has a value equal to that of the cell (1MΩ is a convenient load). This provides a high source impedance

(about 500kΩ). A compromise can be made between signal level and reduced source impedance by using a lower load resistance (470k Ω) with the cell.

OPTICAL SYSTEM

The optical system preceding the radiation detector can have one of two forms: a light-pipe system for close-range measurements or a lens system for longer-range observations.

Light-pipe system

The equipment was initially designed for monitoring targets at a close range by means of a light-pipe. This takes the form of a short length (typically 20cm) of gold-flashed fused silica rod. Fused silica is a suitable transmitting medium since its spectral transmission band (0·19 to 3·5μm) embraces the 3dB spectral response of the cell. The gold-flashing provides a highly polished surface which minimises the losses at each internal reflection. However, reflective attenuation effectively suppresses all incident rays deviating from the axis by more than 10 to 20°. This is shown in the polar diagram in Fig. 6.2.

The maximum sensitivity is attained when the cross-sectional area of the rod is similar to the effective area of the cell. For this particular

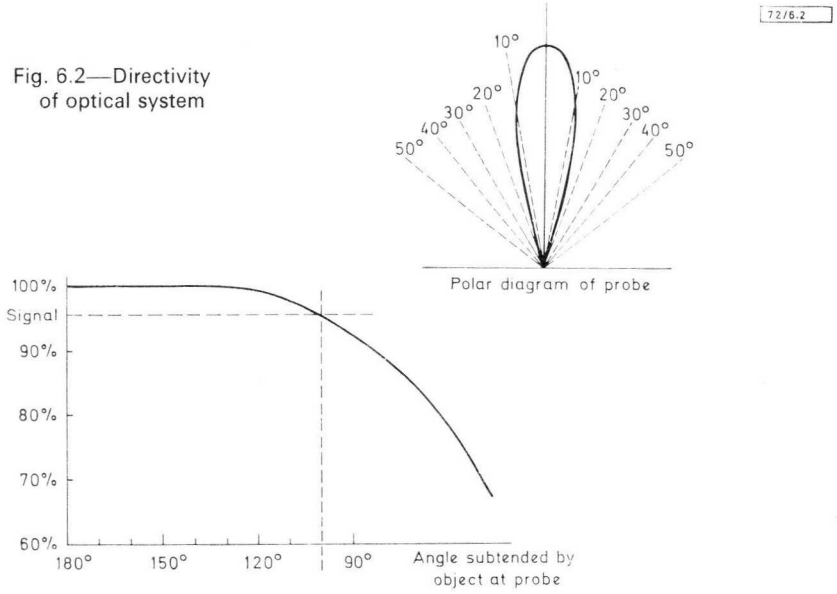

Fig. 6.2—Directivity of optical system

application, a 5mm diameter rod has been used with a 6mm square cell. For high-temperature applications, where some degree of optical attenuation is actually desirable, a smaller diameter rod, or a tapered probe, may be used.

This simple light-pipe is fragile and, for use with a general-purpose instrument such as this portable thermometer, protection is desirable. A stainless steel sheath, which does not deteriorate with use in high-temperature environments, has been found to be suitable. For other applications, where protection is deemed unnecessary, for example in an enclosed control system, the rod may be bent or tapered to any desired form to suit the particular requirement.

High-temperature measurements have also been made with a stainless steel tube as a light pipe. The open-ended tube proved unsatisfactory in that the internal surface deteriorated with life. This limitation could be overcome by inserting fused silica plugs at each end.

For general-purpose equipment, the siting of the probe for any particular measurement is extremely important. As may be seen from the polar diagram, the light pipe collects radiation only within a cone angle of about 100°. Therefore the radiometer can measure the average temperature of a target only from the radiation collected within this cone. Consequently the probe may be moved a distance D/4 from a target of diameter D without any change in signal level. Beyond this distance, the angle subtended at the probe decreases and the signal will be reduced as indicated in Fig. 6.2. With a target diameter of D, the rule of thumb is that the distance between probe and target is D/3 to D/4. Under these conditions, the angle subtended by the target is about 120°, which ensures that there is a negligible loss of signal. In practice, the distance may be determined by moving the probe tip away from the target and noting if there is any significant reduction in the temperature reading.

Lens system

Although the initial design was for a light-pipe optical system, an alternative long-range collecting system, consisting of a double convex lens, also proved satisfactory. With a lens 38mm in diameter and a 60mm focal length, the collecting area is increased so that the overall sensitivity should be improved by a factor of 25. This is achieved in practice, and a black-body target at 100°C gives an indication two scales higher after the lens has been fitted. With this optical system, range 1 (the highest gain amplifier setting) is completely inoperative since normal room radiation produces a standing signal level of 10% of the full range 2 deflection. Under these conditions, the lowest temperature that could be detected is 170°C corresponding to 20% full range 2 deflection.

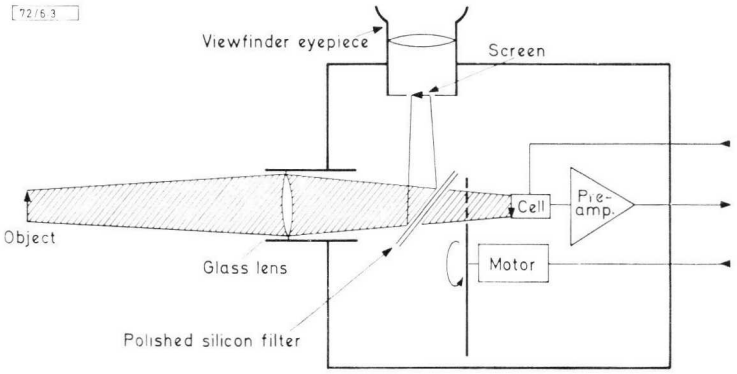

Fig. 6.3—Remote focusing head

With a 6×6mm cell and a lens with a focal length of 60mm, although the instrument has increased sensitivity, the target-diameter-to-distance ratio is only 1:10. For applications where a lower sensitivity can be tolerated, the effective area of the cell can be reduced to improve the target-diameter-to-distance ratio. With a 1·5mm aperture in front of the cell, the ratio is reduced to 1:40 while the basic sensitivity (100°C minimum) is retained.

A variable focus sighting system is employed to ensure that the target completely fills the effective cell aperture. The transmission properties of the bloomed silicon filter (set at an angle of 45°) are utilised by employing it both as a filter to the cell and as a mirror to the visible radiation (Fig. 6.3). To facilitate sighting, a magnified image of the target, which is focused onto the viewing screen, is provided by a further lens.

OPTICAL CHOPPER

To generate an alternating signal across the cell, the radiation from a target is interrupted by a chopper disc. Since the disc itself will radiate energy corresponding to the disc temperature, the amplitude of the signal is dependent on the energy difference between the two radiation levels. In this application, the sensitivity is such that the cell is not responsive to radiation from low-temperature bodies, so the radiation from the disc can be ignored. The amplitude of the signal can therefore be considered as a function of the target temperature alone. The chopper disc is made of metal and has suitably placed holes around its circumference. The hole diameter is not critical, but should be similar to the cell width. A signal waveform approximating to a sinewave is produced by spacing the holes with a separation distance equal to the hole diameter. If the effective area

of the cell in the design using the lens system is reduced to improve the target-diameter-to-distance ratio, then there must be a corresponding reduction in the hole diameter to maintain this sinusoidal output.

For a 16-hole disc, a motor speed of 3000 rev/min is required to produce a chopping frequency of 800Hz. The current drain of the motor is the main load on the battery supply, hence increased battery life can be obtained by underrunning the motor. There is the further advantage that brush noise is reduced. With the prototype model, the motor does not have a completely separate supply, and brush noise could be of prime importance. In practice, the chopping frequency is maintained at 350Hz. At this frequency, there is no loss in cell sensitivity, and low-frequency noise does not present a major problem.

With an ungoverned motor, the motor speed is controlled by using a constant-voltage supply. This takes the form of a simple series voltage regulator in which the e.m.f. applied to the motor is set by a potentiometer to give the required speed and thus chopping frequency.

ELECTRONIC SYSTEM

At a constant cell bias, the signal level increases by about 1000:1 over the desired temperature range (100 to 500°C). A linear amplifier is used to cover this 400degC span in five ranges, giving a nominal 14dB attenuation per range. The amplifier may be subdivided as follows:

1) Head amplifier, which is mounted close to the cell and has two main functions, that of gain compensation to correct the variation of cell sensitivity with temperature, and impedance transformation.
2) Main amplifier, which is a comparatively low-gain stage. The gain may be preset between the limits $\times 20$ and $\times 40$.
3) Variable gain amplifier which has a variable gain ($\times 1$ to $\times 10$), and provides a continuously variable overall gain setting to allow for target emissivities from 0·1 to 1.
4) Output amplifier which has negative current feedback and, in conjunction with a bridge detector, provides linear a.c. to d.c. conversion for the moving-coil meter readout.

Apart from the 120V h.t. cell bias supply, all circuits are powered by a common 12V l.t. line. Since this is a battery-operated instrument, the current drain is kept as low as possible. Although a stabilised 12V supply is used, the circuit employs extensive negative feedback so that variations in the line voltage may be tolerated. The chopping frequency is low, therefore filters would tend to be rather cumbersome. It has been possible to obtain a suitable bandwidth by means of high- and low-frequency attenuation at various stages in the amplifier.

Head amplifier

The head amplifier (Fig. 6.4) performs, as already stated, two main functions:

1) it provides the necessary high-impedance to low-impedance transformation;
2) in conjunction with a negative temperature coefficient thermistor, it provides variable gain to compensate for the decrease in cell sensitivity with increasing ambient temperature.

The unit is built into a small module and mounted close to the cell.

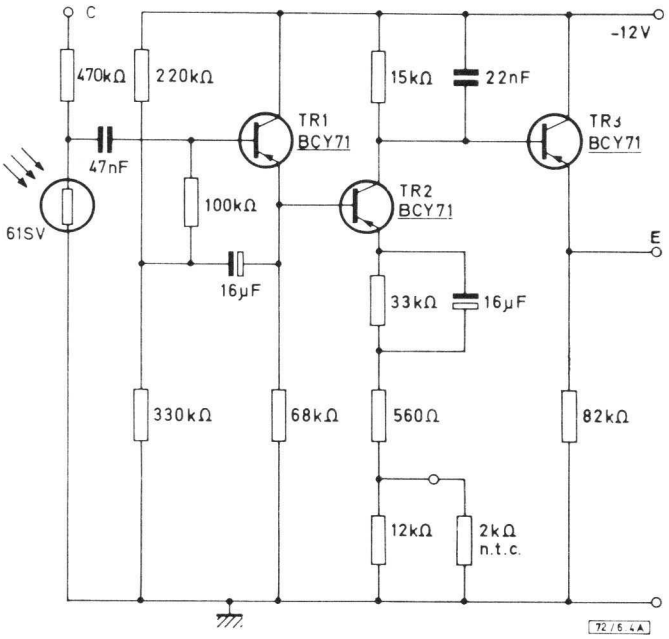

Fig. 6.4—Head amplifier

The circuit consists of three stages: an emitter follower TR_1, a variable-gain amplifier TR_2, and a further emitter follower TR_3.

The first stage, a boot-strapped emitter follower, provides a simple method of producing the high input impedance necessary for a source of 300kΩ. A high-gain, low-noise transistor (BCY71) is used in all stages. For an n-p-n circuit the transistor could be the BC109.

Low-noise conditions in the input transistor are achieved by using a low operating current (100μA) with a low collector-to-emitter voltage

(V_{CE} = 5V). Unfortunately, it is impossible to satisfy the other optimum low-noise condition by providing a source impedance of several kΩ. For this particular application, the performance is adequate, but for lower-noise performance, a field-effect transistor would provide a better solution. The transistor is biased at approximately 7V, and the 100μA current level is defined by an emitter resistor of 68kΩ. With a typical current gain of 100, the corresponding input resistance of the transistor is about 7MΩ.

The overall input resistance is kept high by boot-strapping the bias chain. This produces an effective increase in the value of the 100kΩ bias resistor of 1/(1—A). The emitter resistance R_E (68kΩ) is so much greater than r_e (250Ω) that the voltage gain A, given by $R_E/(R_E+r_e)$, approximates to unity. The output impedance ($Z = R_{source}/h_{FE}$) is low, approximately 3kΩ, and is therefore suitable for low-noise matching to the following stage.

This second stage is a variable-gain voltage amplifier incorporating negative feedback. The second stage also contributes significantly to the overall noise level and is therefore biased to low-noise conditions. With direct coupling, the base potential lies between 6 and 7V. A decoupled emitter resistor of 33kΩ sets a 200μA bias level. The decoupling capacitor of 16μF provides an impedance level of less than 50Ω at 350Hz, and the 200μA bias level a low value of r_e (125Ω). Both these values are considerably lower than the undecoupled emitter resistors which therefore predominantly determine the voltage gain.

A negative temperature coefficient thermistor forms part of the emitter load, so that as the ambient temperature increases the emitter load decreases. The gain of the amplifier, which depends on the ratio of collector load to emitter load, therefore increases, compensating for the decrease in cell sensitivity. The thermistor resistance must be of the order of several kΩ to have an adequate temperature coefficient. By using a 2kΩ thermistor and a comparable value of series resistor, the necessary temperature coefficient is obtained.

The input resistance with the undecoupled emitter load is greater than 100kΩ and produces a negligible loading effect on the previous stage. With a base potential of 6 to 7V and a collector current of 200μA, the maximum value of collector load that can be tolerated is 27kΩ. Under these conditions, the transistor is close to bottoming and the signal handling capacity is reduced. Since high gain is not a prime consideration, a lower resistance (15kΩ) can be tolerated, giving a corresponding improvement in signal-handling and a lower output impedance.

With the motor noise encountered in the prototype, a considerable amount of h.f. attenuation is required. This is provided at an early stage (before the amplifier becomes overloaded) by decoupling the collector

load. In this particular case, a 22nF capacitor has been used, but at the cost of reduced gain.

It is possible to couple from this stage directly to the main amplifier. However, with the remote head a low output impedance was deemed desirable to minimise electrical pick-up, consequently a further stage, an emitter follower, has been added.

Main amplifier

As with the head amplifier, the requirement for the main amplifier (Fig. 6.5) is to keep the design simple and compact. For this reason a circuit has been used which favours d.c. coupling between stages.

The first two stages of the main amplifier consist of a compound p-n-p/n-p-n amplifier (TR_4, TR_5) which has a high input impedance and a low output impedance. The input transistor (TR_4) is operated at a current level of 400μA at which the value of r_e (60Ω) is low compared with the emitter resistance. The variable control R_1 enables the emitter resistance to be set between the limits 270Ω and 770Ω. With a BCY71, the typical base current requirement at this level is 4μA. The bias chain current is significantly greater than this, that is, 60μA. Boot-strapping has been employed to keep the effective value of the bias resistor high.

The typical operating voltages of TR_4 are as follows:

at mid-point of base potential divider (V_{BB})	5·8V
at base (V_B)	5·4V
at emitter (V_E)	4·8V
at collector (V_C)	9·7V

The decoupled 12kΩ emitter resistor, being far greater than r_e, determines the current level of 400μA. The 32μF decoupling capacitor ensures that the impedance at 350Hz (20Ω) is far less than the emitter resistance.

The 5·6kΩ collector load of TR_4 sets the d.c. operating levels of TR_5. With a collector current of 400μA, the voltage drop across this load is 2·3V. If allowance is made for a base-emitter voltage V_{BE} of 0·6V, the potential drop across the emitter load of TR_5 is 1·7V. The 4·7kΩ load in turn defines the emitter current of TR_5 at about 300μA. The output voltage level is predominantly determined by this current and the collector load of 22kΩ, and is typically 7V. The additional voltage drop is that developed across the emitter resistance of TR_4.

At an operating level of 300μA, the value of r_e for TR_5 is about 70Ω, which, in conjunction with the high current gain ($h_{FE} \simeq 300$), provides an input resistance of 22kΩ. The 5·6 kΩ collector load of TR_4 therefore provides a low-impedance shunt path for the signal.

For simplicity, it may be assumed that all signal current flows into the base of TR_5 and that the effective current gain of the amplifier has been

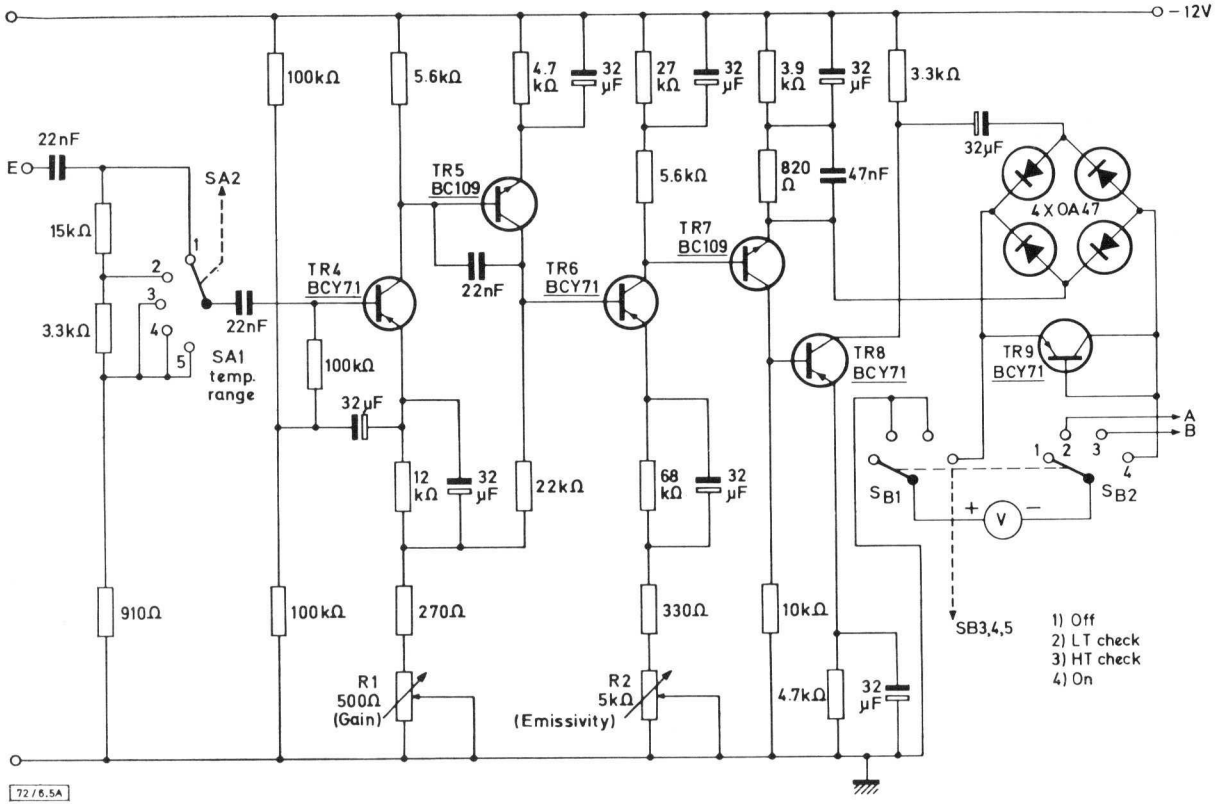

Fig. 6.5—Main and output amplifiers

proportionally reduced to 75. On this assumption the voltage gain may be derived as follows:

$$I_{b(5)} = I_{c(4)} = I_{e(4)}$$

where these are respectively the base current of TR_5 and the collector and emitter currents of TR_4. Therefore the input voltage V_{in} is given by the equation

$$V_{in} = R_E(I_{b(5)} + I_{c(5)})$$

where R_E is the emitter resistance and $I_{c(5)}$ is the collector current of TR_5. Thus the output voltage V_{out} is given by

$$V_{out} = R_E I_{b(5)} + I_{c(5)}(R_E + R_{c(5)})$$

where $R_{c(5)}$ is the collector resistance of TR_5. The value of $I_{b(5)}$ is very much less than that of $I_{c(5)}$ and can be neglected, so that the voltage gain A is given by

$$A = \frac{V_{out}}{V_{in}} = \frac{R_{c(5)} + R_E}{R_E}.$$

With the values shown in Fig. 6.5, measured gain has the limits 30 and 90 depending on the value of the variable resistor R_1.

With a high-gain transistor and an undecoupled emitter resistor, the input resistance of TR_4 tends to be high. The input resistance is increased to the 100kΩ order by the fact that the current multiplication caused by TR_5 increases the effective value of R_E (as presented to the emitter of TR_4) by the effective gain of TR_5. Although the actual collector load of TR_5 is high (22kΩ), the current multiplication in the circuit has the effect of reducing this value, by a factor equal to the effective gain of TR_5, to produce an output impedance of 300Ω.

The standing voltage of 7V at the output allows for direct coupling to the following stage. Initially, under the maximum-gain conditions of the complete instrument, this stage tended to be unstable. The instability was cured by connecting a 22nF capacitor between the collector and base of TR_5. This had the effect of reducing the gain limits to 20 and 40, which were tolerable but also introduced undesirable frequency selectivity. A more uniform frequency response has been obtained by introducing low-frequency attenuation at the input. This is accomplished by reducing the coupling capacitor to 22nF.

Variable gain stage

The output from the main amplifier is directly coupled to the following stage, which is a variable gain amplifier. The transistor (TR_6) is biased to a nominal 100μA level by the decoupled 68kΩ emitter resistor. At this

current, the value of r_e is 250Ω which, in conjunction with the 330Ω resistor, sets the minimum limit of emitter resistance at 580Ω (assuming that the control R_2 is set to zero). With a current gain of 100, the corresponding input resistance is of the order of 50kΩ, so that there is a negligible loading effect on the previous stage.

The variable 5kΩ emitter resistor (R_2) enables any required value of emitter resistance to be set between the limits 580Ω and 5·6kΩ. With a 5·6kΩ collector load, the gain of the amplifier (collector resistance/emitter resistance) may be correspondingly set between the limits 10 and 1. The decoupled collector load of 27kΩ in conjunction with the 5·6kΩ provides a required voltage drop of 3·3V so that this stage in turn may be directly coupled to the output amplifier.

Output amplifier

The output amplifier (Fig. 6.5) provides a moving-coil meter readout. The signal is rectified by a bridge, and the integrating action of the meter produces a d.c. level corresponding to the average value of the waveform. The rectifying diodes have a non-linear characteristic, therefore negative current feedback is used in the output stages to provide the required linearity.

The circuit used is a compound p-n-p/n-p-n amplifier (TR_7, TR_8) which is directly coupled to the previous stage. The potential drop across the collector load of TR_6 is 3·3V, which, with an allowance for a value of V_{BE} of 0·6V, sets the emitter load voltage of TR_7 as 2·7V. The total emitter resistance of TR_7 is about 4·7kΩ, so that the transistor is biased to a level of 0·5mA. If the 820Ω resistor were undecoupled, the input resistance of this stage would be high. With the 10kΩ load, the voltage gain (as given by collector resistance/emitter resistance) is about 10.

The d.c. voltage across the 10kΩ load is 5V, which sets the bias condition for TR_8. At the current level of approximately 1mA, the value of r_e of this device is low (25Ω), consequently the input resistance is low (2·5kΩ). This has the effect of reducing the gain of the previous stage to a nominal value of 2. However, with a collector load of 3·3kΩ this low value of r_e provides a high gain in TR_8, so that the overall gain, with no feedback, is about 250.

At various points in the overall system it has been necessary to introduce h.f. attenuation. By decoupling the 820Ω feedback resistor, h.f. boost can be introduced, thus improving the frequency response. This allows for a $\pm 10\%$ variation in chopping frequency.

Temperature ranges

The prototype instrument covers a temperature range of 100 to 500°C.

Over this range, the cell responsivity is such that the signal amplitude increases by a factor of 1000:1. This temperature span has been covered in five ranges, using linear amplification. The attenuation between each range is about 5:1. The first 20% of the scale reading is extremely non-linear, but for the remaining region (20% to 100%) the response is more open. Each range covers a typical temperature span of 80degC.

With this five-range instrument, a single linear meter scale is used in conjunction with a calibration chart. For a single-range or dual-range instrument, the meter could be scaled directly in temperature.

Attenuation of the signal can be accomplished by the following methods:

1) *Optical method.* The incident radiation of the cell may be attenuated by reducing the diameter of the light pipe. For targets at temperatures considerably above 500°C, this method is essential to prevent the cell from overloading.
2) *Cell sensitivity method.* Since the sensitivity is directly proportional to the cell supply voltage, attenuation may be introduced by reducing the cell supply.
3) *Resistive method.* The amplitude of the signal may be reduced by a simple resistive network.

In this instrument, two forms of attenuation have been used: the cell supply method (switch SA_2) up to the head amplifier, and the resistive method (switch SA_1) up to the main amplifier.

On the most sensitive range, the general order of r.m.s. output signal levels is:

Cell output	= 0·3mV
Head amplifier output	= 1mV
Main amplifier output	= 20mV

This gives 10% deflection on a 200μA meter, with an 820Ω feedback resistor providing about 20mV feedback. Attenuation is necessary before the head amplifier to prevent overloading. Attenuation before the main amplifier ensures that the input signal range is restricted.

Supplies

A commercial d.c. to d.c. converter (as used in the Philips portable transistorised d.c. millivoltmeter, type PM2430) is used to provide the stabilised 12V line for the electronic circuits. The converter can be operated either from four ordinary U2 (1·5V) cells or from four rechargeable nickel-cadmium (1·3V) accumulators. Provision has been made to charge the latter type in situ. The supply circuit is shown in Fig. 6.6.

The battery supply also provides the source for the motor supply regulator. The reference potential for this voltage regulator is derived from the stabilised 12V line.

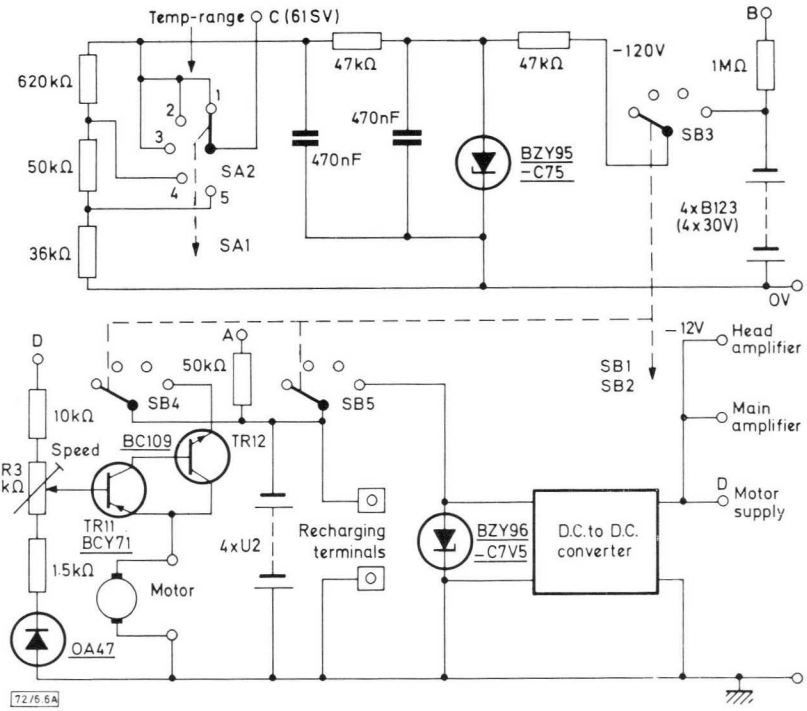

Fig. 6.6—Supply circuits

The cell supply is provided by four B123 (30V) batteries (Fig. 6.6), which can discharge to 90V without affecting the secondary reference of about 75V. This voltage is provided by a voltage regulator diode type BZY95–C75. An RC filter is used to minimise the noise generated in the reference diode. This is followed by a simple resistive chain which sets the required cell supply levels necessary for signal attenuation.

The state of both l.t. and h.t. supplies is indicated on the meter (2nd and 3rd contacts of switch SB). The minimum level is 88μA corresponding to 88V (h.t.) and 4·4V (l.t.).

USE OF INSTRUMENT

With the type of thermometer described, the temperature is derived from a measurement of the radiant power of the target. The instrument is initially calibrated against the radiant power emitted by a black-body

source. For such a target the radiant emission as given by the Stefan-Boltzmann law is exactly proportional to the fourth power of absolute temperature.

Since the radiant power increases much faster, proportionally, than absolute temperature, the calibration of this instrument over the temperature span 100 to 500°C is covered in five ranges (Fig. 6.7). There is the advantage in this scaling that the temperature discrimination, particularly in the lower ranges, is very good.

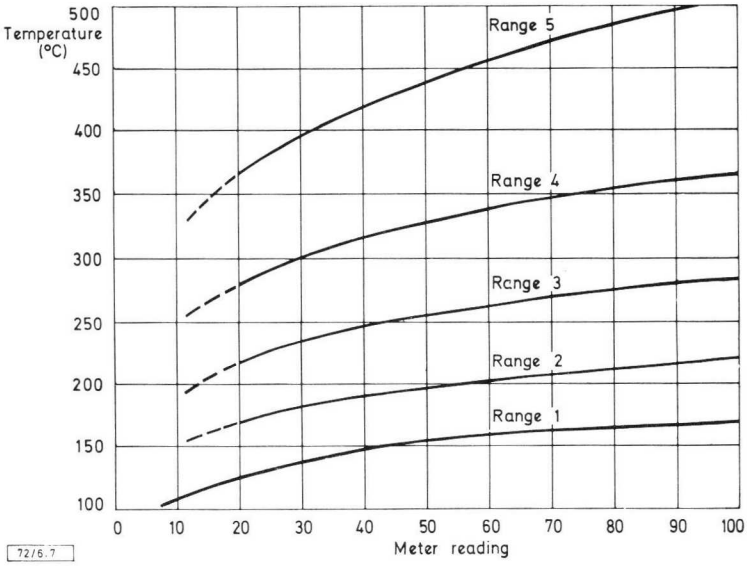

Fig. 6.7—Calibration graph of thermometer

Real bodies reflect or transmit radiation or do both, and are imperfect radiation emitters. The emittance of a real body (W) is always less than that of a black body (W_{bb}). Consequently the emissivity (ε) of a real body ($\varepsilon = W/W_{bb}$) is always less than 1.

The instrument should only be used with an emissivity setting of 1 when the target is simulating a black-body source. One standard method of doing this is to drill a hole in the target to produce a black-body cavity. This provides increased emittance because of the multiple reflections within the cavity; but to be effective, the hole depth should be typically six times the diameter. An alternative method is to apply a surface coating of a high-emissivity material such as colloidal graphite. The emittance of

colloidal graphite is typically 0·92 hence, with an emissivity setting of 1, there will be a 10% error in the scale reading. For some applications such an error in emissivity may be tolerated since this represents a much smaller temperature error (for example, 5degC at 275°C). However, to allow for greater accuracy if required, and also for targets of a much lower emissivity, a variable gain control has been incorporated to allow for target emissivities from 0·1 to 1.

For general-purpose temperature indication, where a high degree of accuracy is not required, the following emissivity values provide a guide. However, for accurate measurements or when the emissivity is not known, the particular emissivity must be measured. The usual method requires a direct measurement of true temperature with a simultaneous measurement with the radiation thermometer. The true temperature can be measured with a thermocouple or, where possible, by the radiation thermometer sighting into a black-body cavity.

Material	**Emissivity**
Aluminium	
smooth polished	0·1
smooth oxidised	0·2
Cardboard	
light coloured	0·4 to 0·8
dark coloured	>0·9
Ceramics	0·7 to 1·0
Copper	
smooth polished	0·04
smooth oxidised	0·7
Firebrick	0·7 to 1·0
Glass (commercial soda-lime, 150mm thick)	0·9
Graphite	0·65
Nickel	
smooth polished	0·15
smooth oxidised	0·9
Tungsten	
smooth polished	0·1
smooth oxidised	0·6
Wood	>0·8

EQUIPMENT SPECIFICATION

General

Detector	61SV, uncooled lead sulphide cell
Peak spectral response	2·2μm
Ambient temperature range	10 to 40°C
Accuracy	
Constant ambient temp	Better than 2%
Over ambient temp. range, 10 to 40°C	4%
Object temperature range	100 to 500°C in five ranges (upper limit may be increased)
Emissivity range	0·1 to 1
Target distance	
Light-pipe version	D/3 where D = target diameter
Lens version	Up to about 6m

Battery Supplies

LT	4 nickel-cadmium rechargeable cells (D.E.A.C., type BD2·5) or 4×1·5V dry cells
HT	4 dry batteries (Ever Ready, type B123) 30V

Operating Life

LT	40 hours continuous (per charging)
HT	200 hours continuous (per set of batteries)

CHAPTER 7

ROOM TEMPERATURE RADIATION THERMOMETER

The equipment described uses the ability of the uncooled indium antimonide photoconductive element, type ORP10, to measure the temperature of objects near room temperature by means of the energy radiated from them. The radiation is interrupted at about 600Hz by a mechanical chopper driven by a clockwork motor. The resulting alternating signal from the cell is amplified by a wideband amplifier of flat response so that variations in chopping frequency do not affect the amplitude. The amplified signal is then mixed with a signal corresponding to room temperature. Finally a phase-sensitive rectifier, deriving its reference signal from the interruption of a secondary beam of radiation (between a BPX25 detector and CQY11A emitter) by the chopper blade, rectifies the signal to produce a direct current through the meter.

OPTICAL SYSTEM

For demonstration purposes it was decided that the instrument be built in the form of a clinical thermometer, covering the range 30 to 40°C, intended for the measurement of the temperature of the external auditory canal (which has been shown by Bowling Barnes (Ref. 2) to approach closely that measured orally). To define the area of measurement, a steel light-guide of diameter 10mm and length 80mm is used.

The radiation from the target is chopped by a disc having radial slots before falling on the cell. Thus the cell 'sees' alternately the target and the chopping disc. If the chopping disc is at room temperature, the amplitude of the radiation signal received by the cell is given by the following expression, which takes no account of reflections:

$$\sigma(T_2^4 - T_1^4)A_1A_2/\pi d^2$$

where

σ = Stefan-Boltzmann constant $\simeq 5{\cdot}7\times10^{-12}\text{Wcm}^{-2}\text{degK}^{-4}$
T_2 = target temperature (K)
T_1 = ambient temperature (K)
A_1 = area of cell (cm^2)
A_2 = cross section of pipe (cm^2)
d = length of pipe (cm)

When internal reflections in the pipe are taken into account, this is further multiplied by a factor

$$\left(1+\frac{8r}{1-r^2}\right)$$

in which r is the reflectance of the pipe.

For a target at 35°C in an ambient of 20°C, and given a reflectance of 0·75, the amplitude of the radiation signal falling on the ORP10 detector is about 200μW. From the spectral response curve given for the ORP10 and the black-body emission curve for 35°C, it is seen that about 4% of the incident signal has effect on the cell. Thus the accepted radiation is about 8μW which, with the cell biased at 10mA (for long battery life), will give rise to an electrical signal of 2μV for a typical cell.

THERMAL CONSIDERATIONS

To obtain an absolute measurement of temperature, it is necessary both to measure the difference between the temperature of the chopper blade and the temperature of the target, and to measure the temperature of the chopper blade (assumed ambient). The previous section indicated the correlation between the difference temperature and the signal from the cell under fixed ambient conditions. However, as ambient temperature changes, both the sensitivity and resistance of the cell vary. Changes in sensitivity may be compensated by adjusting the gain of the amplifier; variations in resistance affect the gain. Preliminary investigations show that these effects tend to cancel approximately, and the residual variation was within the error of experiments.

The measurement of ambient temperature is performed by an n.t.c. thermistor in an attenuating network.

ELECTRICAL CONSIDERATIONS

Since the a.c. signal from the detector (Fig. 7.1) is small, the system as a whole must not introduce noise. To this end, the motor driving the chopper blade, being necessarily close to the detector in a small instrument, is clockwork. This has two advantages: electrical noise from commutators and changing magnetic fields is obviated, and battery life is considerably

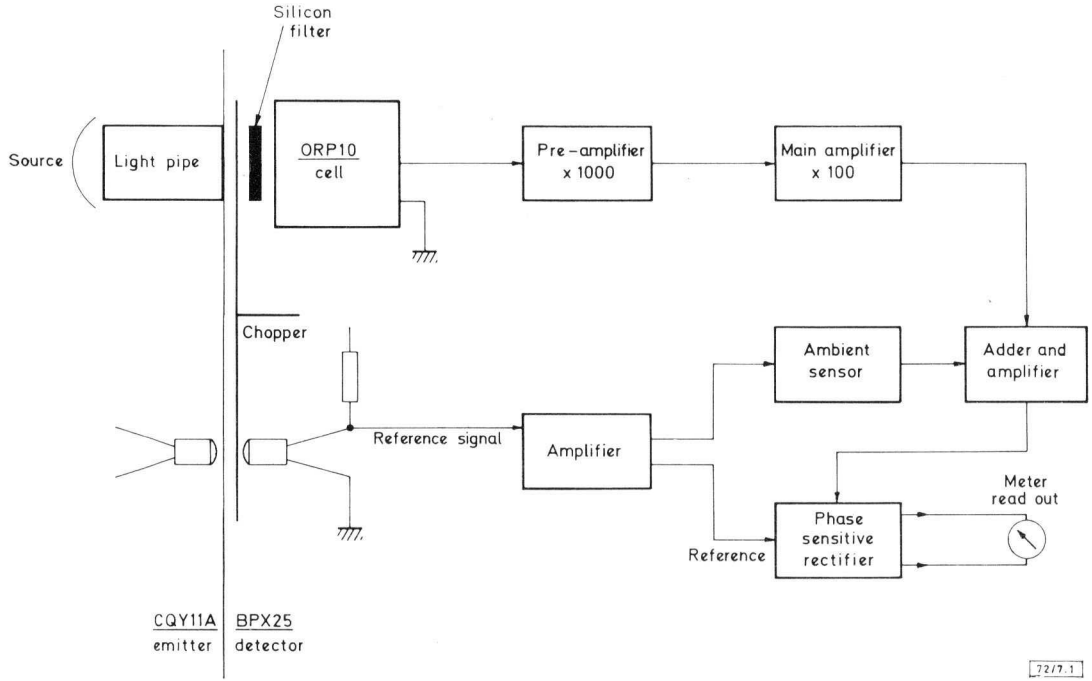

Fig. 7.1—Room temperature radiometer

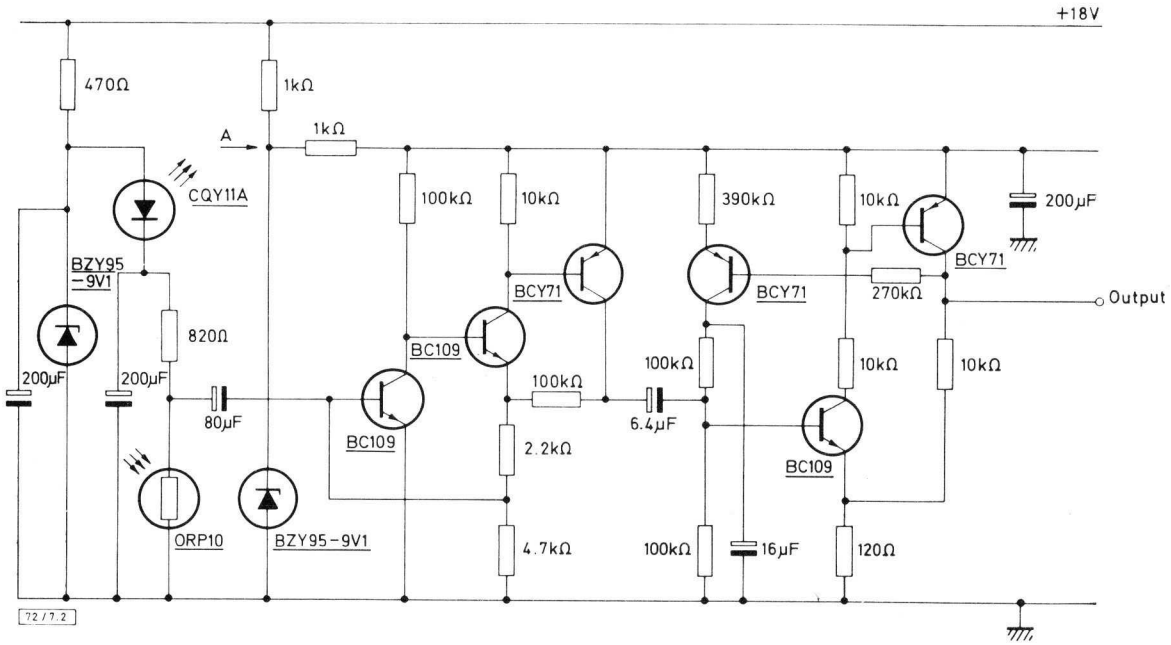

Fig. 7.2—Cell bias, preamplifier, and main amplifier

lengthened. A major disadvantage is the variation in chopping frequency as spring tension alters, so that a narrow-band amplifier (with a corresponding low noise) cannot be used. However, this difficulty is overcome and, in fact, turned to advantage, by the use of a phase-sensitive rectifier in conjunction with a wideband amplifier. This produces the required narrow bandwidth while the fundamental frequency can vary considerably. The output is in a form that can readily be turned into a meter reading.

The phase-sensitive rectifier requires a reference signal which switches it at the correct phase relative to the chopper blade. This is provided by the two devices, the CQY11A, which is a gallium arsenide emitter, and the BPX25 phototransistor acting as the detector. The reference signal, when amplified, is also used in the sensing of ambient temperature.

Cell bias, preamplifier and amplifier

The bias current for the cell is chosen to be 10mA to keep the size of batteries to a minimum while retaining a reasonable battery life. A stable low-impedance supply (Fig. 7.2) in the form of a decoupled 9V voltage regulator diode is used to provide the current, which incidentally is passed through the CQY11A emitter and further decoupled.

The preamplifier is a three-transistor amplifier combining a virtual-earth amplifier with a feedback pair. This has a very low input impedance, and the gain depends inversely on the cell resistance. Since both the sensitivity and resistance of the cell decrease with increased temperature, some degree of compensation is afforded.

The preamplifier is coupled to a further feedback pair amplifier having a gain of 80, and an output impedance of 150Ω.

Reference signal amplifier

The chopped radiation falling on the BPX25 detector (Fig. 7.3) produces a signal of 10mV across the 10kΩ load resistor. This is amplified by a factor of 100 by a conventional amplifier. The preset emitter resistor allows adjustment of the shape of the output signal so that the waveform crosses the mean level symmetrically.

Ambient sensor and adder circuit

Both the ambient sensor and adder circuit (Fig. 7.4) use the differential amplifier technique. The reference signal is fed to both sides of the first differential amplifier via both a fixed preset attenuator chain and a temperature-dependent (n.t.c. thermistor-controlled) chain. The preset control R_3 is adjusted to feed through the correct amount of reference signal variation relative to the radiation signal. The preset resistor R_2 is adjusted to back off excess reference signal and radiation signal so that the meter

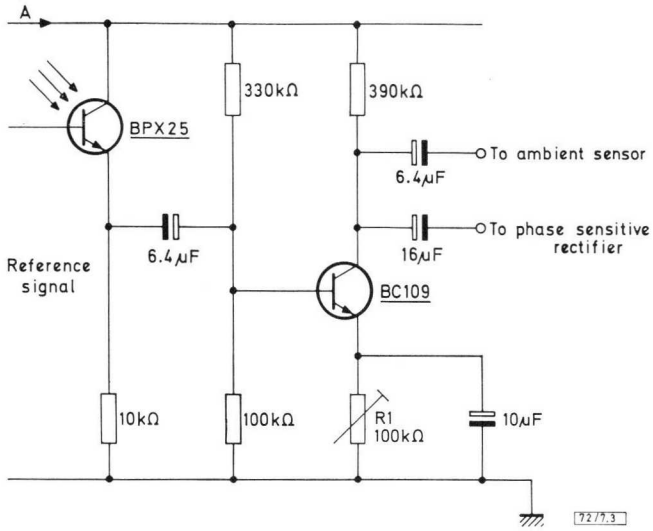

Fig. 7.3—Reference signal amplifier

range starts at 30°C. A voltage gain of 5 is incorporated to match the output level of the ambient sensor with the radiation signal.

The output from the ambient sensor is taken from the collector which is 180° out of phase with the radiation signal. By feeding this and the radiation signal into opposite sides of the second differential amplifier, the output corresponds to the sum of the two signals. The preset control R_4 in the output collector provides adjustment of gain to set the meter range correctly.

This is followed by a feedback pair amplifier (Fig. 7.5) having a gain of 10 and low output impedance (100Ω) suitable for feeding the phase-sensitive rectifier.

Phase-sensitive rectifier

The reference signal switches the transistors ACY21 and OC140 on and off alternately, 180° out of phase since one is a p-n-p device and the other an n-p-n device (Fig. 7.5 and Ref. 3). When one is short-circuited, the signal current flows in one direction through the meter. At the end of half a cycle, the conditions are reversed, but so also is the sense of the signal. Hence signal current flows through the meter in the same direction at all times, except when the target temperature is lower than the 30°C threshold. The capacitor across the meter reduces the bandwidth of the system to about 10Hz with the result that noise is considerably reduced.

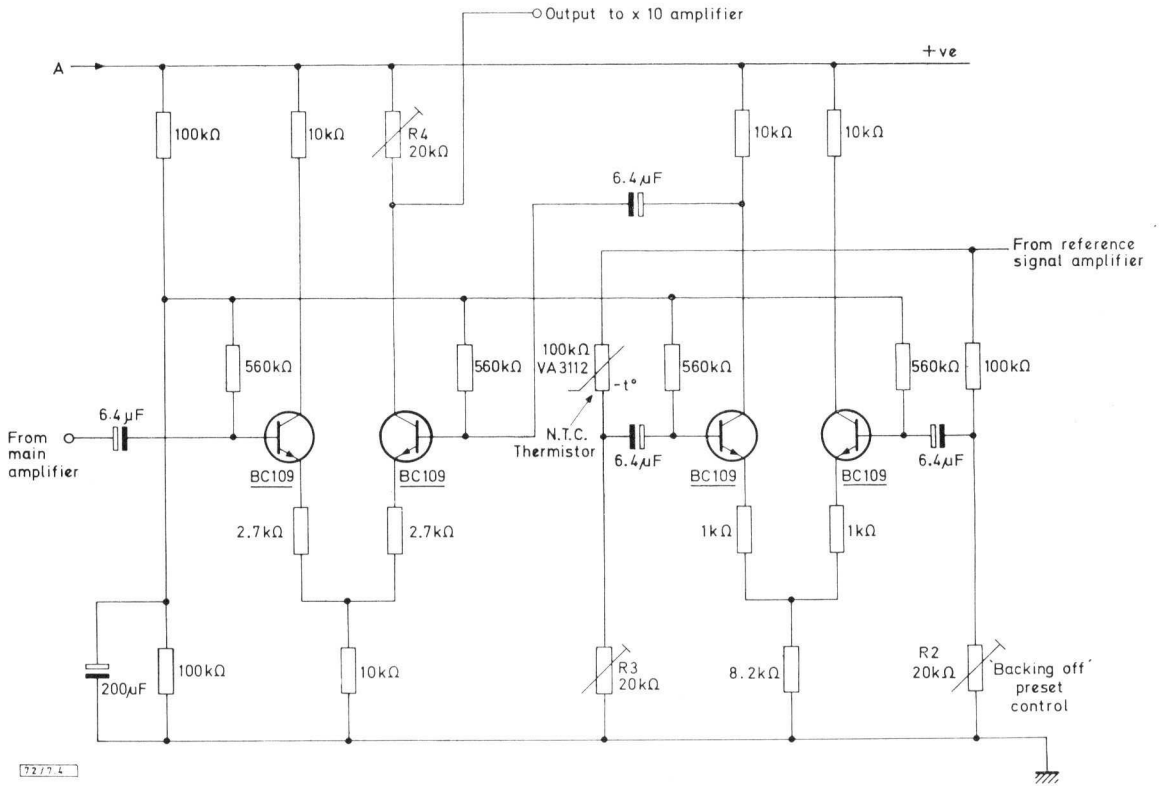

Fig. 7.4—Ambient sensor and adder circuit

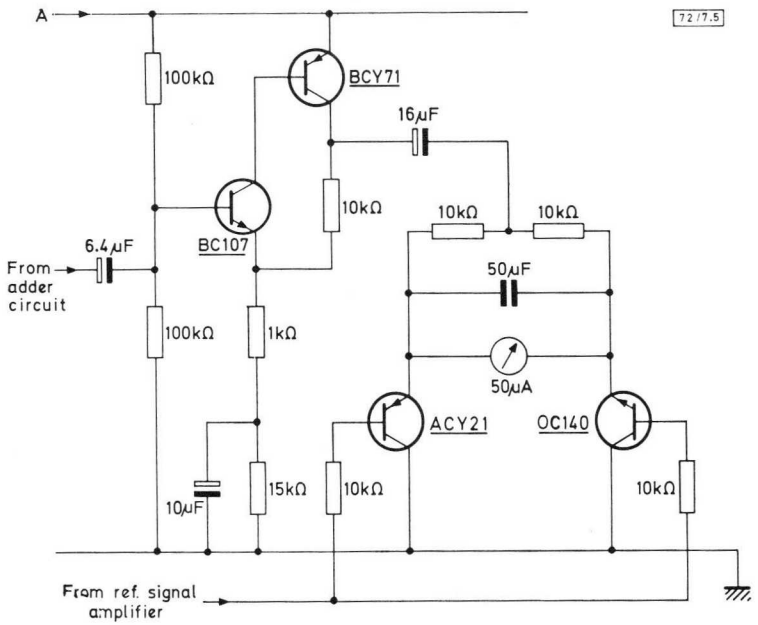

Fig. 7.5—Amplifier ($\times 10$) and phase-sensitive rectifier

CHAPTER 8

INFRARED MICROSCOPE FOR TEMPERATURE MEASUREMENT OF SMALL AREAS

The infrared microscope described was developed primarily to examine the temperature distribution over the surface of transistors and integrated circuits. The instrument incorporates an RPY51 indium antimonide infrared detector.

MICROSCOPE LAYOUT AND OPTICAL SYSTEMS

The optical and mechanical arrangement of the system are shown in Fig. 8.1. The microscope optical system is very simple, consisting of a single objective and an eyepiece, through which the specimen is viewed in the ordinary way.

An infrared image is formed by interposing a semi-transparent mirror, angled at 45°C, in the microscope column: this mirror reflects the infrared radiation and transmits light for normal viewing. Both image planes are arranged to be at the same distance from the objective, so that the images are focused together and are the same size.

A second mirror is used to deflect the infrared image through 90° so that the RPY51 detector can be mounted vertically. This has been done to enable liquid nitrogen to be poured directly into the cell dewar. The dwell time of the dewar is 15 minutes, so that the equipment is generally used with an automatic Leiden-Frost liquid transfer system.

The reflecting material used on the semi-transparent mirror is a thin gold film. This is very reflective at infrared wavelengths and has a high transmission at visual wavelengths. All the mirror surfaces in the system must have the reflecting material deposited on the incident radiation side to prevent attenuation by the glass or base material of the mirror. A silicon filter (cut-off from 2μm and shorter wavelengths) is placed in the infrared path between the two mirrors to attenuate reflected visible radiation from the microscope viewing lamp.

The RPY51 infrared detector is situated in the infrared image plane,

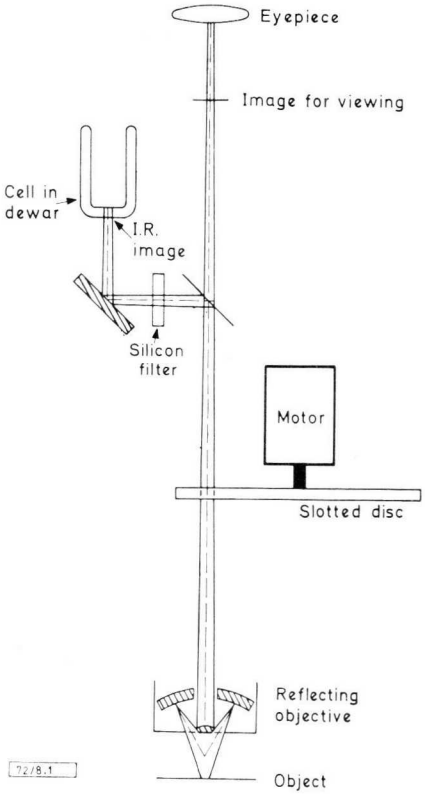

Fig. 8.1—Infrared microscope

and lateral adjustments are provided to facilitate moving the cell into the correct position. At the centre of the field of the visual image, two pairs of parallel lines cross at right-angles to form a square of the same size as the detector (the RPY51 is a 0·5mm square). The cell must be adjusted to occupy the same position in the infrared image as the crossed lines occupy in the visual image.

The type of objective used on the microscope is a Beck reflecting objective designed for use at 15× magnification. Because a mirror objective is used, the problem of finding a lens material of suitable transmission at the appropriate infrared wavelength (5μm) has been avoided.

A further addition to the normal microscope system is a chopper disc introduced into the microscope column. Because the chopper is used, the output of the RPY51 can be connected to an a.c. amplifier, so that a high degree of amplification can follow the cell. The edge of the disc

is cut to have 16 radial slots which produce a signal of 1:1 mark-to-space ratio. The disc is driven by a synchronous motor running at 3000rev/min to give a basic signal frequency for the entire system of 800Hz.

DEVELOPMENT OF ELECTRONIC SYSTEM

When the type of amplification system to be used with the microscope was considered, it was decided that some form of nulling by feedback would be advantageous. The two possible lines of approach are shown in Fig. 8.2.

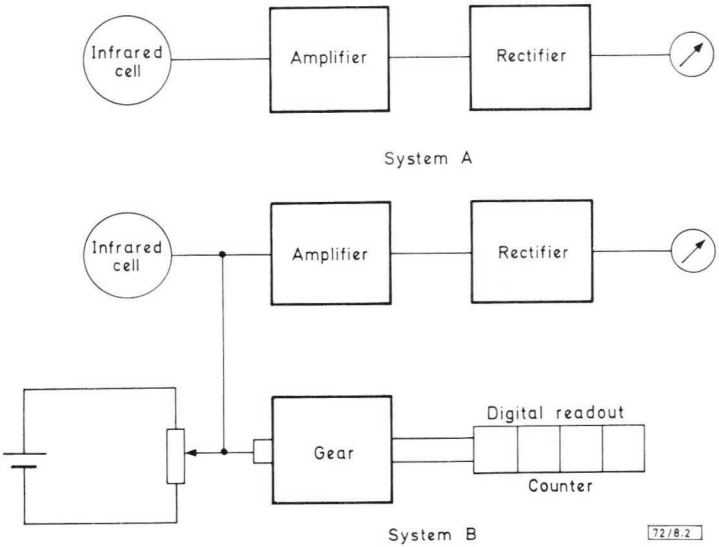

Fig. 8.2—Two amplifying systems

System A is the straightforward open-loop amplifier method; System B shows the nulling method where the meter output is reduced to zero and the position of the potentiometer is proportional to the signal at the nulling point.

System B has the following advantages:

1) The problem of amplifier dynamic range is overcome. The dynamic range required can be met by choosing an appropriate voltage across the potentiometer for the maximum level, and a high resolution potentiometer for good resolution at the lowest level.
2) Amplifier gain changes will not have a first-order effect on the output accuracy.

3) Resolution is a maximum at all levels of input because of the effectively great length of scale of the output meter (or counter); that is, small changes in cell output will be equally apparent at high and low levels of output.

There are, however, several practical problems with a nulling system. The cell output is a.c., so the feedback signal must be an exactly similar waveform to produce zero input to the amplifier: at high cell output levels in particular, this is a difficult requirement to meet. Nulling will also be difficult if there is excessive noise at the amplifier output. It will therefore be necessary to limit the bandwidth to some extent.

To obtain a good zero, it was decided to make this a d.c. point. This immediately necessitates a compromise in that there must then be some amplification and rectification outside the loop, the system being dependent on this for accuracy.

The cell output level is too low for immediate rectification, and amplification is necessary first. The gain of this first amplifier should therefore be just sufficient to bring the signal up to a level suitable for rectification; this will then ease the problem of keeping the gain stable by application of negative feedback.

Use of phase-sensitive rectifiers

An ordinary diode bridge rectifier is not suitable for use in this circuit. The forward voltage drop of the diodes makes them unsuitable for low-level operation.

A phase-sensitive rectifier using transistors will function at the millivolt signal level and is ideally suited for this application. This type of rectifier also provides a convenient means of reducing the bandwidth to almost any desired degree.

The phase-sensitive rectifier requires an a.c. reference voltage which must be of the same frequency and in the same phase as the signal. This reference is available from the mechanical chopper disc when a lamp and photocell are arranged on either side of it at some suitable point to give the correct phase. This method of bandwidth limitation has the advantage that if the signal frequency alters, then the reference will also change, and there is no change in the d.c. output level of the rectifier. The whole system can therefore be made immune to changes in chopper frequency. To achieve this, however, there must be no phase-shift in the amplifier preceding the phase-sensitive rectifier as this will cause a drop in the d.c. output. The bandwidth of the amplifiers must therefore be sufficient to ensure that over any possible change of chopper frequency, no phase-shift

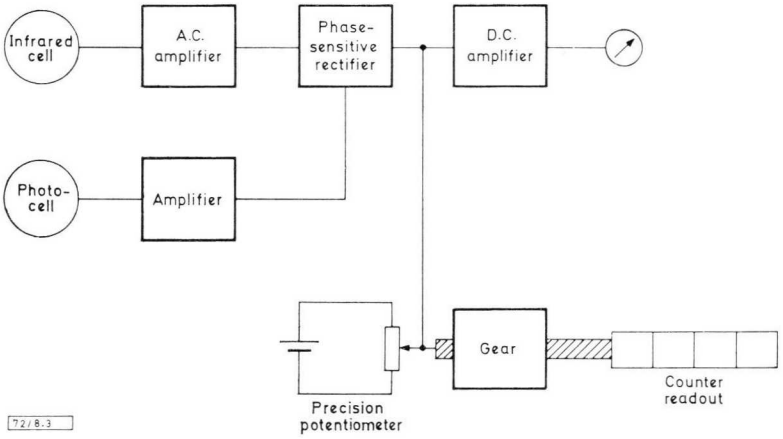

Fig. 8.3—Nulling system

will be introduced. The block diagram has now been developed into that shown in Fig. 8.3.

Automatic read-out

It is now an obvious step to close the mechanical loop by dispensing with the meter and substituting a motor which drives the potentiometer automatically to zero output, thus making a nulling servo-indicator. A small permanent-magnet d.c. motor is well suited to this application.

In the system built, it was decided to use a commercially available mechanical digital voltmeter which contained the potentiometer, counter, motor, motor-amplifier and gearing. The motor used in the voltmeter is an a.c. 50Hz two-phase type.

Second amplifier

The d.c. amplifier in Fig. 8.3 is of the same type as the first amplifier except that the input to it is chopped (modulated) and the output is phase-sensitive rectified. The modulators and phase-sensitive rectifiers have virtually the same circuit.

Meter read-out

An independent meter readout was required and this was calibrated directly in temperature (black body). It is fed from a straight-through amplifier system with the potentiometer feedback switch out. The complete block diagram is shown in Fig. 8.4.

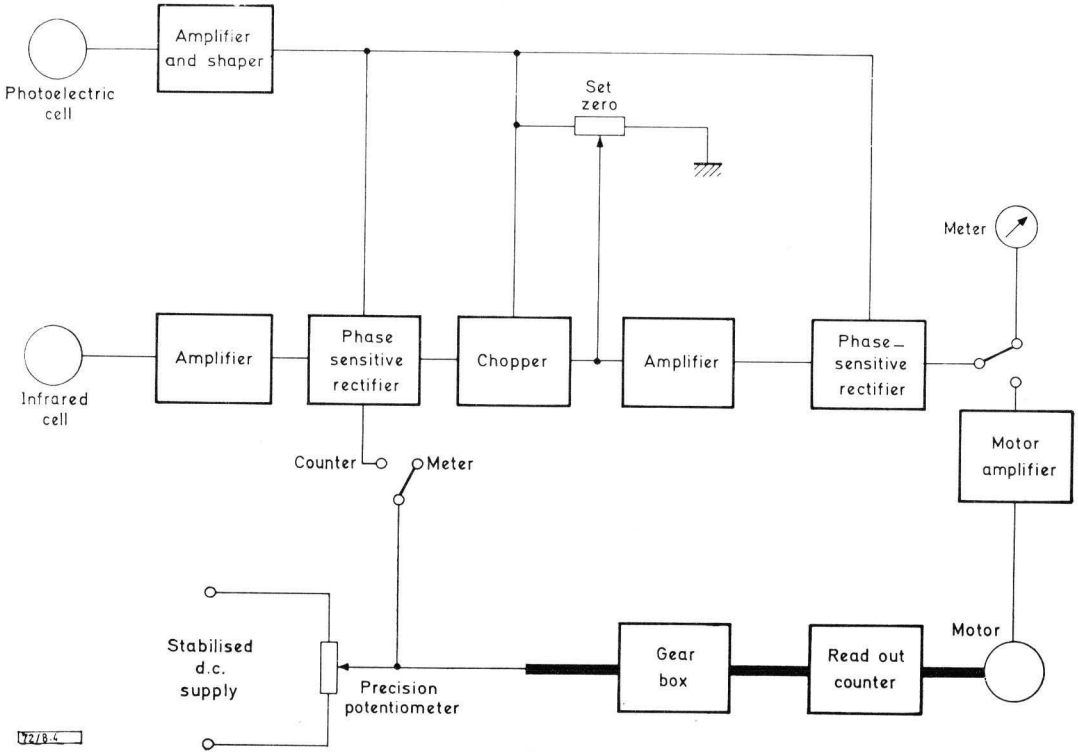

Fig. 8.4—Complete nulling system

Zero set

The reference signal is derived from the output of a phototransistor (BPX25) which is amplified and squared. There is also a preset control to adjust the mark-to-space ratio to be an exact square wave. The phase-sensitive rectifiers and modulators are all full-wave circuits, which means that two reference signals are required, one in antiphase with the other. Their voltages are stabilised by a voltage regulator diode and suitably attenuated, and are used for zeroing the system.

The output from the cell depends on the difference between the radiation from the chopper blades and the radiation from the object under investigation. Since the system is phase-sensitive, if the infrared radiation from the object is less than that from the chopper blades the output voltage will be negative; and if the object radiates more, the output will be positive (Fig. 8.5). Thus, if a square-wave backing-off voltage is injected into the

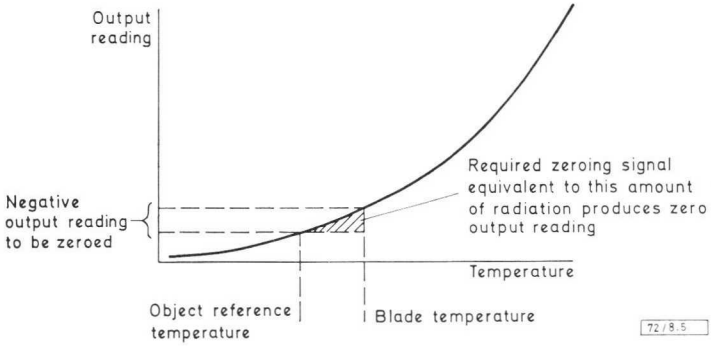

Fig. 8.5—Effect of zeroing method

system, the system can be zeroed at any object temperature, so that any temperatures above the chosen zero level will give a positive output reading. This is possible only with a phase-sensitive system.

PHOTOCELL AMPLIFIER CIRCUIT

The functions of the photocell amplifier (Fig. 8.6) are to amplify the photocell signal to produce a square wave of 1:1 mark-to-space ratio, and to provide two outputs in antiphase as reference signals for the full-wave phase-sensitive rectifier.

A mark-to-space adjustment potentiometer is included, and supply voltages are stabilised by means of a voltage regulator diode, so that the output voltage amplitude remains substantially constant. This is important

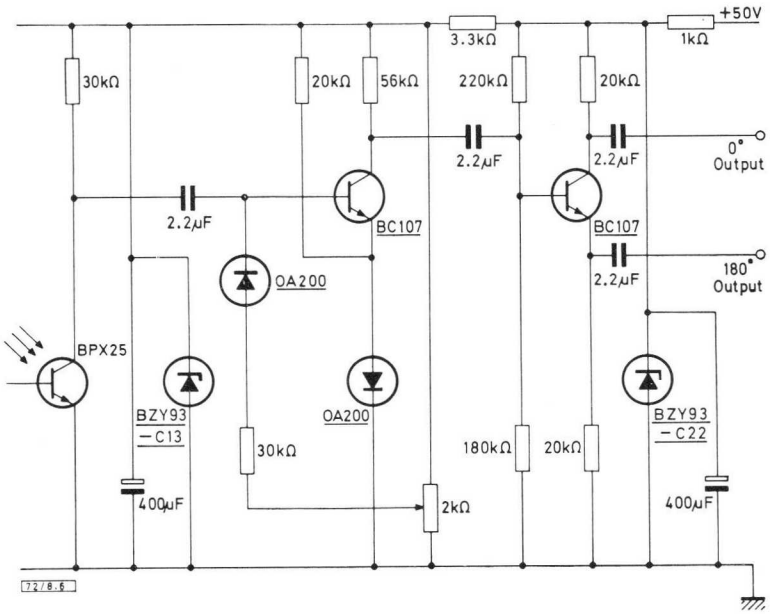

Fig. 8.6—Photocell amplifier and pulse shaper

since the output from this circuit is also used to provide the zero adjustment for the system. The high supply voltage has been chosen because of the drive requirements of the insulated gate FET chopping transistors used in the phase-sensitive rectifiers.

AMPLIFIER CIRCUIT

The two amplifiers in the system are of similar design, and the circuits are shown in Figs. 8.7 and 8.8. The two major design considerations are low noise and stability of gain. BC109 transistors are used; these, when operated at a collector current of between 100μA and 200μA, and with an effective source resistance of 2kΩ, have a very good noise characteristic.

The resistance of the RPY51 is between about 1 and 2kΩ, so that this is suitable for feeding directly into the amplifier. Cell biasing is shown in Fig. 8.7 and this is simple constant-current feed from the stabilised 50V supply.

To achieve good gain stability, a large amount of negative feedback is essential. The accuracy of the basic two-stage amplifier is reasonably

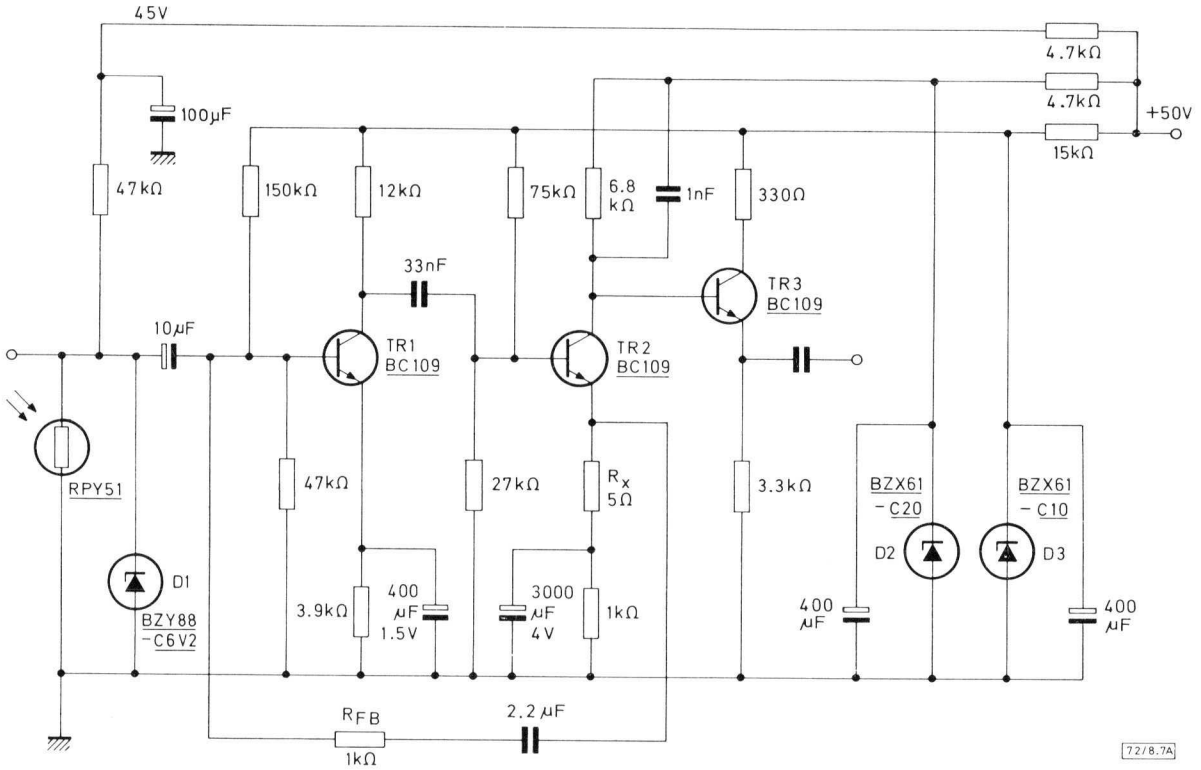

Fig. 8.7—Cell amplifier

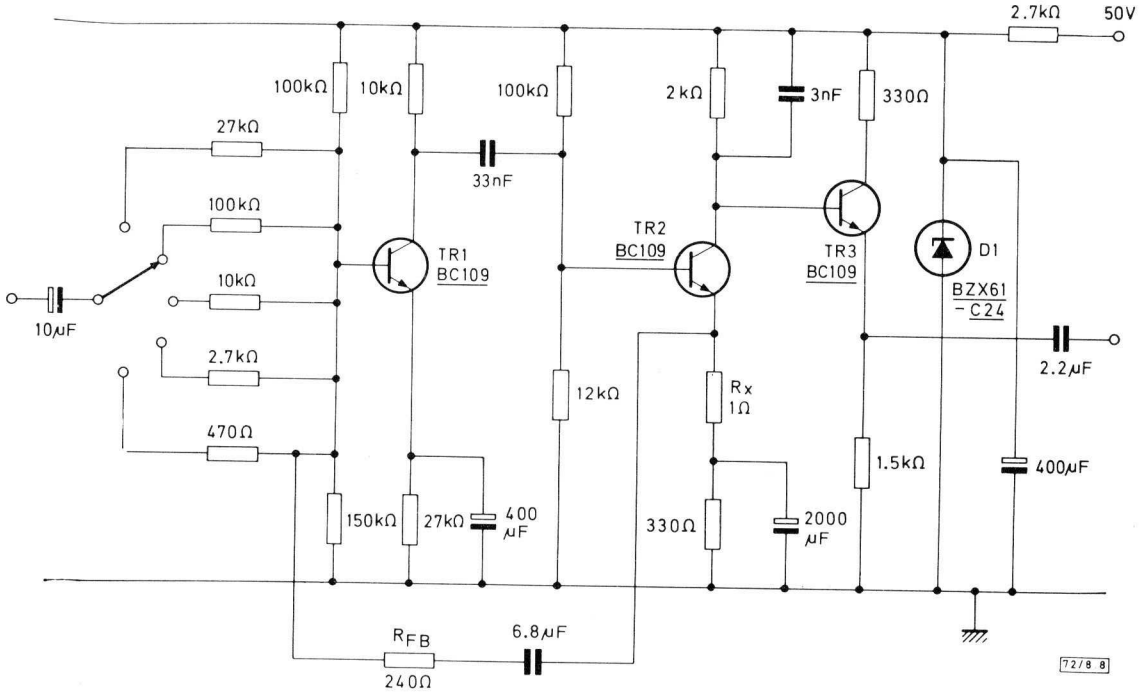

Fig. 8.8—Second amplifier

good. The stability of the current gain of the circuit is good, but this performance is degraded to some extent by the possibility of variations in input impedance. There is, however, some compensation for this effect, as the input to the amplifier from the cell does not represent a voltage drive. If it were a perfect current source then, of course, variations of input impedance would have no effect on amplifier gain.

In predicting what accuracy is to be expected in practice, it is necessary to decide on the worst-case conditions. Production spreads in transistor characteristics are such as to alter the gain of this type of amplifier by several per cent, but since any instrument that is built will be calibrated, this effect was not included in the worst-case considerations.

The two factors affecting gain stability are temperature and ageing. Temperature will change the values of h_{FE}, r_e, and V_{BE}. The change in V_{BE} is -2mV/degC. The value of h_{FE} increases by 1% per degC. The value of r_e increases proportionally with absolute temperature. The change in r_e tends to reduce the effect of changes in h_{FE} and V_{BE}, the latter two tending to increase the stage gain, the former actually producing more negative feedback.

The expression for current gain G_i of this amplifier is:

$$G_i = \frac{A}{1+\frac{AR_x}{R_{FB}}},$$

where A is the open-loop current gain of the amplifier. To convert A to voltage gain G_v, the current gain G_i must be multiplied by the ratio of output resistance to input resistance. The input impedance Z_{in} to the amplifier is given by:

$$Z_{in} = R_{in} + \frac{r}{1+\frac{AR_x}{R_{FB}}},$$

where R_{in} is the external series resistance and r is the effective input resistance into the base of the transistor; at room temperature r is given by the equation:

$$r = h_{FE}(25/I_e)$$

where I_e is measured in mA. The expression for Z_{in} shows that the summing point of the amplifier is not a perfect 'virtual earth'. Thus the true voltage gain G_v of the amplifier is given by:

$$G_v = G_i \frac{R_o}{R_{in} + \left(\frac{r}{1+A\frac{R_x}{R_{FB}}}\right)}$$

where R_o is the collector load of TR_2 in Fig. 8.7 or Fig. 8.8.

Variations in the voltage gain of the amplifier are caused partly by current gain variations in the amplifier and partly by variations in input impedance. These effects are additive. Thus, if amplifier gains fall slightly, the input impedance increases. However, because of the loading of the cell voltage by the amplifier input impedance, the cell output voltage rises, thus reducing the effect of gain variations. If the cell output were a constant current, changing input impedance would have no effect. This effect can be seen from the expression for cell voltage, V_{in}, in terms of cell resistance R_{cell}, and amplifier input impedance Z_{in}, given below.

$$V_{in} = Z_{in} I_{bias} \left(\frac{Z_{in}}{R_{cell} + Z_{in}} \right) .$$

The input to the amplifier is thus proportional to Z_{in} $(R_{cell} + Z_{in})$. The cell voltage is then the effective input voltage to the amplifier.

If the circuit were to contain BC109 transistors of low value of h_{FE}, and if the value of h_{FE} were to increase by 50%, the resulting increase in amplifier voltage gain would be 4·5%. This has been calculated from the above equations.

The top response is limited by the shunt capacitor across the collector load of TR_2 of each amplifier; the low-frequency response is limited by the amplifier input capacitor. The frequency characteristic of the amplifiers is equivalent to about a 15% fall-off in an 800Hz square wave at the output of the amplifier; this is considered to be acceptable for the waveforms in the system.

This amount of droop in the waveform results in a change of d.c. output from a phase-sensitive rectifier when there is a change of signal frequency. A frequency change of 6% (the most that would be expected of the 50Hz mains) would cause a change of output from a phase-sensitive rectifier of 0·5%.

PHASE-SENSITIVE RECTIFIER AND CHOPPER

The type of phase-sensitive rectifier used consists of four switching transistors arranged in a bridge (Fig. 8.9). These operate in a similar manner to the diodes in a bridge rectifier, the difference being that, whereas the diodes are switched by the a.c. signal to be rectified, the transistors are switched on and off by an independent reference signal of fixed frequency and phase.

Thus, the phase-sensitive rectifier will produce a d.c. signal only from a signal of the same frequency and phase as the reference. The d.c. output from this circuit would normally have a floating level between the appropriate two points of the bridge. However, to obtain an output relative to

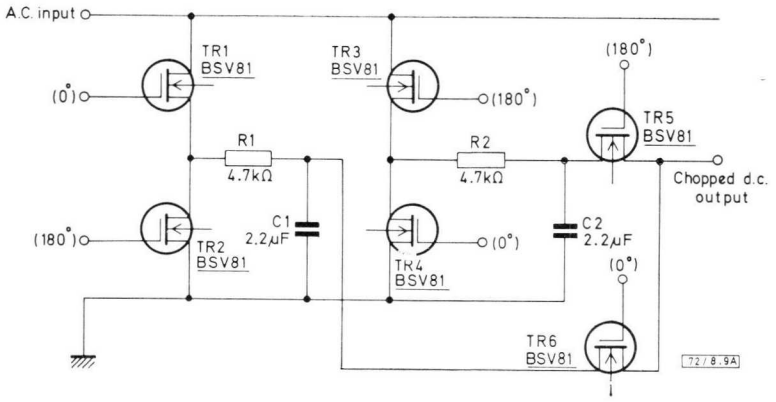

Fig. 8.9—Phase-sensitive filter

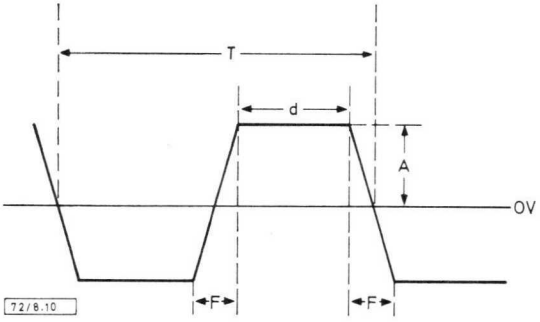

Fig. 8.10—Waveform of chopped radiation

chassis, two halfwave outputs are taken, as shown in Fig. 8.10, one being positive and the other negative.

The a.c. output from the first amplifier is fed into the phase-sensitive rectifier which then provides a d.c. signal which is used for comparison with the d.c. feedback from the potentiometer. The phase-sensitive rectifier also serves as a narrow-band filter when followed by a chopper and further a.c. amplification.

The type of transistor used is the insulated gate FET type BSV81. With the bridge arrangement and the following two chopper transistors, all the switching ON and OFF operations are carried out by one transistor in series and another in parallel. With this type of connection, noise generated when the series transistor is cut off is reduced by the parallel transistor being conductive.

The bandwidth of the circuit can be adjusted by altering the smoothing time-constant. The bandwidth is given by $1/\pi CR$, and the bandwidth is

defined as between the points where the d.c. level has fallen to 0·707 of the value at chopping frequency.

There is also a waveform change from the a.c. input to the a.c. output of the filter, the output always being a square wave.

If the input is assumed to be a sinewave of peak value V, then the d.c. output V_{dc} at each half-wave point is V/π. Since there is a positive and a negative output of this value, the peak-to-peak value of the output waveform is $2V/\pi$. Thus the attenuation of a sinewave input measuring peak-to-peak at input and output is $1/\pi$ or 0·32. This is correct only if the output loading is a high resistance compared with the resistance in the filter. The waveform from the cell is of the form shown in Fig. 8.10. The attenuation of this waveform by the phase-sensitive filter is given by

$$\frac{V_{out}}{V_{in}} = \frac{\left(\frac{F}{2}\right)+d}{T}.$$

The first phase-sensitive rectifier has RC values of 4·7kΩ and 2μF. This gives a calculated bandwidth of 15·5Hz each side of chopper frequency.

Both amplifiers have a bandwidth of 20kHz. The phase-sensitive rectifier at the output feeds directly into the readout system and has the same circuit configuration as transistors TR_1 to TR_4 in Fig. 8.9. The time-constant is chosen to give a bandwidth of ±1Hz.

GAIN OF COMPLETE SYSTEM

The open-loop microscope system gain from input to meter is shown in the block diagram in Fig. 8.11. The gain shown in the first phase-sensitive rectifier block is for a sinewave input. Thus, for a 1μV peak-to-peak sinewave input, the open-circuit output voltage is 77mV d.c.

If a 100μA meter having 1·5kΩ coil resistance is used at the output, and the output resistor of the phase-sensitive rectifier is also 1·5kΩ, then the output current will be given by the equation

$$I_{out} = \frac{0{\cdot}077}{3\times 10^3} A \simeq 25\mu A.$$

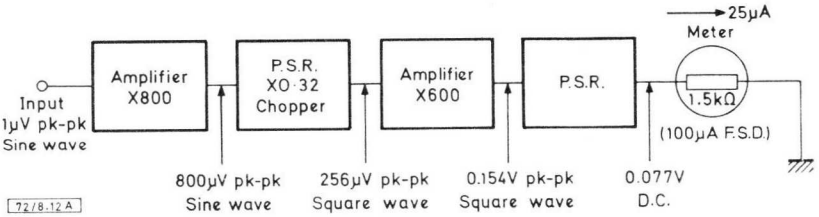

Fig. 8.11—Overall system gain

EQUIPMENT SPECIFICATION

Detector

Type	RPY51, indium antimonide cell
Operating temperature	77K
Cooling system	Drip-feed mechanism fed from liquid nitrogen dewar

Optical

Objective magnification	15×
Spot size	30μm
Visual field of view	1mm diameter
Working distance	24·3mm

Electrical

Bandwidth	
Normal chopping mode	4Hz
Transient measurement mode (no chopper; transient heating of specimen)	50kHz

Performance

Temperature resolution* (meter)	0·5degC at 25°C
Temperature range* (meter)	
1	0 to 15°C
2	10 to 44°C
3	20 to 80°C
4	45 to 200°C
(See Figs. 8.12 and 8.13)	
Temperature range* (counter) (See Fig. 8.14)	15 to 150°C
Cell response time	4μs
Spectral range	1·8 to 5·5μm

*Black-body calibration

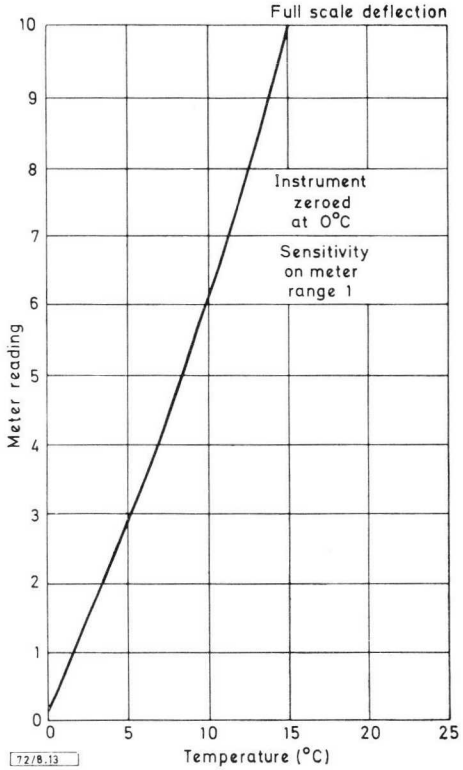

Fig. 8.12—Maximum sensitivity range

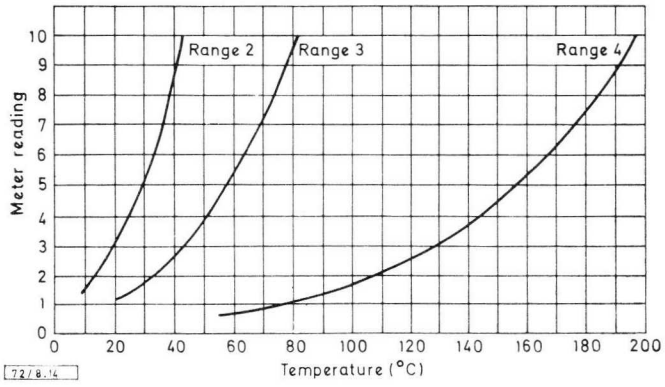

Fig. 8.13—Meter range curves

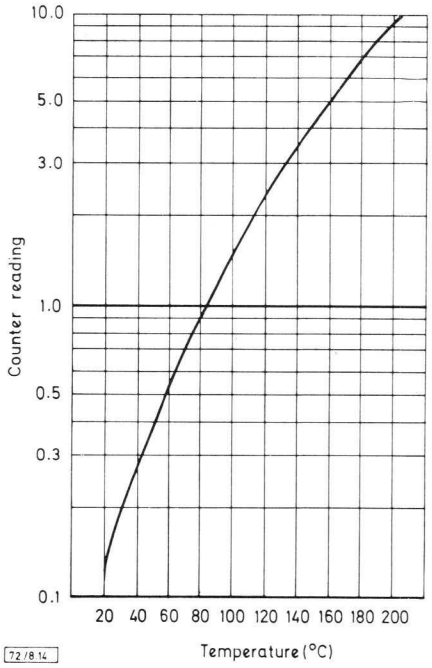

Fig. 8.14—Range of counter

CHAPTER 9

CLOSED-CIRCUIT INFRARED TELEVISION SYSTEM

A number of very expensive thermal scanning systems with high optical definition are commercially available. These systems, however, are generally bulky, and require large power supplies. Many of them also have the disadvantage of taking a long time to generate a picture.

The object in building the prototype scanning system described in this chapter was to determine the performance of a lightweight inexpensive camera employing a simple Nipkow disc as the scanning mechanism. This mechanism comprises a rotating flat disc, perforated with a spiral of holes, which generates 30 scanning lines. Since the disc, rotating at 1000 rev/min, is the only moving part, the camera is small and robust, and it has a low power consumption. The complete equipment consists of two parts, a camera head and an oscilloscope display, as indicated in Fig. 9.1.

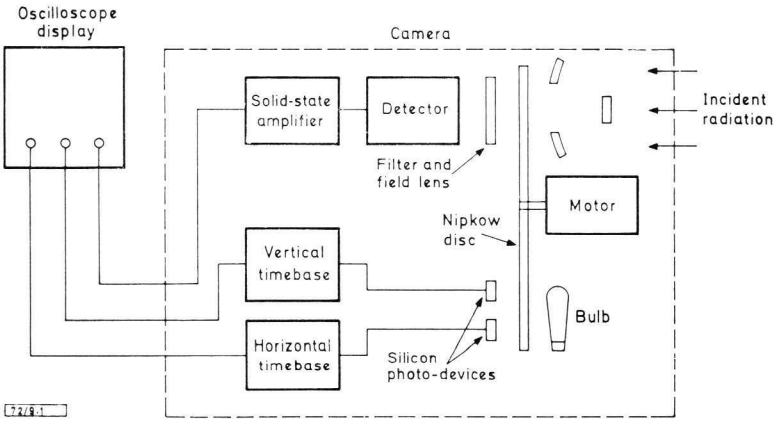

Fig. 9.1—Infrared cctv system

The main problem of the Nipkow disc scanning mechanism is that the detector 'sees' any variation in the radiation emitted or reflected by the disc, as well as that from the scene. In our first experiments, this variation produced a spurious signal level much greater than the signal from a room-temperature scene; but the problem was overcome by means of a specially constructed disc of black Perspex, so that the camera was limited by detector noise.

With the 30-line 17 frames per second picture, the equipment has a temperature sensitivity of 0·5degC with a room temperature background. Thus, it can detect the presence and position of any hot spots on moving and stationary objects within the field of view.

The detector is an RPY56 77K indium antimonide photoconductive infrared detector which has an annular element to match the optical system. Cooling is achieved by using a liquid nitrogen drip-feed system supplied from a dewar vessel placed on the floor at the side of the camera. This enables the camera to be operated in any plane. If a room-temperature lead sulphide detector is used in place of the indium antimonide detector, the minimum detectable temperature becomes 120°C, but detector cooling is then unnecessary.

DESIGN OF OPTICAL SYSTEM

The requirements of the equipment are that it should be portable and relatively inexpensive. This dictates the requirements of the optical system. A germanium lens could be used instead of the simple reflecting Cassegrainian system employed, but this would be expensive and therefore conflict with a basic requirement. The Nipkow disc scanning system, although not theoretically the most efficient, has the advantages of mechanical simplicity and ease of manufacture.

The optical system is shown in Fig. 9.2. The radiation from the scene is collected by the front-silvered concave mirror, and focused via the front-silvered plane mirror on to the Nipkow disc, which has a spiral of 30 holes near its circumference. Each hole scans the image in turn, and the transmitted radiation is focused on to the annular detector by a field lens. The field lens projects an image of the effective annular shape of the collecting optics on to the detector element, hence the radiation transmitted by a scanning hole is uniformly spread over the detector area.

A second set of holes in the disc enables synchronisation pulses to be obtained, thus enabling the raster on the display oscilloscope to be triggered. The signal from the detector is used to intensity-modulate the electron beam of the oscilloscope, thus producing an image on the screen.

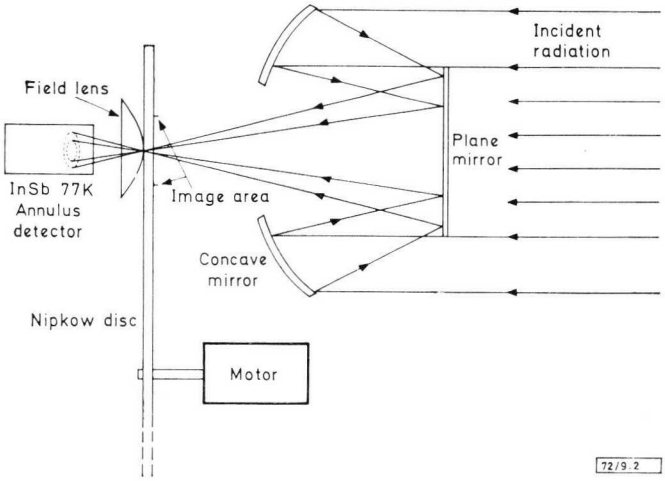

Fig. 9.2—Optical system of camera

The design equation of the Nipkow disc is Eq. 12 in Appendix 1.

$$\int_0^{\lambda_c} T(\lambda)(Q_S - Q_B)d\lambda \geqslant \frac{K\lambda_{pk}(A_D\Delta f)^{\frac{1}{2}}}{D^*(\lambda_{pk})hcJA_H\sin^2\theta}.$$

From this equation the maximum temperature sensitivity of the camera with cooled indium antimonide and lead sulphide detectors is calculated. The temperature sensitivity for the indium antimonide detector is shown to be 0·5degC at 25°C, and this figure has also been obtained from actual measurements with the camera. For the lead sulphide detector, it is shown that a temperature difference of 80degC between a black-body source and room temperature should be detectable, and this again corresponds fairly closely to the easily observable 100degC difference measured with the camera.

VARIATIONS ON PRESENT DESIGN

The main parameters that can be varied in the Nipkow disc scanner are:

1) field of view,
2) optical resolution,
3) temperature sensitivity,
4) frame rate,
5) camera size and weight,
6) cost of system.

Each of these can generally be varied only at the expense of another: for example, the optical resolution can be increased at the expense of the temperature sensitivity and vice versa. The first three of these six variables are discussed below.

Field of view

The present 6° field of view of the system is most easily increased or decreased by using a collecting optical system of shorter or longer focal length. If the f-number of the optical system is kept constant, the convergence of the radiation at the Nipkow disc is constant, hence from Eq. 10 of Appendix 1 the temperature sensitivity remains the same.

Optical resolution

The optical resolution of the present system (7mrad) is determined mainly by the number of scanning lines, the field of view of the optical system, and the hole size in the Nipkow disc. It is given by the equation

$$\text{Optical resolution} = \frac{\text{Field of view}}{\text{Number of holes}} \times \times \frac{\text{Actual diameter of holes}}{\text{Maximum diameter of holes with no overlap}} \quad \ldots(1)$$

If the optical resolution is doubled by doubling the number of scanning lines and the rest of the optical system is kept constant, then the diameter of the scanning holes must be halved and the electrical bandwidth increased.

The electrical bandwidth Δf required to give a square picture is given approximately by

$$\Delta f \simeq Fn^2/2$$

where F is the frame rate and n is the number of scanning lines. This bandwidth is essentially the fundamental sine frequency generated by alternate hot and cold picture elements.

It can be seen from the design equations in Appendix 1 that doubling the number of lines and keeping the rest of the system the same, reduces the hole area A_H by a factor of four and increases the bandwidth Δf by a factor of four, thus reducing the temperature sensitivity by a factor of eight. It is possible to compensate for this reduction in temperature sensitivity by using a more expensive collecting optical system with a smaller f-number, or by reducing the frame rate, or by doing both. If collecting optical systems of smaller f-number (that is, higher convergence) are used, then the field lens and detector combination must also be changed, as will be shown.

In the present system, the scanning lines overlap by 50% on each side,

so a factor of two in optical resolution can be easily obtained at the expense of temperature sensitivity by halving the diameter of the scanning holes.

It is also relevant that one advantage of using the low-definition system described here is that an aberration-free optical system is not necessary. This enables the cost of the optical system to be substantially reduced.

Temperature sensitivity

The temperature sensitivity of the scanning system is determined by the detectability criterion equation quoted on page 109.

To obtain greater temperature sensitivity, the right-hand side of this equation should be made as small as possible. One method of increasing the temperature sensitivity is to use detectors with higher detectivities (D^*_λ) or longer wavelength response, or both. The degree to which this can be done, however, is limited by the detectors that are available. The area of the detector (A_D) is also determined by the optical system and therefore cannot be independently changed.

The two main ways of increasing the temperature sensitivity are:

1) to reduce the bandwidth Δf of the system by reducing the number of lines or the frame rate, or
2) to increase the optical efficiency, the hole size A_H, or the convergence of the radiation at the Nipkow disc.

As described in the previous section, either decreasing the number of scanning lines or increasing the hole size decreases the optical resolution.

The effect of reducing the bandwidth to below that given by $Fn^2/2$ is quite interesting. If the bandwidth is restricted at the high-frequency end, then the sharp edges of objects are blurred. If, however, the low-frequency end of the bandwidth is restricted, the edges of hot objects are accentuated and the temperature sensitivity of the system is increased. Restricting the low-frequency end of the bandwidth also enables hot and relatively cool objects to be seen in close proximity without overloading the picture.

OPTICAL SYSTEM

Because a small, inexpensive, portable scanning system was desired, the optical system also had to be readily available and inexpensive. The optical system finally chosen was shown in Fig. 9.2. It is a simple Cassegrainian system consisting of a 7·3cm diameter collecting mirror and a 4·7cm diameter plane mirror, to focus the image on to the Nipkow disc. An arsenic trisulphide lens with a focal length of 1·4cm is then used to focus the radiation on to the detector. The detectors used are 8mm × 5mm diameter annular elements which are comparable with the shape of

the collecting optical system. In the PbS camera, a 61SV detector can be used, but the field lens must be replaced by a cone channel optical system. The full details are:

Collecting mirror*:	Front-silvered concave mirror 7·3cm diameter; 13cm focal length.
Plane mirror:	Front-silvered plane mirror 4·7cm diameter (the area of concave mirror that is obscured is 5cm in diameter).
Nipkow disc:	A 19cm diameter disc of black Perspex. The scanning and synchronisation holes are 1mm in diameter.
Field lens:	Material, arsenic trisulphide; diameter, 2cm; focal length, 1·4cm.
Detector	
InSb:	8mm × 5mm diameter annulus, operating at 77K. Type RPY56.
PbS:	8mm × 5mm diameter annulus, operating at room temperature. Type RPY57.

The focusing arrangement on the camera moves the whole collecting optics, thus enabling the scene to be continuously focused up in the Nipkow disc. The size of the detector is such that the image of the collecting optical system lies on the annular sensitive area for focusing distances between 1·2m and infinity.

Nipkow disc

Nipkow disc scanning is a means of scanning in the image plane of a system. The disc has a spiral of 30 holes round its circumference as shown in Fig. 9.3, each of which scans across the image in turn. The radiation passing through these holes is focused on to the detector. The signal from the detector is then used to intensity-modulate the raster on the display oscilloscope. Secondary holes diametrically opposite the scanning holes are used to give pulses with which the line and frame timebases providing the raster are synchronised. The synchronisation pulses are produced by using a 12V festoon bulb and two BPX25 silicon phototransistors.

It is very important to align the synchronisation holes and the scanning holes on the same disc diameters, otherwise distortion will occur in the displayed picture.

The scanned image size on the Nipkow disc is about 1·5 × 1·5cm.

*A shield is used on the concave mirror to prevent stray radiation from passing, unreflected, through the optical system.

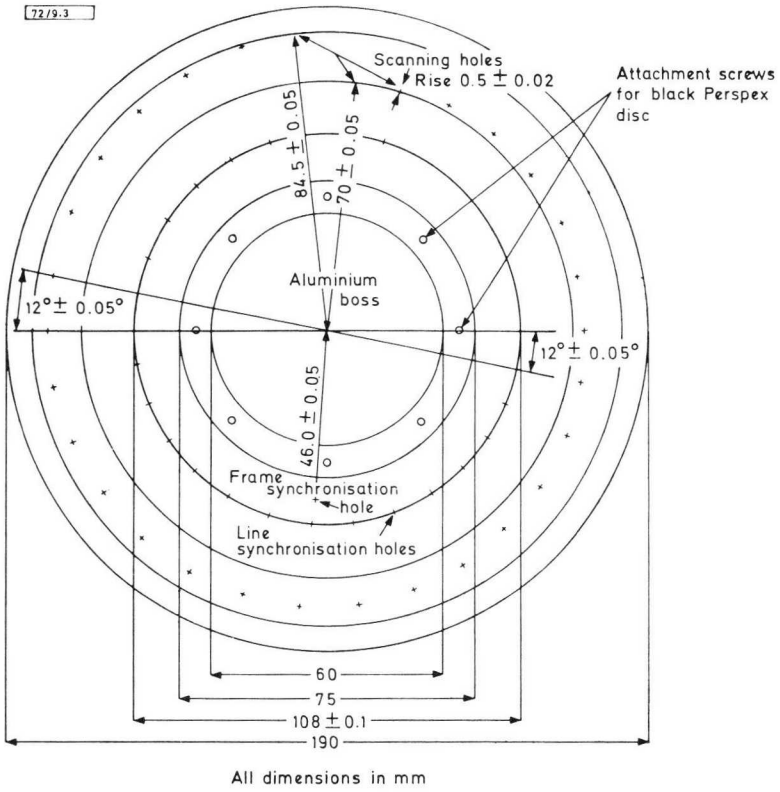

Fig. 9.3—Dimensions of Nipkow disc. The scanning and synchronisation holes are circular and 1·0 ± 0·05mm in diameter. The 30 scanning holes are placed in a spiral at 12° ± 0·05° intervals with a rise between two consecutive holes of 0·5 ± 0·02mm. The disc is constructed of $\frac{1}{8}$ in black Perspex with a centre boss of aluminium. The scanning holes are countersunk, on the side facing the collecting optical system, to within 0·1mm of the other surface with a 5mm drill.

The 30 scanning holes are placed on radii of the disc, with equal angular displacement between any two consecutive radii. Partly to compensate for the fact that the drilled scanning holes are round rather than square and partly to increase the temperature sensitivity, the scanning lines were made to overlap by 50% on both sides; that is, the holes were made 1mm in diameter.

The main difficulty in making the disc for the indium antimonide system was that the first discs gave a large spurious signal when rotated. The amplitude of this spurious signal was up to 50 times that of the noise from the detector and was caused by variations in reflectivity and emissivity, and by wobble along the surface of the discs. Various metal discs were made with polished or mat surfaces but, although the spurious signal was reduced, it was still much greater than the detector noise.

Finally, a different principle was tried. A disc was made of clear Perspex which, in thin sheets, transmits infrared out to 5·5μm. This disc was found to produce a very low spurious signal. Because most of the radiation is emitted from beneath the surface of the disc, surface imperfections and small scratches did not cause high standing signals as the disc was rotated. One problem that occurred when using clear Perspex, however, was that radiation from the bulb driving the phototransistors was channelled through the disc to the scanning holes, where it interfered with the video signal. This was overcome by using black Perspex.

The black Perspex discs still had, however, the wobble associated with the first discs. This produced a low-frequency spurious standing signal on the thermal picture. To reduce this to a minimum, the metal boss on the disc was extended as far as possible, and thicker Perspex discs were made. The loss of signal radiation due to vignetting by the thicker disc was reduced to a minimum by countersinking the scanning holes on the side of the disc facing the collecting optics.

Complete elimination of the wobble was found to be unnecessary because of the other sources of low-frequency noise in the system, such as noise caused by the Leiden-Frost cooling system, and low-frequency noise in the indium antimonide annular detector.

All the sources of low-frequency noise were rendered almost unnoticeable by using a clamping technique, in which the signal is d.c. restored before the start of each line scan. With the lead sulphide version of the camera the standing signal from the disc is of course negligible compared with the detector noise.

Field lens

The purpose of the field lens is to focus the radiation from the scanned image on to the detector. This is achieved by imaging the collecting optical system on to the detector. Thus the field lens can be placed close to the Nipkow disc, enabling its diameter to be not much larger than the diameter of the image. This method also has the advantage that the radiation falling on any one point in the scanned image is spread uniformly over the detector, thus overcoming any problems of nonuniformity of response in the detector.

The required diameter D of the detector is given by the equation:

$$D \simeq fd/(L - f) \qquad ..(2)$$

where

f = focal length of the field lens,
L = separation distance of the field lens from the collecting optical system, and
d = diameter of the collecting optical system.

An aperture of angular width 10° is placed in the plane of the field lens to allow about 2° of disc rotation while clamping takes place.

Cooling system for indium antimonide detector

The indium antimonide detector type RPY56 used in the infrared camera is designed to operate at liquid nitrogen temperature (77K). This is achieved by using a system which utilises the Leiden-Frost effect whereby beads of liquid nitrogen ride inside a layer of vapour in the transfer line. The vapour insulates the liquid beads from the walls of the transfer line; hence the length and material of the transfer line are not critical, and lengths up to two metres may be used. However, constrictions and sharp bends in the line must be avoided.

The actual system used consists of a 4 litre flask of liquid nitrogen coupled to the camera by a transfer line of p.v.c. tubing having a 3mm internal diameter. The flask is sealed with toggle clamps to generate enough pressure to force the liquid nitrogen beads through the transfer line. The actual rate of flow is controlled by restricting the vapour effluent from the cooling head in the detector.

The flow rate should be kept to the minimum required to cool the detector, which is generally about three-quarters of a turn of the needle valve used on the camera. If excess flow rates are used, then the beads may wet the wall of the transfer line, thus causing only nitrogen vapour to reach the detector.

The effluent vapour from the detector is heated to a few degrees below room temperature by the heatsink on the needle valve. It is then passed into the cavity between the detector and the field lens and subsequently blown on to the Nipkow disc. This use of the effluent gas serves several purposes:

1) to prevent the detector window and the field lens from misting,
2) to cool the Nipkow disc and, therefore, cause it to emit less radiation,
3) to reduce the background radiation falling upon the detector and hence increase its detectivity.

Because the effluent gas is blown on to the disc, it is important to switch the motor on before switching the cooler on, otherwise a large

standing signal will occur from the cooled portion of the disc.

The standby time of the 4 litre flask is about 60 hours, and the continuous running time is about 30 hours. Thus, under most conditions of intermittent use, 4 litres is enough for two days.

The main advantage of the Leiden-Frost cooling system is that it enables the camera to be used in any plane. Its main disadvantage is that the beads of nitrogen generate bursts of low-frequency noise as they are forced into the detector. This noise has largely been eliminated in the present camera by the clamping.

ELECTRONICS

The main functions of the electronic circuits are:

1) To amplify the signal from the detector and present it in such a form as to modulate the brightness of a CRT spot.
2) To generate a raster for the display.
3) To drive the motor which rotates the disc at constant speed.

It has been convenient to display the thermal pictures on an oscilloscope, since the additional electronics required to produce a raster and to modulate the brightness are minimum. For example, the frame and line timebases (Fig. 9.4) are similar circuits providing linear ramp waveforms with fast flyback triggered by the synchronisation holes. The trigger circuit is shown in Fig. 9.5.

The preamplifier (Fig. 9.6) and intermediate amplifier (Fig. 9.7) for the indium antimonide detector and the preamplifier for the lead sulphide detector (Fig. 9.8) raise the 'video' signal to a level sufficient for the clamping circuit to operate (Fig. 9.9). The clamp circuit restores the voltage at its output to a fixed level at the end of each line scan, during which time the cell detects radiation from the disc, since the scanning holes are masked by the 10° aperture. Thus if the radiation from the disc varies from line to line, this variation does not appear at the output of the clamp. Other low-frequency variations which do not originate in the field of view are dealt with in the same manner, there remaining only the small variations which take place during a line scan. The clamp is triggered from the line synchronisation pulses and operates for a period of 70μs.

The output from the clamp is fed to a differential amplifier (Fig. 9.10) which allows the peaks of the waveform to be displayed, to enhance contrast of the 'hot-spots'.

One minor drawback in normal oscilloscopes is the low value of capacitance used to couple the grid of the CRT, leading to a high value of low-frequency cut. This is overcome by impressing the video signal on a

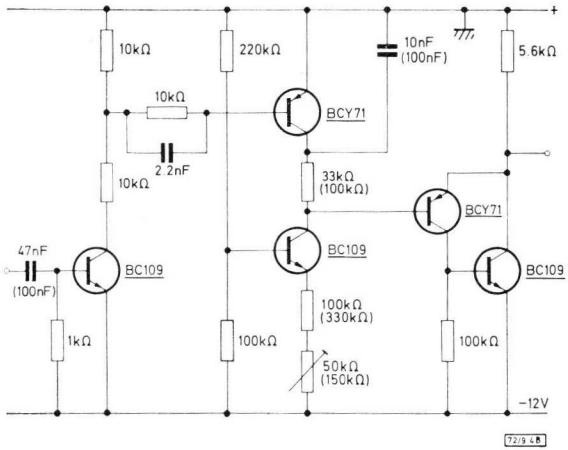

Fig. 9.4—Frame and line timebases (Frame timebase values in brackets).

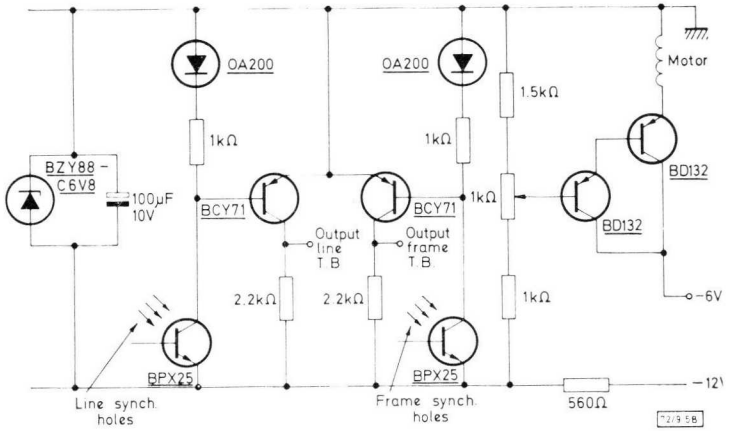

Fig. 9.5—Trigger and motor drive circuits

50kHz carrier (Fig. 9.10). The two outputs of the differential amplifier are used to limit the amplitude of the carrier. This stage is followed by a simple amplifier using a high breakdown voltage transistor, which has a low output impedance and large voltage swing.

Attenuation of the video signal is achieved in three ways:

1) the cell bias is reduced by 3 factors of 10,
2) the output of the preamplifiers can be switched between high and low gain positions,
3) the coupling from the preamplifier to the following stage is variable.

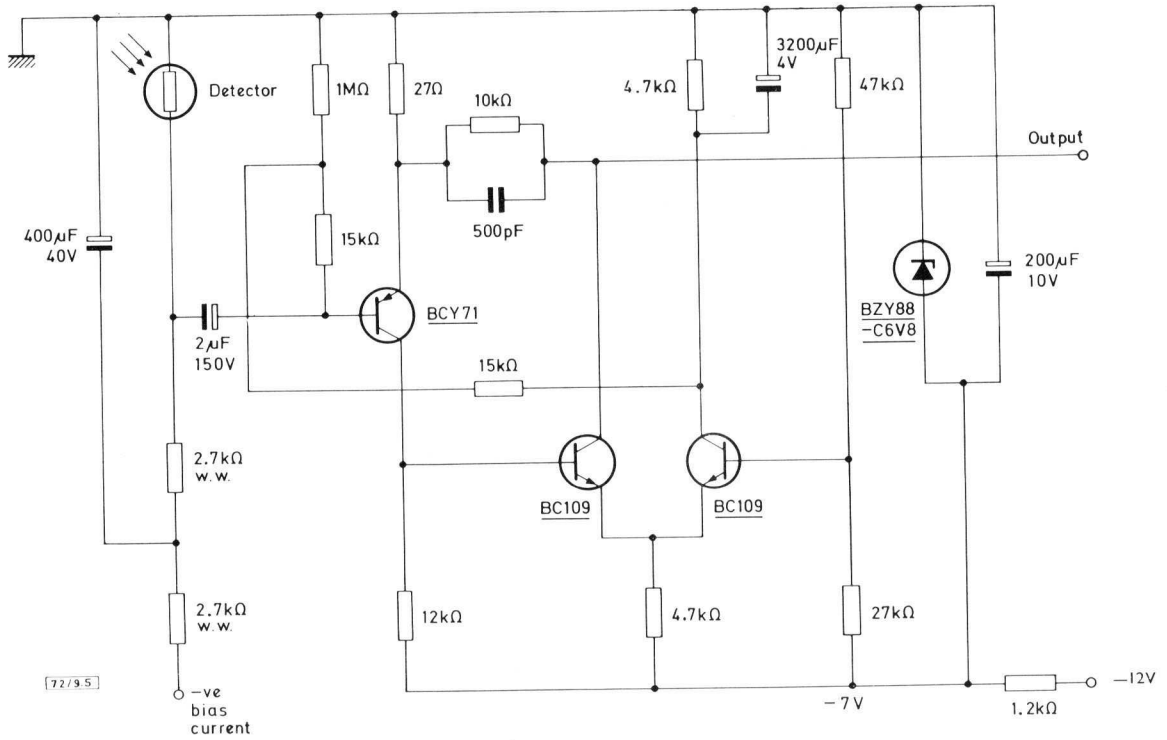

Fig. 9.6—Preamplifier for indium antimonide detector

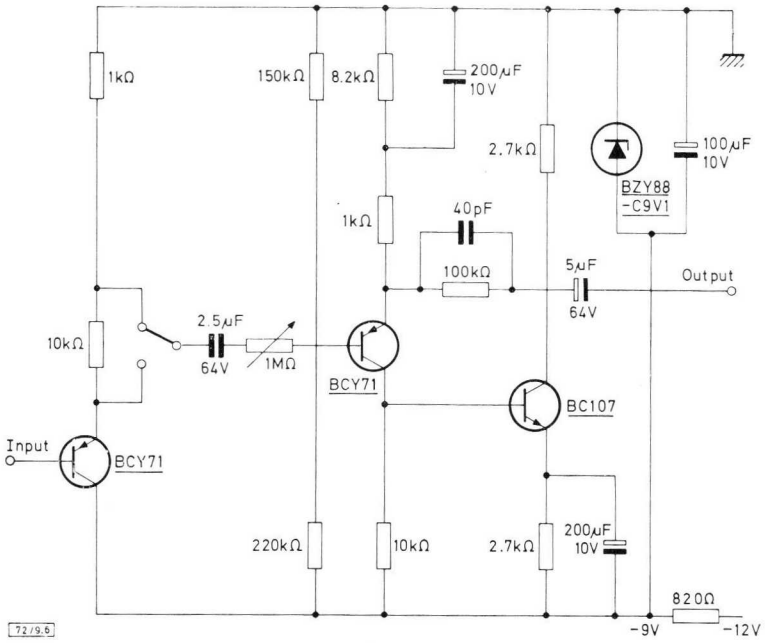

Fig. 9.7—Intermediate amplifier

In the case of the cooled detector, the bias voltage across the cell is displayed on an edge meter. This serves as an indication of the correct cooling of the detector, since its impedance rises from a few ohms to about 200Ω when cool.

An alternative method of displaying the thermal picture is available: the video signal from the clamp can be superimposed on the raster, rather than on the spot brightness. This deflection modulation provides more visual information in that smaller temperature fluctuations are more easily seen, and relative temperature differences can be accurately measured. A combination of the two display modes lends a third dimension to the picture which requires less interpretation than the deflection modulation alone.

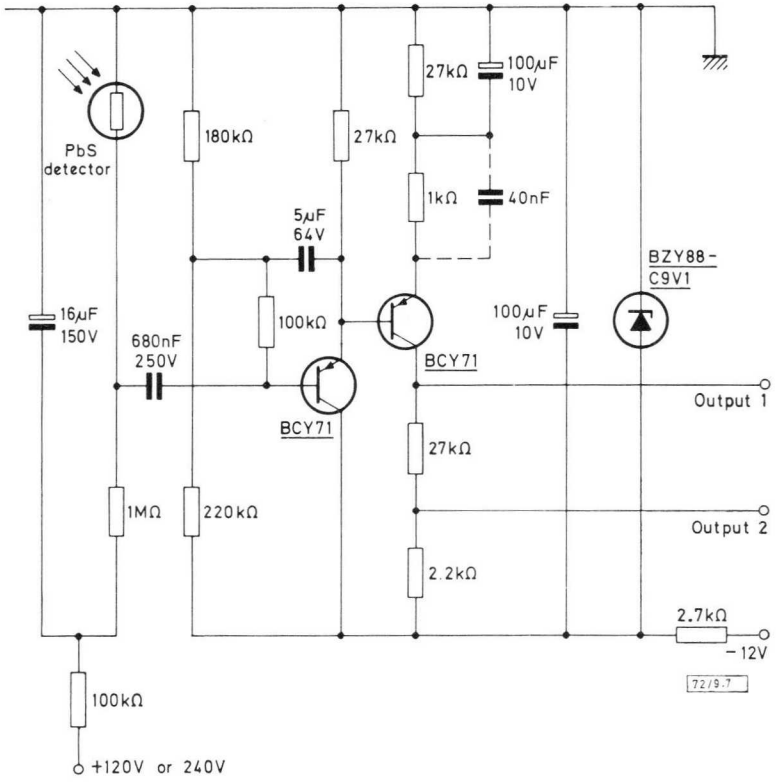

Fig. 9.8—Preamplifier for lead sulphide detector

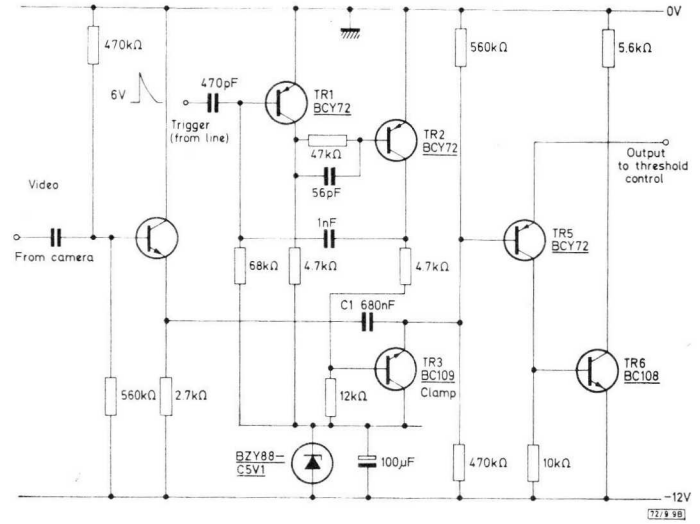

Fig. 9.9—Black level clamp

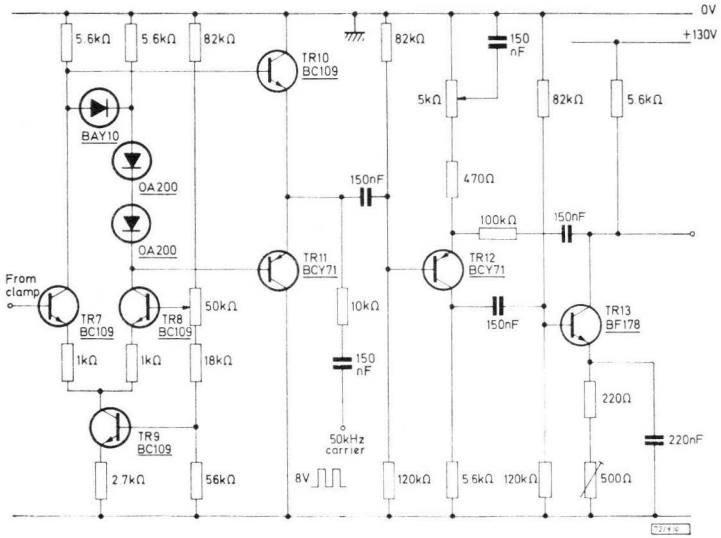

Fig. 9.10—Threshold control, modulator, and output stage

APPENDIX 1

Design equation of Nipkow disc

The design equation of the Nipkow disc will enable the maximum temperature sensitivity of a given scanning system to be calculated. In this calculation it will be assumed that the system is limited by detector noise. This will be shown to be a justifiable assumption provided that the disc is made of the right material and correctly balanced.

OPTICAL SYSTEM

The scanner must be able to distinguish between the infrared source of interest and the background in the scene. The difference between the radiant emittance of source and background is

$$W = \int_0^\infty (H_S(\lambda) - H_B(\lambda))\,d\lambda \qquad ..(3)$$

where λ = wavelength

$H_S(\lambda)$ = source spectral radiant emittance

$H_B(\lambda)$ = background spectral radiant emittance.

A proportion of this radiation is collected by the optical system of the scanner and focused onto the Nipkow disc. From a basic theorem for ideal optical systems, the radiant power falling on a single scanning hole of area A_H in the disc is given by

$$H_H = A_H W \sin^2 \theta, \qquad ..(4)$$

where θ is the half angle of the cone of the convergence of the optical system at the disc.

In practice, allowance must be made for the efficiency of the optical system (J), and for absorption and scattering by the atmosphere, which is a function of wavelength $T(\lambda)$. Introducing these factors into Eqs. 3 and 4 gives

$$H_H = JA_H \sin^2\theta \int_0^\infty T(\lambda)(H_S(\lambda) - H_B(\lambda))\,d\lambda. \qquad ..(5)$$

DETECTOR

The radiant power passing through the scanning hole in the disc is uniformly focused, by means of a field lens, on to the annular detector. The

signal voltage V_S developed in the detector is given by

$$V_S = JA_H \sin^2\theta \int_0^\infty R(\lambda)T(\lambda)(H_S(\lambda) - H_B(\lambda))d\lambda \quad ..(6)$$

where $R(\lambda)$ is the spectral responsivity of the detector; that is, the output voltage per unit of radiant power, as a function of wavelength.

The criterion for the detection of an object is that the difference signal between the source of interest and its background must exceed the system noise by a factor K. A value of 5 for this factor gives a high probability of detection.

Provided that the system is limited by detector noise, this noise (V_N) can be obtained from the area-normalised detectivity $D^*\lambda$ by the equation,

$$D^*(\lambda_{pk}) = R(\lambda_{pk})\ (A_D\Delta f)^{\frac{1}{2}}/V_N \quad ..(7)$$

where λ_{pk} is the wavelength of peak response, A_D is the detector sensitive area and Δf is the bandwidth. Therefore

$$V_N = R(\lambda_{pk})\ (A_D\Delta f)^{\frac{1}{2}}/D^*(\lambda_{pk}). \quad ..(8)$$

If the detector parameters R and D* are dependent on frequency, then Eq. 8 should be written as follows:

$$V_N = \left[\int_{f_2}^{f_1} \left(\frac{R(\lambda_{pk})}{D^*(\lambda_{pk})}\right)^2 A_D df\right]^{\frac{1}{2}} \quad ..(9)$$

where f is frequency. For the detectors used in the scanning systems described here, Eq. 8 holds approximately.

Thus, the detectability criterion can be written, using Eqs. 6 and 8, as:

$$JA_H \sin^2\theta \int_0^\infty R(\lambda)T(\lambda)(H_S(\lambda) - H_B(\lambda))d\lambda \geqslant K[R(\lambda_{pk})/D^*(\lambda_{pk})](A_D\Delta f)^{\frac{1}{2}} \quad ..(10)$$

The detectors used in the equipment described are photon detectors. With such a detector it is convenient to use the photon responsivity $P(\lambda)$, where

$$P(\lambda) = R(\lambda)/\lambda.$$

Eq. 10 can then be simplified to the following form:

$$\int_0^\infty P(\lambda)T(\lambda)(Q_S - Q_B)d\lambda \geqslant K\lambda_{pk}P(\lambda_{pk})(A_D\Delta f)^{\frac{1}{2}}/D^*(\lambda_{pk})\ hcJA_H \sin^2\theta \quad ..(11)$$

where Q_S = source photon flux density per unit wavelength,
$= \lambda H_S(\lambda)/hc$,
Q_B = background photon flux density per unit wavelength,
$= \lambda H_B(\lambda)/hc$,
h = Planck's constant,
c = velocity of light.

For an ideal photon detector, $P(\lambda)$ is constant for wavelengths up to the cut-off wavelength λ_c, and is zero beyond. The detectability criterion then becomes:

$$\int_0^{\lambda_c} T(\lambda)\ (Q_S - Q_B)d\lambda \geqslant K\lambda_{pk}(A_D\Delta f)^{\frac{1}{2}}/D^*(\lambda_{pk})hcJA_H \sin^2\theta. \quad ..(12)$$

MAXIMUM TEMPERATURE SENSITIVITY

The design equation is applied to the scanning systems described in this chapter in order to calculate their maximum temperature sensitivities. The values of the following parameters in the criterion equation are:

Detector sensitive area, A_D	= 30·6mm^2 (annulus; 8mm outer diameter; 5mm inner diameter)
Bandwith, Δf	= 8kHz
Area of scanning hole, A_H	= 7·85 $\times$ 10^{-3} cm^2 (1mm diameter hole)
Convergence, sin θ	= 0·2706
Planck's constant, h	= 6·625 $\times$ 10^{-34} joule second
Velocity of light, c	= 3 $\times$ 10^{10}cm s^{-1}
Efficiency of the optical system, J	= 0·51
Detectability criterion, K	= 5

InSb detector system

The indium antimonide detector used in this system has a spectral responsivity that closely follows that of an ideal photon detector. In fact, it can be assumed to be an ideal photon detector with a value of D^*(4·4μm, 800, 1) equal to 5$\times$10^{10}cmHz$^{\frac{1}{2}}$W^{-1} and an effective cut-off wavelength λ_c of 5·5μm.

Substituting these values and the other parameters into Eq. 12 gives the condition

$$\int_0^{\lambda_c} T(\lambda)(Q_S - Q_B)d\lambda \geqslant 3{\cdot}7 \times 10^{14} \text{ photons cm}^{-2}\text{s}^{-1}.$$

With a black-body slide-rule, or with a similar instrument, it can be directly shown that this condition is satisfied for a black-body source temperature 0·5degC above a background temperature of 25°C for short path lengths where the atmospheric transmittance is close to unity.

This figure of maximum temperature sensitivity of 0·5degC at 25°C has also been obtained from actual measurements with the camera.

PbS detector system

The PbS room temperature detector can be treated as an ideal photon detector with a value of $D^*(2{\cdot}3\mu m, 800, 1)$ of $1{\cdot}8 \times 10^{10}\text{cmHz}^{\frac{1}{2}}\text{W}^{-1}$ and an effective cut-off wavelength λ_c of $2{\cdot}8\mu m$.

Substituting these values into the detectability criterion equation gives

$$\int_0^{\lambda_c} T(\lambda)(Q_S - Q_B)d\lambda \geqslant 5{\cdot}5 \times 10^{14} \text{ photons cm}^{-2}\text{s}^{-1}.$$

With a black-body slide-rule it can be found that, for short optical path lengths (that is, $T(\lambda) \simeq 1$) and the daylight filter transmission of 55%, a temperature difference of 80degC between a black-body source and a room temperature background is enough to satisfy this criterion. This figure again corresponds fairly closely to the easily observable 100degC difference measured with the camera.

APPENDIX 2

Equipment specification

Picture quality	30 × 30 element raster generated at 17 frames per second
Field of view	6° × 6°
Focusing range	60cm to infinity
Detector types	
Low temperature camera	RPY56 InSb detector cooled to 77K annular element, 8 × 5mm
High temperature camera	RPY57 PbS detector operated at room temperature; annular element 8 × 5mm

Temperature ranges	
InSb detector	−40 to +800°C
PbS detector	+120 to several thousand degrees C, depending on optical attenuation filters used
Temperature sensitivity	
InSb detector	± 0·5degC at 25°C
PbS detector	±5degC at 200°C (accuracy, ±10%)
Effective spectral response	
InSb detector	3·0 to 5·5μm
PbS detector	2·0 to 2·8μm (Type G1 daylight filter incorporated)
Battery life	
Camera head (InSb)	
67·5V, B101 supply	50h
6V, rechargeable NiCd supply	4h
Intermediate control box	
2 off, 67·5V, B101	80h
Camera head (PbS)	
67·5V, B101 supply	120h
6V, rechargeable NiCd supply	4h
240V, 8 off B123	450h
Oscilloscope display	
12V, rechargeable supply (or mains operated)	4h
Power consumption	
Camera	3W
Oscilloscope display	20W
Coolant for InSb detector	
Liquid nitrogen fed by Leiden-Frost drip-feed mechanism from dewar.	
Dewar capacity	4 litre
Cooling period (intermittent use)	2 days
Dimensions	
Camera	34 × 25 × 28cm
Intermediate box	23 × 15 × 14cm
Four-litre dewar	20cm high; 40cm diameter

Weight	
Camera	7·4kg
Intermediate box	2·1kg
Four-litre dewar	7·7kg

APPENDIX 3

Equipment controls

Camera controls	
Focus	60cm to infinity in the directions shown (InSb equipment has a calibrated scale).
Attenuation controls	
Coarse	5 ranges each with an attenuation factor of approximately 10.
Fine	Variable attenuation factor of approximately 10.
Battery check	Enables condition of batteries to be ascertained; they should be either replaced or recharged when needle no longer lies in red region of scale.
Detector temperature check (InSb detector camera only)	Needle valve controlling flow of coolant should be turned approximately three-quarters of revolution, at which point needle should slowly move into red region of scale; flow rate may need adjusting from time to time but should be kept to minimum required to cool detector.
6V charging point	Enables 6V NiCd supply to be recharged, the charging period being 14 hours at maximum of 250mA; Philips charger, PM9000, is suitable.
Approximate black-body temperature calibration	When the oscilloscope display controls on PbS equipment are set as described below, an approximate effective black-body temperature calibration can be obtained by decreasing attenuation until the display phosphor just reaches its maximum brightness; temperature of object under consideration can then be read from instrument chart.

Outputs	Video signal and two timebase outputs are provided on B.N.C. sockets; screwdriver adjustments are provided for line and frame holds.

Intermediate box controls

Display mode switch	Enables the display to be brightness modulated, deflection modulated, or both.
Differential control	Enables peaks of video signal to be displayed on oscilloscope; this enables fine detail on relatively-high-temperature object to be seen in sharp contrast.
Attenuation controls	Two variable attenuation controls are provided, one for each display mode.

Oscilloscope display controls

Focus, brilliance, astigmatism	For calibration purposes on the high-temperature PbS equipment, these should be set with the white lines positioned centrally.
Y-amplifier	500mV/cm, d.c.
Sweep	X-input
Y-input	Frame timebase from camera
X-input	Line timebase from camera
Z modulation on back panel	Video signal
X- and Y-gain and shift	Should be adjusted until centrally positioned square picture is obtained.

CHAPTER 10

INFRARED GAS ANALYSIS

For many years the absorption of radiation at certain wavelengths by gases and liquids has been used as a means of identifying and estimating them. The absorption of radiation involves a transition in a molecule between discrete energy levels, and the wavelength of the radiation absorbed corresponds to the energy difference. The types of absorption process are:

Electronic transitions	0 to 1·5μm
Bond vibrations	1·5 to 30μm
Rotations of molecules	30 to 1000μm

In general, the rotational spectrum, as well as causing absorption in its own region, is superimposed on the vibrational spectrum, and both vibrations and rotations on the electronic spectrum, forming a very fine structure of absorption which may sometimes be resolved.

In the case of gases the vibrational spectra are of the most practical interest, since electronic absorption often occurs in the vacuum ultraviolet (<0·2μm) and the rotation bands are in the far infrared, both regions presenting experimental difficulties. Stretching (asymmetric and symmetric), bending, and rocking vibrations occur, and the more atoms that form a molecule, the more absorption bands occur.

It should be noted that in conventional infrared spectroscopy the vibrations of symmetric molecules such as N_2, O_2 and H_2 are not excited although they may be observed by Raman techniques.

For quantitative estimation of gases that have absorption bands in the infrared, the attenuation of radiation at a given wavelength is given by:

$$I = I_i e^{-\alpha 1 p L}$$

where

I_i, I are the incident and emergent beam intensities
α^1 is the absorption coefficient
p is the partial pressure of the absorbing gas
L is the optical path length.

In practice a convenient form of this equation is

$$\log_{10} I/I_i = -\alpha pL$$

where

$$\alpha = 2{\cdot}303\alpha^1.$$

This equation is only approximate when the radiation is of finite bandwidth, but is adequate for most purposes.

APPLICATIONS

Gas analysis is important in medicine for lung function tests, in control of furnaces for efficiency and pollution purposes, in the control of the composition of gas in heat-treatment furnaces, in chemical engineering plants, in monitoring of atmospheric pollution, and in monitoring car exhausts. Recent legislation in the U.S.A. and the prospect of European legislation has stimulated much effort by motor-car manufacturers to control exhaust emissions, and a corresponding need has arisen to measure these. Infrared absorption techniques offer the advantage of high-speed continuous read-out of changing concentrations, and are already in widespread use in the industrial field. It is believed that a need has arisen for a low-cost infrared instrument for use in testing stations for automobiles, for checking on carbon monoxide (CO) emissions in particular.

METHODS OF INFRARED GAS ANALYSIS

The available methods are illustrated by the generic diagram:

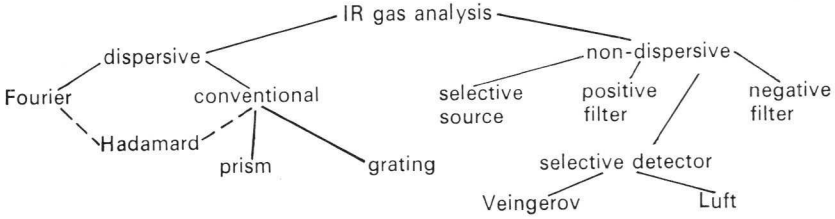

Dispersive methods are generally only suitable for laboratory use because of cost and fragility. Non-dispersive methods have been developed and are in widespread use, particularly the ingenious selective detector method (Fig. 10.1) in which a chamber filled with the gas to be analysed absorbs radiation of the appropriate wavelength and deflects a diaphragm.

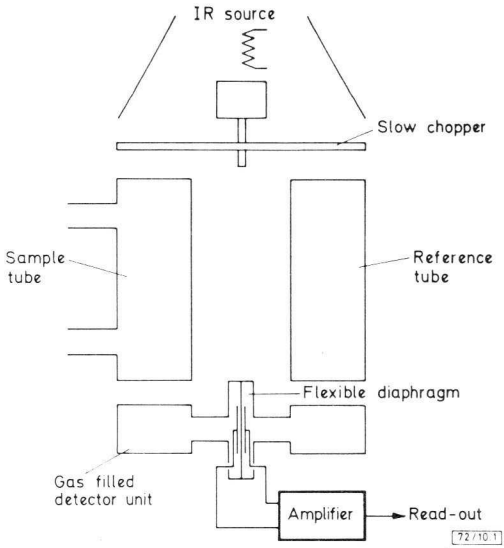

Fig. 10.1—Luft analyser, schematic and simplified

This analyser has achieved a high degree of development and has been applied to most IR absorbing gases of industrial importance. The possible disadvantages are sensitivity to vibration and temperature changes. In recent years narrow-band interference filters, IR detectors, and lasers have become available, making feasible other arrangements and the possibility of greater robustness and reliability as well as cost-saving. The most obvious approach is to replace the gas-filled detector with a positive narrow-band filter of the wavelength that the gas to be analysed absorbs. There are several configurations of analyser possible, each offering a trade-off between performance and cost. Some of these are shown in Fig. 10.2.

ABSORPTION CHARACTERISTICS OF GASES

Some of the gases which are of interest have the following predominant absorptions (Ref. 4):

	Wavelength (μm)	α (peak value) (torr $^{-1}$cm^{-1})
Carbon dioxide	4·35	$7{\cdot}5\times10^{-4}$
Carbon monoxide	4·7	1×10^{-4}
Sulphur dioxide	7·25	$1{\cdot}9\times10^{-3}$
Ethane (and many hydrocarbons)	3·4	$1{\cdot}4\times10^{-3}$
Nitrogen dioxide	6·2	$2{\cdot}4\times10^{-3}$

(1 torr $\simeq$ 133N/m^2 in SI units)

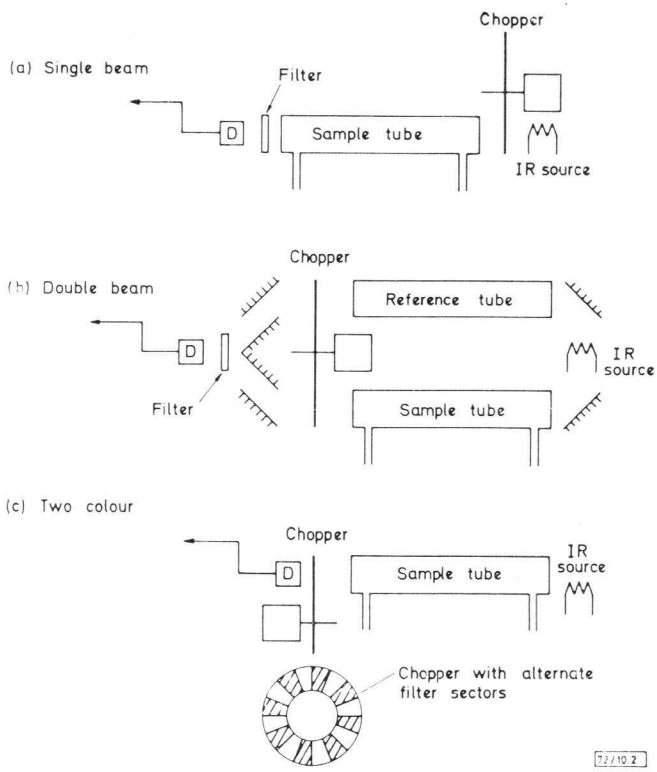

Fig. 10.2—Gas analyser schemes

All the above gases except carbon monoxide have significant absorptions at other wavelengths. It should be noted that hydrocarbons containing the $-CH_3$ group will have absorption in the 3·2 to 3·6μm region, and that they are difficult to discriminate one from another by IR means. Frequently they are estimated as "hexane equivalent", and legislation so far proposed is on this basis.

A spectrum of a sample of car exhaust is shown in Fig. 10.3.

APPLICATION OF IR DETECTORS

The detector materials available are discussed in Chapter 1 of this book. For the detection of radiation of the wavelengths absorbed by the above

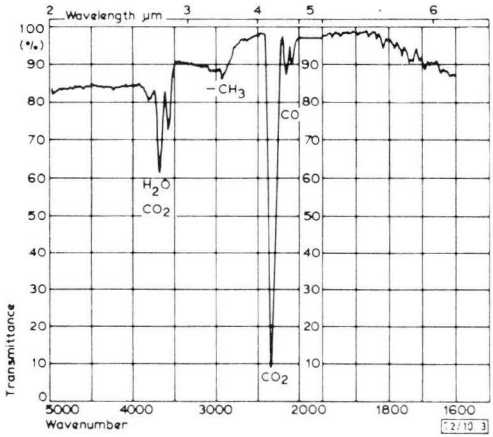

Fig. 10.3—Car exhaust sample spectrum

gases the following materials can be considered:

Indium antimonide, room temperature operating
Indium antimonide, 77K operating
Mercury cadmium telluride, room temperature operating
Triglycine sulphate bolometer

The actual choice of detector is dependent on spectral response, D*, element area, and cost.

PROTOTYPE CO_2/CO ANALYSER

A prototype CO_2/CO analyser has been developed to obtain information in the application of IR detectors to gas analysis, and in particular to car exhaust analysis at relatively low cost. For this reason a single beam design (Fig. 10.2a) using the room temperature indium antimonide RPY77 detector was adopted. The design variables are the source area, its temperature and emissivity, the absorption tube length, the detector area, and the type of optics to be used. The requirements of this analyser were:

CO measurement	0 to 5% concentration
CO_2 measurement	0 to 15% concentration

The sample cell length was estimated from the graphs of Figs. 10.4 and 10.5 on the basis that the minimum absorption when gas is introduced should be 10% and the maximum 90%. For up to 10% absorption the output of the analyser may be linearised, but otherwise a non-linear scale may be produced by calibrating with standardised gas mixtures.

A tube length of 10cm was decided on which would give 18% absorption

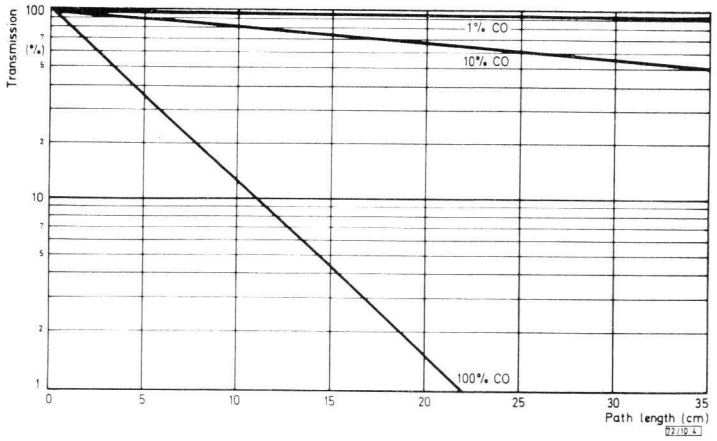

Fig. 10.4—Estimated transmission through CO gas mixtures at 4·7μm versus path length

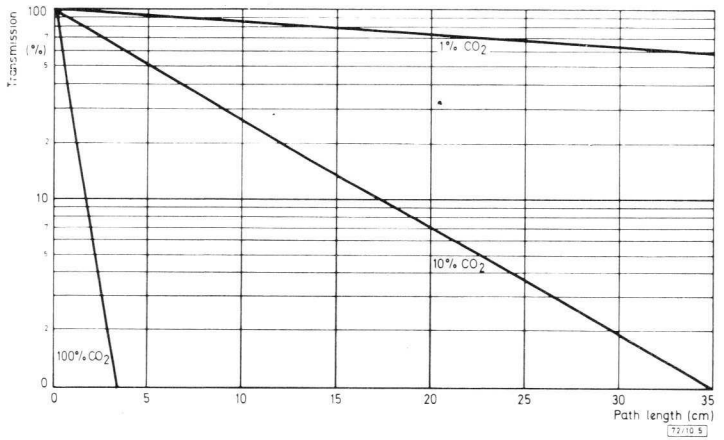

Fig. 10.5—Estimated transmission through CO_2 gas mixtures at 4·35μm, versus path length

for 10% CO and 70% absorption for 10% CO_2. A length of 30cm has also been used experimentally. Sapphire windows which may be fused or waxed to a glass tube were used.

The source presents problems. Ideally one should use a temperature which gives a peak output at the filter wavelength and increase the area as necessary to give a sufficient irradiance. This would imply a temperature

of about 650K. However, there might be considerable losses of heat from a large low-temperature source, and for convenience a tungsten filament lamp of 15W that had been fitted with a periclase (MgO) window was used. The source was obviously inefficient to the extent that it operated at about 2000K and that the emissivity of tungsten is low at 4 to 5μm, although the coiled filament will have a cavity effect to mitigate this.

Filters for the instrument have been supplied by STC–ITT, and consist of narrow-band filters with transmissions of 4·4μm for CO_2 and 4·7μm for CO, with about 0·1μm bandwidth. Auxiliary cut-on and cut-off filters are used to reject breakthrough at other wavelengths.

The use of focused optics was considered, but initially no focusing through the analyser tube was used. The design equations to estimate the irradiance at the detector are:

$$H_\lambda = G\frac{W_\lambda}{\pi d^2}\Delta\lambda A_S \qquad \text{for no focusing}$$

$$H_\lambda = J\frac{W_\lambda \Delta\lambda}{4F^2} \qquad \text{for a single lens system with an extended source}$$

where

H_λ is the irradiance
G is a constant >1
W_λ is the radiance of the source in $Wcm^{-2}\ \mu m^{-1}$
$\Delta\lambda$ is the system spectral bandwidth in μm
A_S is the area of source in view
d is the source detector distance
J is the lens or mirror efficiency (<1)
F is the f-number.

It should be noted that the factor G has been incorporated in the unfocused case to allow for the light-guide effect of the sample tube. Even a plain glass tube causes an increase in signal of several times that produced by the source-detector distance, and the signal can be further increased by the usual techniques of making lightpipes.

Once an estimate has been made for irradiance, the open-circuit signal and signal-to-noise ratio are given by:

$$V_S = C_t H_\lambda A_D R_\lambda$$

$$\frac{V_S}{V_N} = \frac{D^* H_\lambda A^{\frac{1}{2}}}{C_t \Delta f^{\frac{1}{2}}}$$

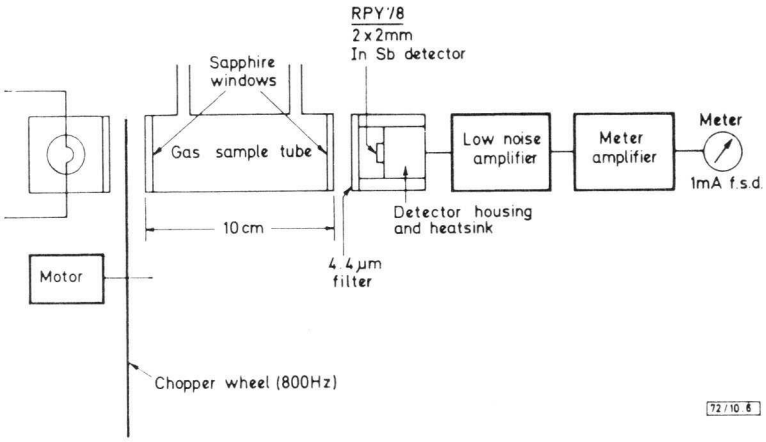

Fig. 10.6—Simple gas analyser

where

C_f is the chopping factor and is about 2·2 for square-wave chopping
A_D is the detector area
R_λ is the responsivity at the wavelength λ
D^* is the area-normalised detectivity.

In the prototype, the signal level was about 10μV and the signal-to-noise ratio was 50.

Circuit Design

The electronic system was designed to be part of a simple and cheap gas analyser. This approach was based on the existence of a large potential market in the field of motor-car exhaust pollution testing.

The type of gas analyser under consideration is shown in block diagram form in Fig. 10.6 and has the following features:

A single gas sampling tube with a narrow-band infrared filter and a fairly high energy source.

A single control in the electronics to enable the output meter to be set to full scale at the 100% transmission point when no gas is present in the sample tube. This point could be set conveniently before each test.

When the sample tube is filled with a gas mixture at atmospheric pressure the output meter reading will indicate the percentage of gas on a previously calibrated scale.

Design considerations

With a simple electronic system it is necessary to select a suitable tube length that will provide a $>10\%$ change of transmission when the sample is introduced into the tube. A further criterion for accuracy of the system is signal-to-noise ratio. If this ratio is not high enough, noise will contribute to the meter deflection and will introduce calibration errors. If we are to use the simple electronics proposed, then a source of sufficiently high energy must be used. The alternative is to reduce the electronic bandwidth. However, any reduction of this will demand a higher degree of stability of chopper speed. Both of these problems would be overcome by use of a phase-sensitive rectifier, but of course this would mean greater expense.

Fig. 10.7 shows how noise will affect reading accuracy. The gain has been adjusted to give full-scale deflection, which is the condition set just before

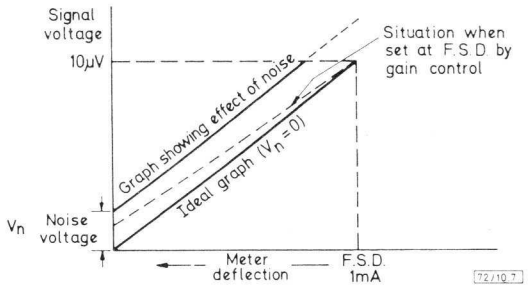

Fig. 10.7—Effect of noise on calibration

measurement. However, due to noise error, if the signal is now reduced by some percentage the output level departs from the ideal line and heads toward an elevated zero.

Calculation of percentage error due to noise

In the ideal noiseless system

$$I_o = G\ V_S$$

where

I_o = current output

G = amplifier overall gain (current/voltage).

If the noise is V_N but the system is set up at f.s.d. then

$$I_o = G'\ (V_S + V_N) = \text{f.s.d.}$$

where

G′ is the set up gain.

To calculate the error at $1/x^{th}$ of V_S (reading should be $1/x$ of f.s.d.)

$$I_{ox} = G'[(V_S/x)+V_N]$$

where

I_{ox} is the current output
V_S is reduced by $1/x$.

The percentage error is given by

$$\left(1 - \frac{I_{ox}}{\text{f.s.d.}/x}\right) 100.$$

In practice the gain was set so that meter f.s.d. was obtained for $10\mu V$ signal from the cell. This produced a zero error of $20\mu A$ on the output meter; that is $0{\cdot}2\mu V$ at the detector. From the above expressions for percentage error:

$$\text{Idealised gain } G = \frac{I_o}{V_S} = \frac{1\times10^{-3}}{10\times10^{-6}} = 100.$$

Setting up gain to give 1mA f.s.d. with $0{\cdot}2\mu V$ of noise:

$$G' = \frac{I_o}{(V_S+V_N)} = \frac{1\times10^{-3}}{10\times10^{-6}} + 0{\cdot}2\times10^{-6} = 98.$$

If $x = 3$ then at $V_S/3$

$$I_{ox} = G'(V_S+V_N) = 98\left(\frac{10\times10^{-6}}{3} + 0{\cdot}2\times10^{-6}\right) = 0{\cdot}343\text{mA}.$$

$$\text{Percentage error} = [1-(343/333)]100 = 3\%.$$

A standing error of this type due to noise can of course be calibrated out, but then any variation of noise level will change the calibration, and the meter scale will vary with different instruments.

AMPLIFIER UNIT

The amplifier (Fig. 10.8) has been designed for use with the 2×2mm indium antimonide labyrinth cells RPY77 or RPY78. It was decided that the electronics should be capable of operating from a 9V to 12V supply. This may then be suitable for a portable equipment as batteries could be reasonably small at a current drain of up to 50mA. This supply voltage is also compatible with car electrics, which may prove to be advantageous.

A low-noise input stage was considered to be of prime importance. Gain stability is not quite so vital since the equipment will be adjusted immediately before measurement.

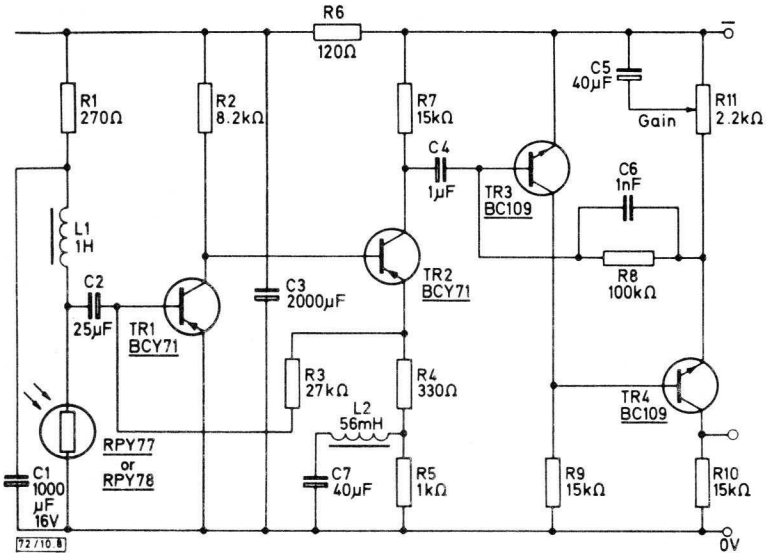

Fig. 10.8—Bias supply and amplifier

The unit consists of a pair of amplifiers each being of the current feedback type, with p-n-p transistors for the first amplifier because of their low-noise properties. The second amplifier is complementary to the first as this makes for better rejection of spurious supply-line voltages.

Both the first stage and the detector are supplied from a heavily decoupled point to reduce noise and prevent feedback due to the supply.

The detector is biased via a 1 henry choke from which the following advantages are obtained:

1) Noise contribution from the detector load is eliminated.
2) A higher bias current is available from a given supply line.
3) The input impedance of the amplifier is not so critical, and its noise contribution can be reduced.

With reference to point (3), it can be shown that the noise figure of this type of amplifier is degraded as more feedback is applied. The equation for noise factor is:

$$\text{N.F.} = 1 + \frac{i_n^2 R_{in}}{K} + \frac{e_n^2}{K R_{in}} \frac{(R_F + R_{in})^2}{R_F^2} + \frac{R_{in}}{R_F}$$

where

i_n = transistor equivalent noise current generator
e_n = transistor equivalent noise voltage generator
K = $4kT\Delta f$
R_{in} = total source resistance
R_F = feedback resistor.

This method of biasing and amplification does not fall exactly into any of the categories mentioned in Chapter 2. The amplifier input impedance is fairly low (100Ω) and the d.c. resistance between the cell and its supply is comparable with cell resistance. This arrangement is nearest to the category of constant power biasing followed by a current amplifier. It reduces signal-to-noise variation and also responsivity variations to some extent (see Chapter 2). The bandwidth of the amplifier is determined by the LC filter in the emitter of TR_2. The choke has an inductance of 56mH and a d.c. resistance of 16Ω.

Amplifier specification

Supply voltage	9V to 12V
Current drain (amplifier only)	2mA
Gain	500 000 to 50 000
Bandwidth	600Hz (3dB points)
Total noise voltage referred to input	5×10^{-9} $VHz^{-\frac{1}{2}}$ (F = 800Hz, R_S = 1kΩ)
Noise figure	1·8dB (F = 800Hz, R_S = 1kΩ)
Maximum available cell bias current	10mA.

METER DRIVE CIRCUIT

The meter drive circuit is shown in Fig. 10.9. The output meter is a 1mA f.s.d. instrument, preferably with a long scale. The meter impedance should not be greater than 500Ω to avoid bottoming of the amplifier at low supply voltage (9V).

The purposes of this circuit are (a) to convert the a.c. voltage output from the amplifier unit into a suitable d.c. current for the 1mA meter, and (b) to overcome the inherent non-linearity of the diode rectifiers so that the meter current is nearly linear with input voltage.

Principle of operation

This is an amplifier circuit where d.c. feedback is present via R_5 and R_6 to make the output voltage level approximately equal to the input d.c.

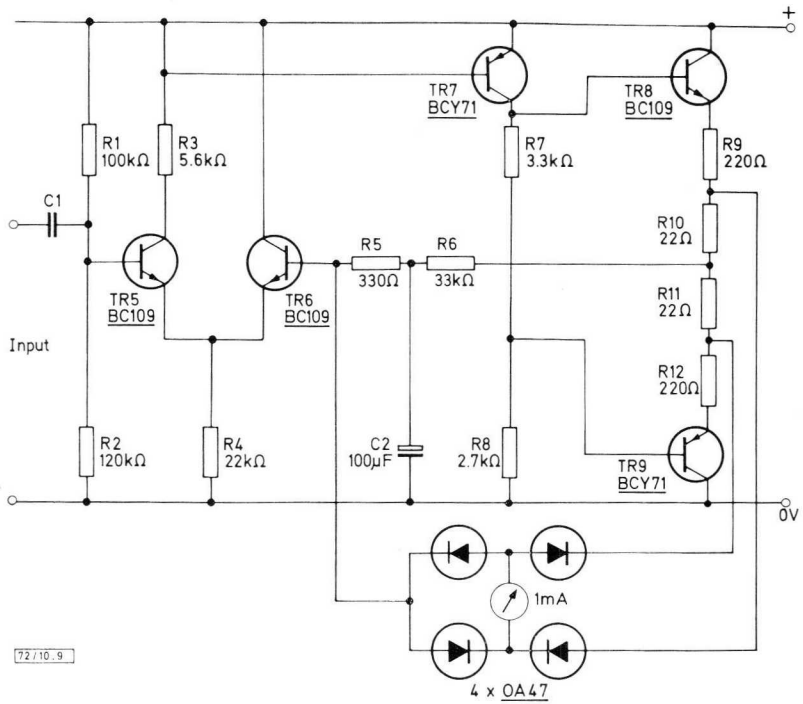

Fig. 10.9—Meter drive

voltage set by R_1 and R_2 across the supply. There is no a.c. feedback in this path, a.c. being shunted to earth by C_2. A.C. feedback is available only through the diode bridge and the meter.

At low values of a.c. input, where the diode rectifiers tend to be of high impedance, the amplifier voltage gain is high and a large voltage swing is applied to the rectifiers, thus minimising their non-linearity.

The meter current develops an a.c. feedback voltage across R_5 (330Ω) which is approximately equal to the input voltage.

The effective loop gain is 1500. Linearity of the meter circuit is not worse than 2% of f.s.d. from 1mA to 5μA. The meter should be protected from current surges.

Performance

The performance of this type of electronic system, when used with a practical gas analyser, will depend on the energy of the infrared source and the length of the sample tube.

For the electronic system to function adequately it must be provided

with a signal from the cell of 10μV when no gas is present. The meter will then show full scale deflection and will give 3% inaccuracy due to noise, down to 1/3 of full scale deflection.

With a 300°C source of $1cm^2$ and a sample tube of 10cm length a signal of 10μV was developed at the amplifier input terminals. A 4·4μm narrow-band (0·1μm) filter was used. Under these conditions, 10% CO_2 at atmospheric pressure produced a meter indication 50% of f.s.d. From the line in Fig. 10.5 a 27% meter indication would be predicted. The difference is explained by the filter being about 0·05μm off the centre of the CO_2 absorption peak.

CHAPTER 11

MCT DETECTORS AT 5μm AND NORMAL AMBIENT TEMPERATURE

The performance characteristics of mercury cadmium telluride detectors in the 8 to 13μm band and at a temperature of 77K are already well established. Substantially background-limited performance can be achieved under these conditions. In this chapter an investigation into the properties of these detectors in the 4 to 6μm band, at room temperature and with moderate cooling, is described. Detectors of various cutoff wavelengths within the 4 to 6μm band were made by adjusting the ratio of mercury telluride to cadmium telluride in the material. The detectors, of sensitive area 0·25mm square, were mounted on a ceramic substrate in a modified integrated-circuit flatpack.

At 5μm and a temperature of 77K the performance of mercury cadmium telluride detectors is comparable with that of indium antimonide devices. However, at room temperature (300K) indium antimonide is not ideal for applications involving transmission through the atmosphere because the material responds to 7μm, whereas the atmosphere is opaque beyond 5μm. Thus, much of the radiation emitted by broadband sources to which indium antimonide is sensitive is absorbed by the atmosphere. This investigation shows that not only are good detectivities achieved under these conditions with mercury cadmium telluride detectors, but resistance and noise levels are such that amplifier design is greatly simplified.

PERFORMANCE AT 300K

Detectivity

Fig. 11.1 shows measured values of area normalised detectivity D* (500K, 20kHz, 1) plotted against cutoff wavelength (defined as the wavelength at which response is half the peak value), and calculated values of peak detectivity D* (λp, 20kHz, 1). It will be seen that the peak detectivity increases as wavelength decreases, reaching almost

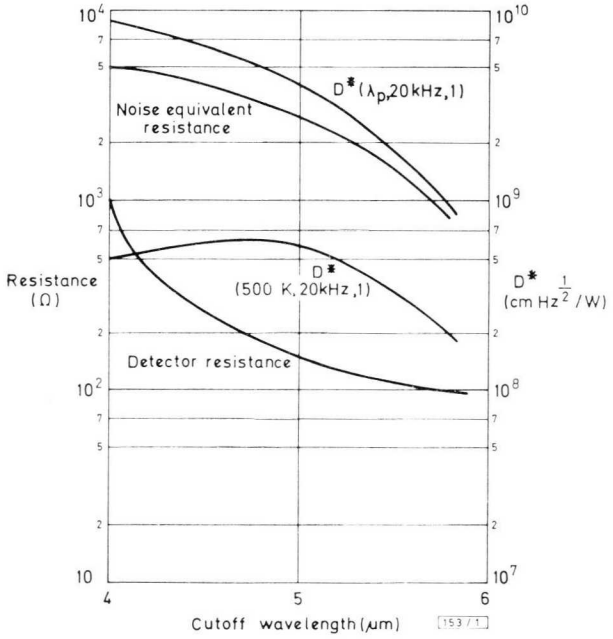

Fig. 11.1—Variation of detectivity, noise equivalent resistance and ohmic resistance with detector cutoff wavelength

10^{10}cmHz$^{\frac{1}{2}}$ W^{-1} at 4μm. At 5μm the peak detectivity is typically $3{\cdot}5\times 10^9$cmHz$^{\frac{1}{2}}$ W^{-1}. (Indium antimonide detectors have a typical peak detectivity of 3×10^8cmHz$^{\frac{1}{2}}$ W^{-1} at 6·5μm, which is close to the value obtained by extrapolation of the curve for the detectors under consideration.)

Noise and resistance levels

Fig. 11.1 also shows the typical noise equivalent resistance (defined as the resistance value which would give Johnson noise equal to that measured in the detector) plotted against cutoff wavelength. To obtain these values the bias current was chosen to give maximum detectivity. The detector ohmic resistance is also plotted to illustrate two advantages of these detectors:

1) The noise equivalent resistance is an order of magnitude higher than the ohmic resistance, so very-low-noise amplifiers are not necessary;

2) for the square elements used in this investigation the resistance levels are high enough to allow direct coupling to amplifiers, and it is not necessary to increase the element resistance by using a 'labyrinth' construction or to use transformer coupling.

Typical performance figures at two wavelengths are tabulated below.

Cutoff wavelength	4·7	5·6	μm
D* (λp, 20kHz, 1)	5×10^{9}	$1{\cdot}3\times10^{9}$	$cmHz^{\frac{1}{2}}W^{-1}$
Peak responsivity	1600	300	V/W
Noise equivalent resistance	4	1·25	kΩ
Resistance	200	100	Ω
Time constant	400	150	ns
Noise knee frequency†	2	5	kHz
Bias current	3	5	mA

†this is the frequency at which the low-frequency 1/f noise and white noise curves intersect.

PERFORMANCE WITH MODERATE COOLING

Figs. 11.2a, b, and c show the variation of detector parameters with temperature for a typical detector of cutoff wavelength 4·6μm at 300K. Increases in detectivity and responsivity are obtained if the detectors are cooled, and Fig. 11.2b shows that cutoff wavelength shifts to higher values. At −40°C the peak detectivity has reached $2\times10^{10}cmHz^{\frac{1}{2}}W^{-1}$ and the responsivity has increased by an order of magnitude over the room temperature value. The high ratio of noise equivalent resistance to ohmic resistance is maintained. Further cooling to −196°C (liquid nitrogen temperature) gives a detectivity of $5\times10^{10}cmHz^{\frac{1}{2}}W^{-1}$, with a cutoff wavelength of 5·8μm, values which are comparable with figures for indium antimonide detectors. However, cooling to the −40 to −80°C region is likely to be of most interest, since these temperatures can be achieved with thermoelectric and freon cooling systems.

OPTIMISATION OF CUTOFF WAVELENGTH

For essentially monochromatic applications, such as spectrometry and gas analysis, the choice of detector cutoff wavelength is governed by the requirements of the measurement. If mercury cadmium telluride detectors are used at room temperature, a response reaching only that required by the application will give the best overall performance.

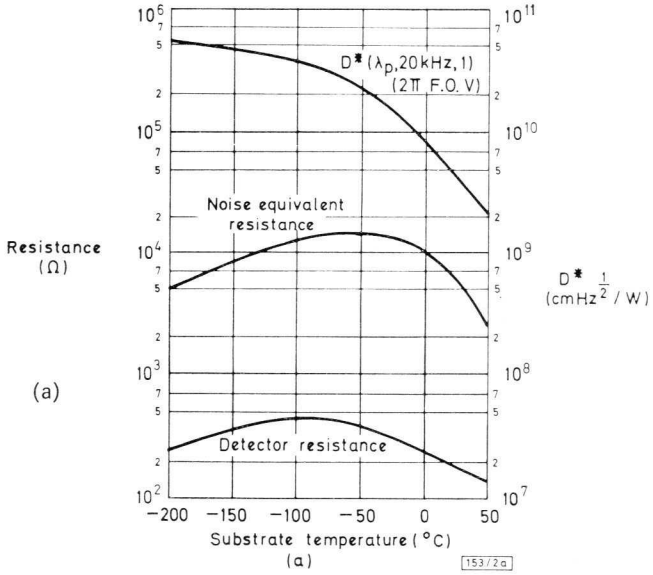

Fig. 11.2—Variation with substrate temperature of
(a) detectivity, noise equivalent resistance and ohmic resistance
(b) cutoff wavelength
(c) responsivity

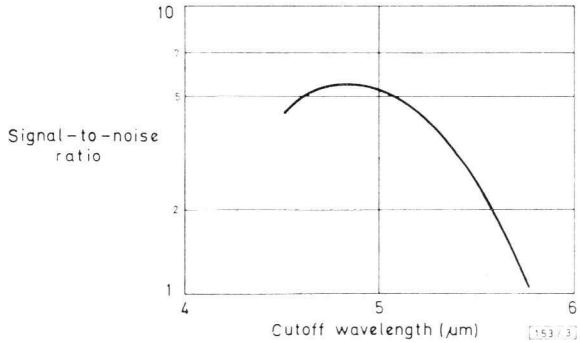

Fig. 11.3—Variation of signal-to-noise ratio with cutoff wavelength

(b)

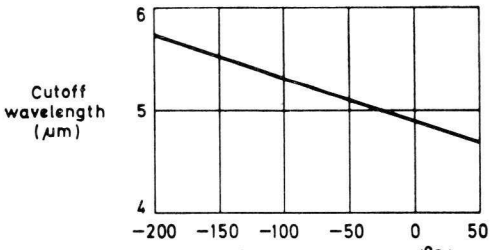

(b) 153/2b

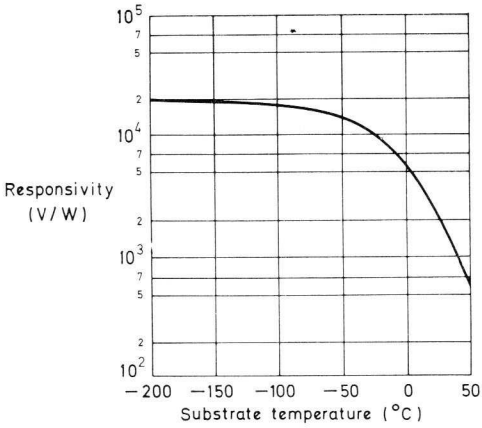

(c)

153/2c

However, in the case of detection or measurement of thermally radiating sources an optimum detector cutoff wavelength occurs, the value depending on the temperature of the source and being influenced by the spectral transmission of the atmosphere, especially over long ranges. Fig. 11.3 shows typical calculated values of signal-to-noise ratio for mercury cadmium telluride detectors, assuming a source at 300K and a value of atmospheric transmission appropriate to a distance of one mile. It can be seen that the best performance is obtained with detectors of cutoff wavelength about 4·8μm.

The techniques used in the manufacture of these detectors can be extended to the fabrication of linear arrays for imaging and other applications, as is already the practice with cooled detectors.

REFERENCES AND BIBLIOGRAPHY

1. GAYDON, A. G., and WOLFHARD, H. G., 'Flames, their structure, radiation, and temperature'. Chapman and Hall, 1953.

2. BARNES, R. B., 'Determination of body temperature by infrared emission.' **J. Appl. Physiology,** Vol. 22, No. 6, June 1967, pp. 1143 to 1146.

3. WILLIAMS, P., 'An improved phase-sensitive detector'. **J. Sci. Instr.,** Vol. 42, July 1965, pp. 474 to 476.

4. PIERSON, R. H., FLETCHER, A. N., and GANTZ, E. ST. C., 'Catalog of infrared spectra for qualitative analysis of gases'. **Analytical Chemistry,** Vol. 28, No. 8, Aug. 1956, pp. 1218 to 1239.

5. HILL, D. W., and POWELL, T., 'Non-dispersive infrared gas analysis in science, medicine and industry'. Adam Hilger, 1968.

6. SIMON, I., 'Infrared radiation'. Van Nostrand, 1966.

7. SMITH, R. A., JONES, F. E., and CHASMAR, R. P., 'The detection and measurement of infrared radiation'. Oxford, 1957.

8. CONN, G. K. T., and AVERY, D. G., 'Infrared methods'. Academic Press, 1960.

9. HOUGHTON, J. T., and SMITH, S. D., 'Infrared physics'. Oxford, 1966.

10. KRUSE, P. W., MCGLAUCHLIN, L. D., and MCQUISTAN, R. B., 'Elements of infrared technology'. Wiley, 1962.

11. HOLTER, M. R., NUDELMAN, S., SUITS, G. H., WOLFE, W. L., and ZISSIS, G. J., 'Fundamentals of infrared technology'. MacMillan (New York) 1962.

12. JAMIESON, J. A., MCFEE, R. H., PLASS, G. N., GRUBE, R. H., and RICHARDS, R. G., 'Infrared physics and engineering'. McGraw-Hill, 1963.

INDEX

Argentina
FAPESA I.y.C.
Melincué 2594
Tel. 50-9941/8155
BUENOS AIRES

Australia
Philips Industries Ltd.
Elcoma Division
95-99 York Street
Tel. 20223
SYDNEY, N.S.W. 2000

Austria
WIVEG
Zieglergasse 6
Tel. 93 26 22
A 1072 WIEN

Belgium
M.B.L.E.
80, Rue des Deux Gares
Tel. 230000
1070 BRUXELLES

Brazil
IBRAPE S.A.
Av. Paulista 2073-S/Loja
Tel. 278-1111
SAO PAULO, SP

Canada
Philips Electron Devices
116 Vanderhoof Ave.
Tel. 425-5161
TORONTO 17, Ontario

Chile
Philips Chilena S.A.
Av. Santa Maria 076
Tel. 39 40 01
SANTIAGO

Colombia
SADAPE S.A.
Calle 19, No. 5-51
Tel. 422-175
BOGOTA D.E. 1

Denmark
Miniwatt A/S
Emdrupvej 115A
Tel. (01) 69 16 22
DK-2400 KØBENHAVN NV

Finland
Oy Philips A.B.
Elcoma Division
Kaivokatu 8
Tel. 10 915
HELSINKI 10

France
R.T.C. - La Radiotechnique-Compelec
Avenue Ledru Rollin 130
Tel. 357-69-30
PARIS 11

Germany
VALVO G.m.b.H.
Valvo Haus
Burchardstrasse 19
Tel. (0411) 3296-1
2 HAMBURG 1

Greece
Philips S.A. Hellénique
Elcoma Division
52, Av. Syngrou
Tel. 915.311
ATHENS

Hong Kong
Philips Hong Kong Ltd.
Components Dept.
St. George's Building, 21st Fl.
Tel. K-42 82 05
HONG KONG

India
INBELEC Div. of Philips India Ltd.
Band Box House
254-D, Dr. Annie Besant Road
Tel. 453386, 456420, 452986
Worli, BOMBAY 18 (WB)

Indonesia
P.T. Philips-Ralin Electronics
Elcoma Division
Djalan Gadjah Mada 18
Tel. 44 163
DJAKARTA

Ireland
Philips Electrical (Ireland) Ltd.
Newstead Clonskeagh
Tel. 693355
DUBLIN 6

Italy
Philips S.p.A.
Sezione Elcoma
Piazza IV Novembre 3
Tel. 69.94
MILANO

Japan
NIHON PHILIPS
32nd Fl. World Trade Center Bldg.
5, 3-chome, Shiba Hamamatsu-cho
Minato-ku,
Tel. (435) 5204-5
TOKYO

Mexico

Electrónica, S.A. de C.V
Varsovia No. 36
Tel. 5-33-11-80
MEXICO 6, D.F.

Netherlands

Philips Nederland N.V.
Afd. Elonco
Boschdijk, VB
Tel. (040)-43333
EINDHOVEN

New Zealand

EDAC Ltd
70-72 Kingsford Smith Street
Tel. 873159
WELLINGTON

Norway

Electronica A/S
Middelthunsgate 27
Tel. 463970
OSLO 3

Peru

CADESA
Jr. Ilo, No. 216
Appartado 10132
Tel. 27 7317
LIMA

Portugal

Philips Portuguesa S.A.R.L.
Rua Joaquim Antonio de Aguiar 66
Tel. 683121/9
LISBOA

South Africa

EDAC (Pty) Ltd.
South Park Lane
New Doornfontein
Tel. 24/6701-2
JOHANNESBURG

Spain

COPRESA S.A.
Balmes 22
Tel. 232 66 80
BARCELONA 7

Sweden

ELCOMA A.B.
Lidingövägen 50
Tel. 08/679780
10250 STOCKHOLM 27

Switzerland

Philips A.G.
Edenstrasse 20
Tel. 051/442211
CH-8027 ZUERICH

Taiwan

Philips Taiwan Ltd.
San Min Building, 3rd Fl.
57-1, Chung Shan N. Road
Section 2
Tel. 553101-5
TAIPEI

Turkey

Turk Philips Ticaret A.S.
EMET Department
Gümüssuyu Cad. 78-80
Tel. 45.32.50
Beyoglü, ISTANBUL

United Kingdom

Mullard Ltd.
Mullard House
Torrington Place
Tel. 01-580 6633
LONDON WC1E 7HD

United States

AMPEREX ELECTRONIC CORP.
Electron Tube Division
Tel. 516 WE 1-6200
HICKSVILLE N.Y. 11802

Sem. and Microcircuits Div.
Tel. 401-762-9000
SLATERSVILLE R.I. 02876

Electro-Optical Devices Div.
Tel. 401-762-3800
SLATERSVILLE, R.I. 02876

Component & Entertainment Tube
Tel. 516-234-7000
HAUPPAUGE N.Y. 11787

FERROXCUBE CORP.
(Memory Products)
P.O. Box 359
Tel. (914) 246-2811
SAUGERTIES, N.Y. 12477

Uruguay

Luzilectron S.A.
Rondeau 1567, piso 5
Tel. 9 43 21
MONTEVIDEO

Venezuela

C.A Philips Venezolana
Elcoma Department
Colinas de Bello Monte
Tel. 72.01.51
CARACAS

Printed in The Netherlands

③ 10-'71

9399 256 00901